IDENTIFICATION OF MACRO- AND MICRO- COMPLIANT MECHANISM CONFIGURATIONS RESULTING IN BISTABLE BEHAVIOR

by

Brian D. Jensen

A thesis submitted to the faculty of

Brigham Young University

in partial fulfillment of the requirements for the degree of

Master of Science

Department of Mechanical Engineering

Brigham Young University

August 1998

BRIGHAM YOUNG UNIVERSITY

GRADUATE COMMITTEE APPROVAL

of a thesis submitted by

Brian D. Jensen

This thesis is accepted in its present form by the Department of Mechanical Engineering of Brigham Young University as satisfying the thesis requirement for the degree of Master of Science.

_____ Date: _____
Larry L. Howell, Committee Chair

_____ Date: _____
Linton G. Salmon, Committee Member

_____ Date: _____
Timothy W. McLain, Committee Member

_____ Date: _____
Craig C. Smith, Graduate Coordinator

ABSTRACT

IDENTIFICATION OF MACRO- AND MICRO- COMPLIANT MECHANISM CONFIGURATIONS RESULTING IN BISTABLE BEHAVIOR

Brian D. Jensen

Department of Mechanical Engineering

Master of Science

The purpose of this research is to identify the configurations of several mechanism classes which result in bistable behavior. Bistable mechanisms have use in many applications, such as switches, clasps, closures, hinges, and so on. A powerful method for the design of such mechanisms would allow the realization of working designs much more easily than has been possible in the past. A method for the design of bistable mechanisms is especially needed for micro-electro-mechanical systems (MEMS) because fabrication and material constraints often prevent the use of simple, well-known bistable mechanism configurations. In addition, this knowledge allows designers to take advantage of the many benefits of compliant mechanisms, especially their ability to store and release energy in their moving segments. Therefore, an analysis of a variety of mechanism classes has been performed to determine the configurations of compliant segments or rigid-body springs in a mechanism which result in bistable behavior. The analysis revealed a relationship between the placement of compliant segments and the stability characteristics of the mechanism which allows either analysis or synthesis of bistable mechanisms to be performed very easily.

Using this knowledge, a method of type synthesis for bistable mechanisms has been developed which allows bistable mechanisms to be easily synthesized. Several design examples have been presented which demonstrate the method. The theory has also been applied to the design of several bistable micro-mechanisms. In the process of searching for usable designs for micro-bistable mechanisms, a mechanism class was defined, known as “Young” mechanisms, which represent a feasible and useful way of achieving micro-mechanism motion similar to that of any four-bar mechanism. Based on this class, several bistable micro-mechanisms were designed and fabricated. Testing demonstrated the ability of the mechanisms to snap between the two stable states. In addition, the mechanisms showed a high degree of repeatability in their stable positions.

COMMITTEE APPROVAL:

Larry L. Howell, Committee Chair

Linton G. Salmon, Committee Member

Timothy W. McLain, Committee Member

Craig C. Smith, Graduate Coordinator

ACKNOWLEDGMENTS

Several people deserve thanks for their help in completing the work reported in this thesis. The help of Brian Christensen in gathering the data for repeatability of the stable positions for the bistable MEMS is gratefully acknowledged. The work of Dani Johnson in recording and organizing data for the MEMS design improvements is also gratefully acknowledged, as well as the aid of Nathan Crane, Dani Johnson, and Clint Mortensen in machine work to create models demonstrating the points made in the thesis. In addition, I would like to thank Rebecca Cragun and Nathan Masters for their excellent work with the scanning electron microscope used to photograph the micro-mechanisms.

Thanks is also due to my graduate committee, Dr. Tim McLain and Dr. Linton Salmon, for their help in improving the thesis and reviewing the work I have done. I have also received valuable moral support and friendship from Matt Parkinson, Greg Roach, and all the others who worked with me in the lab.

I would also like to thank my wife for the support she has given me during my work on this thesis. She has spent many hours listening to explanations of my work while I put my thoughts in order. My advisor, Larry Howell, has also spent a considerable portion of his time giving guidance, editing drafts, and helping in countless ways. I consider him to

be a man that anyone would be fortunate to know, and a model for what a graduate advisor should be.

Finally, I would like to acknowledge the support of my Heavenly Father throughout my master's degree work. His love and inspiration, and my faith in Him, have been guiding forces in my life.

This work has been supported by a National Science Foundation Graduate Fellowship and through National Science Foundation Career Award No. DMI-9624574.

Table of Contents

List of Figures

List of Tables

CHAPTER 1 *Introduction*

The purpose of this research is to identify the compliant mechanism configurations which result in a bistable mechanism. Using the theory developed here, both macro- and micro- compliant bistable mechanisms may be easily synthesized for a variety of applications. In particular, the design and testing of a number of micro-bistable mechanisms are discussed in this thesis. This chapter defines some of the basic concepts involved in compliant bistable mechanisms, and it reviews some of the past work done in this area. In particular, it reviews compliant mechanisms, MEMS, and mechanism synthesis. This first section introduces some of the terms which will be used extensively throughout the thesis.

In kinematic terms, a “mechanism” is a mechanical device used to transfer or transform motion or energy. Mechanisms carry out much of the useful work in machines; for example, the piston and crank on an engine transform linear motion into rotating motion. Mechanisms typically gain motion from several “kinematic pairs,” or joints, which allow motion in one or more directions. A pin joint, for example, allows rotation about one axis while constraining motion in all other directions. Mechanisms which gain all of their motion from kinematic pairs are called rigid-body mechanisms.

Another class of mechanisms, known as compliant mechanisms, gain some or all of their motion from the deflections of parts of the mechanism. Compliant mechanisms offer several advantages over more traditional rigid-body mechanisms. For example, compliant segments have no friction, noise, or backlash, and they significantly reduce the total part count of the mechanism (Sevak and McLarnan, 1974). Many compliant mechanisms can even be made from one piece of material which bends to achieve desired motion. Of course, compliance also introduces several challenges. Compliant members have only limited motion, and their deflection requires energy input, reducing the energy which a mechanism can output. In addition, they are often difficult to design because of the complexity of predicting large deflections in beams. However, recent developments have produced a pseudo-rigid-body model which models many compliant segments as two or more rigid members joined by a pin joint. This model greatly simplifies the design of many compliant mechanisms.

A bistable mechanism is a mechanism that is stable in two positions within its range of motion. Such mechanisms may be used as switches, closures, hinges, or other applications where two stable positions are desired. Although many examples of rigid-body bistable mechanisms exist, compliance offers a particularly economical way to achieve bistable behavior. As mentioned above, flexible members store energy as they flex. In the proper mechanism configuration, a compliant segment can provide the energy needed to keep the mechanism in its two stable positions.

Compliant bistable mechanisms have particular application to micro-electro-mechanical systems, or MEMS. These microscopic devices are produced using the same fabrication techniques that are used to make integrated circuits. This allows sensors,

actuators, or other useful devices to be batch-fabricated with on-chip circuitry for control of the devices. Compliant bistable MEMS could be used as mechanical switches, micro-positioners, or even micro-valves. Therefore, it is especially desirable to be able to design compliant bistable mechanisms which can operate in the micro-regime.

1.1 Importance of the Research

Bistable mechanisms offer a number of possible advantages in many applications. They are used extensively as electrical toggle switches, clasps, closures, and hinges, to name a few applications. Most existing examples are rigid-body mechanisms consisting of linear and leaf springs and any number of rigid links and joints. Compliant bistable mechanisms offer the added advantages listed above. Thus, a method allowing new compliant bistable mechanisms to be easily synthesized would be very valuable in the development of mechanisms for a wide variety of applications.

In addition to their usefulness as macro-mechanisms, bistable mechanisms offer several advantages as components of MEMS. Because they require no energy input to remain in their positions, they could allow significant power savings for memory systems, switches and relays, micro-positioners, or similar systems. They may also allow the realization of applications which could not otherwise be done mechanically, such as non-volatile memory or mechanical computers.

However, the design of compliant bistable mechanisms is not generally straightforward and easy. Not only must the mechanism motion be considered, as in an ordinary mechanism synthesis problem, but the stability of the mechanism must also be evaluated throughout the motion. The relationship between mechanism motion and stability has not

previously been explored in depth, making the design of these mechanisms difficult. Therefore, this thesis studies the compliant mechanism configurations which result in a bistable mechanism. The theory presented allows the selection of the basic mechanism configuration which will result in a bistable mechanism with the desired characteristics. In other words, this theory makes possible the type synthesis of bistable mechanisms.

Additionally, material and fabrication constraints in MEMS have further complicated the design of useful bistable MEMS. This obstacle to bistable MEMS design has been a motivating factor in this research. Hence, while the theory developed in this thesis may be applied to the design of any bistable mechanism, it will be particularly applied to the design of bistable MEMS.

1.2 Contributions of the Thesis

The most significant contribution of this thesis lies in the area of bistable mechanism synthesis. As outlined in the previous section, no method currently exists to consider the motion and energy states of a mechanism simultaneously during design. As a result, bistable mechanism design is usually based on experience or trial-and-error. However, the theory developed in this thesis allows a designer to determine the best general mechanism class to meet a problem, at the same time as choosing the number and placement of compliant segments within the class to result in bistable behavior. This theory is very simple in its application, requiring no computer code or complex calculations. Previously, no method could be so easily applied to bistable mechanism synthesis.

Another meaningful contribution of this thesis lies in the area of MEMS. No prior work demonstrates in-plane bistable behavior for MEMS. By causing the bistable mecha-

nisms to move within the plane of fabrication, much more complex motion is possible, especially in the choice of stable positions. Compliant bistable mechanism theory was instrumental in leading to the design and fabrication of these devices. It is expected that future work will use these or similar mechanisms in a wide variety of applications, such as non-volatile memory cells, micro-valves, micro-switches, and so on.

1.3 Outline of the Thesis

The next chapter discusses the main issues associated with compliant mechanisms and MEMS, prior work in these areas, and provides an overview of various mechanism type synthesis techniques. Chapter 3 contains a review of past work in bistable mechanisms. Chapter 4 describes the theoretical work done in the identification of mechanism configurations resulting in bistable behavior. This theory is applied to a method of type synthesis in Chapter 5. This method is demonstrated using several examples, including the design of bistable micro-mechanisms. The design of bistable MEMS is developed more fully in Chapter 6, with specific examples of micro-mechanisms designed and fabricated. Finally, the work is summarized in Chapter 7, and a variety of recommendations are given for future research.

CHAPTER 2 *Background*

2.1 Compliant Mechanisms

Mankind has relied on deflections to obtain mechanism motion throughout history. However, until recently, research into compliant mechanisms has been very limited. This section will outline the history of compliant mechanisms and describe the research work that has occurred in this area. Particular emphasis will be given to the pseudo-rigid-body model.

2.1.1 History of Compliant Mechanisms

From almost the dawn of time, inventors have used deflections in mechanisms. For example, bows and catapults rely on the energy stored in a deflected beam to propel their missiles across long distances or over walls. Tweezers grasp small objects between two flexible beams. Various types of springs and some hinges also use deflections to achieve the motion desired. However, scientific study of large-deflection mechanisms came much later.

Euler (1744) described beam deflections mathematically using the well-known Bernoulli-Euler beam equation (see section 2.1.2, “Explanation of Non-Linear Beam Deflections”). This equation was solved for large deflections by Bisshopp and Drucker (1945) using elliptical integrals. Frisch-Fay (1962) also studied large beam deflections. Further research in this area has included finding large deflections of beams with various geometries and developing methods of large-deflection finite element analysis. Gorski (1976) presented a summary of such work. Hill and Midha (1990) and Her et al. (1992) also addressed the numerical analysis of large-deflection beams.

Burns (1964) and Burns and Crossley (1966) analyzed mechanisms constructed with one or more flexible beams. They also presented a graphical method of compliant mechanism synthesis using a compliant segment for the coupler link (Burns and Crossley, 1968). Shoup and McLarnan (1971a) investigated compliant mechanisms using compliant segments with both end forces and end moments. They also explored three-dimensional compliant mechanisms (Shoup and McLarnan, 1971b). Shoup (1972) and Winter and Shoup (1972) furthered the analysis of the deflections of compliant segment used in mechanisms. Sevak and McLarnan (1974) then applied optimization to the design of compliant mechanisms. The effects of compliant members on mechanical advantage in a mechanism have also been investigated (Salamon and Midha, 1992). A system of classification and nomenclature for compliant mechanisms has also been established to aid in the naming and analysis of compliant mechanisms (Midha et al., 1994).

Howell and Midha (1994) introduced the idea of a pseudo-rigid-body model to simplify compliant mechanism analysis. In this model, a flexible mechanism link is modeled as two or more rigid links joined by pin joints. A presentation of a pseudo-rigid-

body model for many types of flexible links was presented in the following years (Howell and Midha, 1995a; Howell et al., 1996; Howell and Midha, 1996a, Edwards, 1996). This model allows many compliant mechanisms to be designed and analyzed much more easily than was previously possible.

In recent years, work has focused on methods of synthesizing new compliant mechanisms. Ananthasuresh (1994) and Ananthasuresh et al. (1994) presented work done on applying topological synthesis to the design of compliant mechanisms. In this method, a computer-driven optimization routine attempts to find the right configuration of flexible material to accomplish a certain task. The work was expanded upon by Frecker et al. (1995, 1996, 1997). Sigmund (1996) also presented work on topology optimization. An optimization approach was also used by Parkinson et al. (1997). In this work, optimization was performed on a parametrically described spline representing a compliant beam. The optimization routine found the best configuration of the beam to perform a certain task.

2.1.2 Explanation of Non-Linear Beam Deflections

The deflection of a beam may be determined from the Bernoulli-Euler assumption, which states that beam moment is proportional to curvature. In mathematical terms, this may be expressed as

$$\frac{M}{EI} = \frac{d\theta}{ds} \tag{2.1}$$

where M is the beam moment, EI is the rigidity, θ is the beam angle, and s is a coordinate measuring length along the beam. In an x-y coordinate system, Eq. (2.1) may be expressed as

$$\frac{M}{EI} = \frac{\frac{d^2y}{dx^2}}{\left[1+\left(\frac{dy}{dx}\right)^2\right]^{3/2}} \tag{2.2}$$

For most load conditions, Eq. (2.2) is impossible to solve using normal differential equation techniques. However, for many applications, beam deflection is very small compared to the length of the beam. In this case, $\left(\frac{dy}{dx}\right)^2$, the square of the slope of the beam, may be assumed to be zero, resulting in the equation

$$\frac{M}{EI} = \frac{d^2y}{dx^2} \tag{2.3}$$

This equation may then be solved to give the beam deflection equations found in many mechanics textbooks.

Unfortunately, the deflections involved in compliant mechanisms are generally large. Large deflection problems may be solved using large-deflection finite element models; in fact, several commercial codes offer large-deflection analysis, allowing compliant mechanisms to be accurately modeled. However, design of compliant mechanisms using finite element analysis can be a tedious process, as the model must be updated after any design changes.

The Bernoulli-Euler equation has also been solved for large deflections using elliptic integrals (Bisshopp and Drucker, 1945). Elliptic integrals are functions involving intractable integrals whose value must be found numerically. With this method, many large-deflection problems may be solved. Unfortunately, the process is fairly complex, and only well-defined problems have solutions. However, the solution to these problems led to the development of the pseudo-rigid-body model, which is presented in the next section.

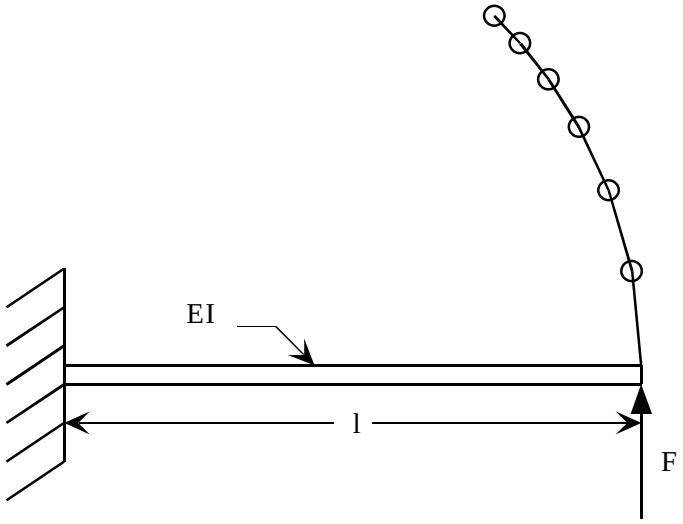

FIGURE 2-1: A flexible cantilever beam showing the deflection path of the beam's end under the application of a vertical force.

2.1.3 The Pseudo-Rigid-Body Model

Consider the flexible beam shown in Figure 2-1. The beam end deflection path under a vertical load, as predicted by elliptic integral solutions, is shown. Notice that the path is nearly circular, allowing it to be approximated by a rigid beam connected to a pin joint at the center of the deflection path (Howell and Midha, 1995a). This model may be drawn as shown in Figure 2-2. In the model, the rigid, rotating beam is of length γl - the "characteristic radius" - where l is the length of the flexible beam and γ is a parameter known as the "characteristic radius factor." The beam's resistance to bending is modeled by a torsional spring placed at the pin joint.

To complete the model shown in Figure 2-2, the value of γ must be found. This is done numerically by finding the value of γ that allows maximum angular deflection of the beam while keeping error within 0.5% of the total beam deflection. The optimal γ has been

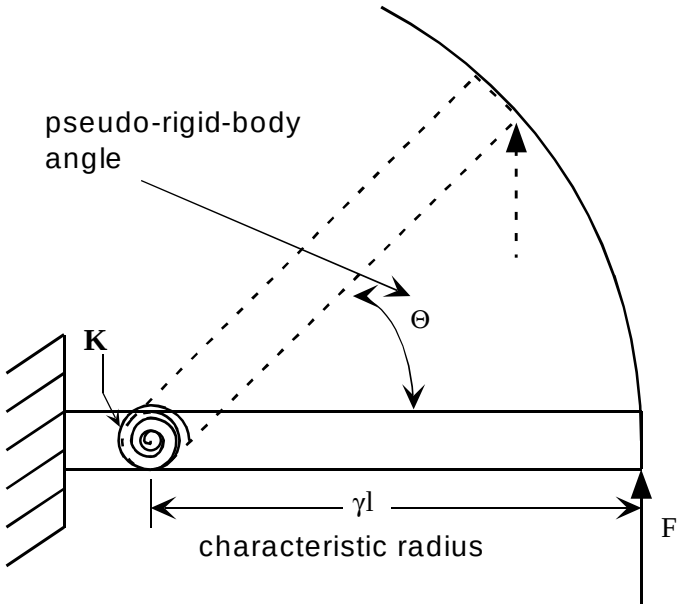

FIGURE 2-2: The pseudo-rigid-body model of a cantilever beam with a force at the free end.

found to be 0.8517 for this case (Howell and Midha, 1995a). The value of γ has been tabulated for a wide variety of load conditions, but it is generally fairly accurate to use an average value of 0.85 (Howell and Midha, 1995a).

The spring constant of the torsional spring may be found from the equation

$$K = \gamma K_\Theta \frac{EI}{l} \tag{2.4}$$

where K_Θ, a parameter called the "stiffness coefficient," is also determined by the load direction. Although it is also tabulated for various loadings, an average value of 2.65 will usually give good results (Howell et al., 1996). It may also be approximated as

$$K_\Theta = \pi\gamma \tag{2.5}$$

A pseudo-rigid-body model has also been developed for a small-length flexural pivot, as shown in Figure 2-3 (Howell and Midha, 1994a). Because the thin flexible

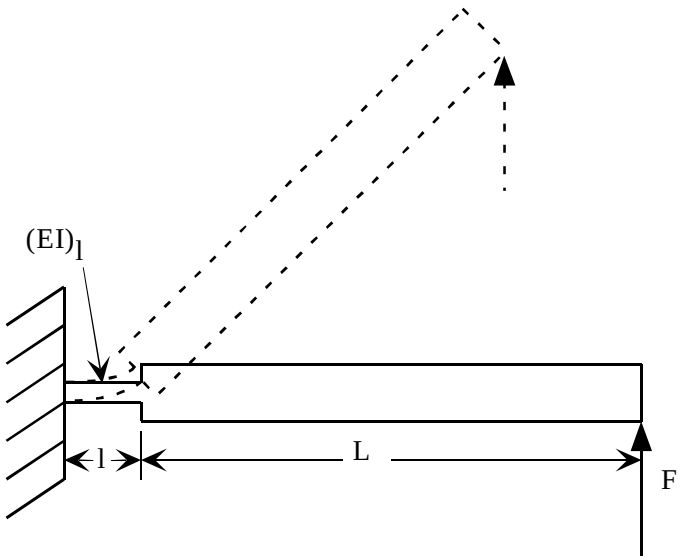

FIGURE 2-3: A small-length flexural pivot under action of a vertical force.

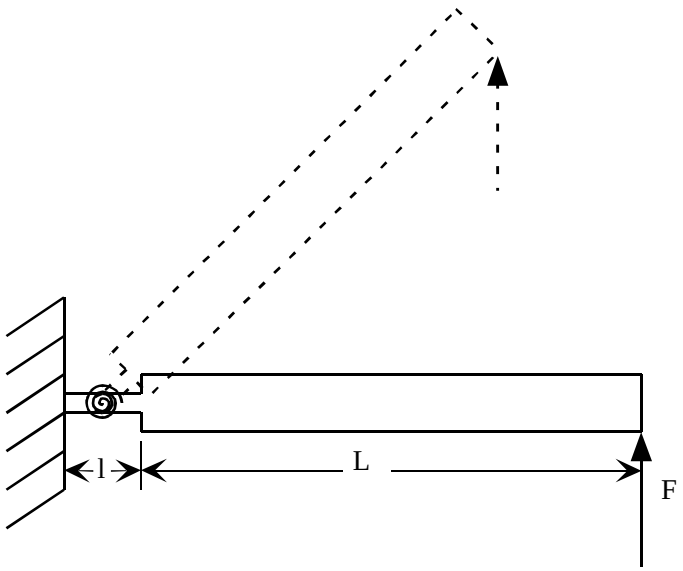

FIGURE 2-4: The pseudo-rigid-body model of a small-length flexural pivot.

segment is much shorter than the rigid segment it attaches to, it may be modeled with a pin joint in the center of the pivot, as shown in Figure 2-4. In this case, the torsional spring shown in the figure has a spring constant

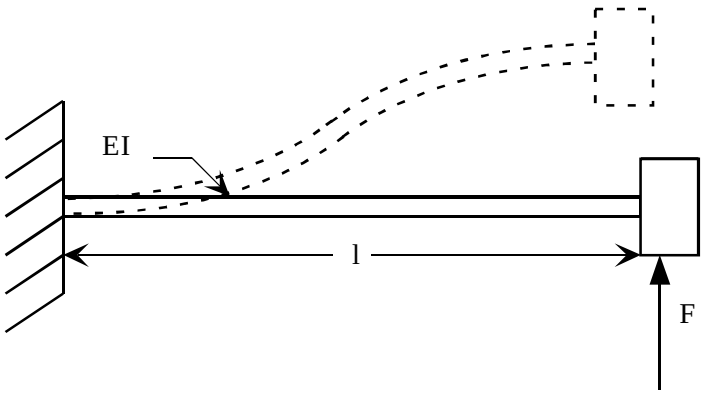

FIGURE 2-5: A parallel-guided segment. The block at the free end is constrained to remain parallel at all times.

$$K = \frac{(EI)_l}{l} \tag{2.6}$$

A living hinge is another case of small length flexural pivots. It is a very short, very thin pivot. Because of its small stiffness compared to other segments usually found in a compliant mechanism, it is often represented simply by a pin joint, with no torsional spring. When using this model, however, care must be taken to remember that the joint does not allow full rotation.

The fixed-guided segment shown in Figure 2-5 also has a corresponding model (Howell et al., 1996). This segment has a moving end which is constrained to always remain parallel to its original direction. The combination of force and moment at the moving end create a moment distribution which is always zero at the center of the beam. Hence, this segment may be modeled as two cantilever beams with forces at the free ends. Placing the beams end to end results in a pseudo-rigid-body model like that shown in Figure 2-6, where the torsional spring constants are given by

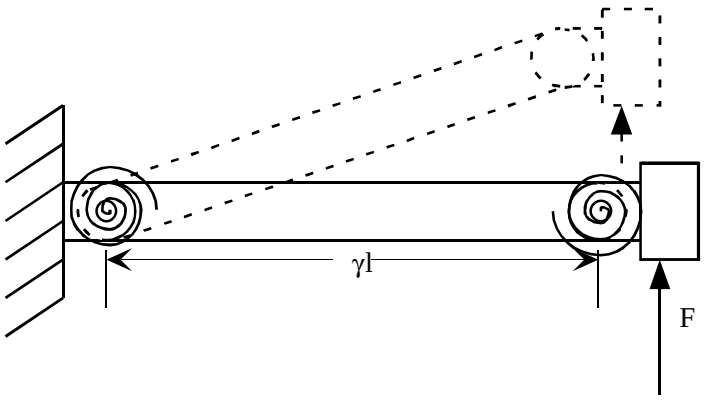

FIGURE 2-6: The pseudo-rigid-body model of a parallel-guided segment.

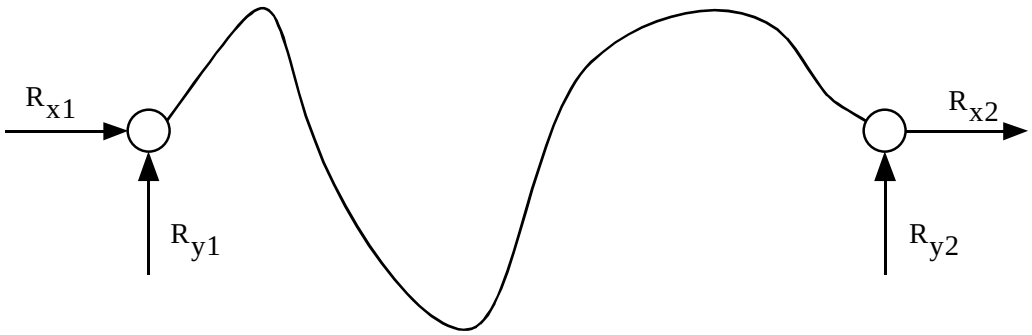

FIGURE 2-7: An arbitrary functionally binary pinned-pinned segment. This segment will only oppose forces acting along the line between its pin joints.

$$K = 2\gamma K_\Theta \frac{EI}{l} \tag{2.7}$$

A pseudo-rigid-body model has also been developed for initially curved cantilever beams with a force at the free end (Howell and Midha, 1996a) as well as a compliant segment pinned on both ends, which is often called a functionally binary pinned-pinned segment (Edwards, 1996). Because functionally binary pinned-pinned segments are especially useful in many bistable mechanisms, only their model will be explained here. Consider the arbitrary functionally binary pinned-pinned segment shown in Figure 2-7. A quick analysis of the reaction forces reveals that for static equilibrium, the segment cannot

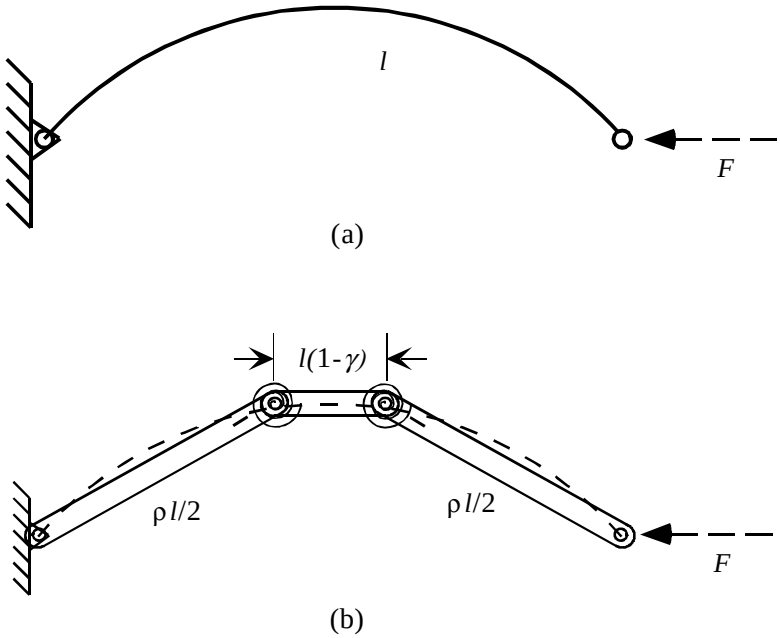

FIGURE 2-8: A semi-circular functionally binary pinned-pinned segment (a) and its pseudo-rigid-body model (b).

sustain any forces in the y-direction; only x-direction forces are possible. In other words, in static equilibrium, the segment can only resist forces acting along the line between its pin joints. This behavior will prove useful in the application of functionally binary pinned-pinned segments to the design of mechanisms.

A full pseudo-rigid-body model has only been developed for semi-circular functionally binary pinned-pinned segments, often called FBPP segments. This segment, shown in Figure 2-8(a), may be modeled using three rigid links joined by two pin joints with torsional springs, as shown in Figure 2-8(b). The length of the two outer segments is $\rho l/2$, where ρ is another constant called the "characteristic radius factor," whose value is given by the loading conditions and the segment's initial curvature (Edwards, 1996). The

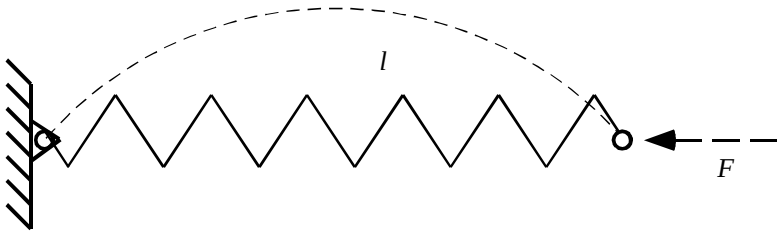

FIGURE 2-9: An alternate model of a semi-circular functionally binary pinned-pinned segment. While this model is less accurate mathematically, it is useful conceptually.

inner segment has length $l(1-\gamma)$, where the value of γ is also given by Edwards (1996). The two torsional springs have spring constants

$$K = 2\gamma K_\Theta \frac{EI}{l} \tag{2.8}$$

where K_Θ for this case is also given by Edwards (1996), and each pin joint is constrained to have the same angular deflection as the other.

The models for a small-length flexural pivot and a fixed-pinned segment are similar, with both segments being modeled by two rigid segments joined by a pin joint. Hence, either segment may be used in the place of a rigid-body pin joint to create a compliant mechanism (Howell and Midha, 1996b). The FBPP segment behaves differently, though. As shown previously, analysis of the forces on the segment shows that, at equilibrium, it can only sustain a horizontal force (one applied along the line between the two pins). This special behavior allows another model to be applied to the FBPP segment which is more useful conceptually, although it is less accurate mathematically. In this model, the resistance of the segment to horizontal forces is modeled by a nonlinear spring, as shown in Figure 2-9. This model is less exact mathematically because it is difficult to estimate the nonlinear spring function. Nevertheless, for fairly small deflections, the nonlinear function

can be approximated with Hooke's law, greatly simplifying the analysis (Edwards, 1996). It is often helpful to think of FBPP segments as representing linear springs, while small-length flexural pivots and fixed-pinned segments represent links joined by pin joints and torsional springs. This point will be demonstrated in section 2.1.4.

The pseudo-rigid-body model works very well in many situations, but it does have several limitations. It is very accurate over fairly large deflections, but it begins to lose accuracy if the deflection angle becomes too high. Maximum deflection angles are tabulated for keeping the deflection error under 0.5% (Howell and Midha, 1995a). Additionally, a model has yet to be developed for a cantilever beam with both an end force and a moment. However, despite these limitations, the model has proven to be extremely useful both in design and analysis of compliant mechanisms (Derderian et al., 1996; Derderian, 1996; Howell et al., 1994a; Howell and Midha, 1995b; Howell and Midha, 1996b; Lyon et al., 1997; Jensen et al., 1997; Jensen et al., 1998; Mettlach and Midha, 1996; Millar et al., 1996; Opdahl, 1996; Salmon et al., 1996).

2.1.4 An Example Using the Pseudo-Rigid-Body Model

Figure 2-10 shows a common, well-known bistable compliant mechanism, the shampoo lid. This closure is made of one piece of material, and it snaps open and closed, allowing easy use in the shower or bathtub. The pseudo-rigid-body model of the mechanism may be developed by realizing that the flexural pivots are living hinges, so that they may be modeled as pin joints. The square-shaped connecting piece may be modeled as two fixed-pinned segments. The completed model is shown in Figure 2-11. Although this model accurately predicts the motion and force characteristics of the shampoo lid, it

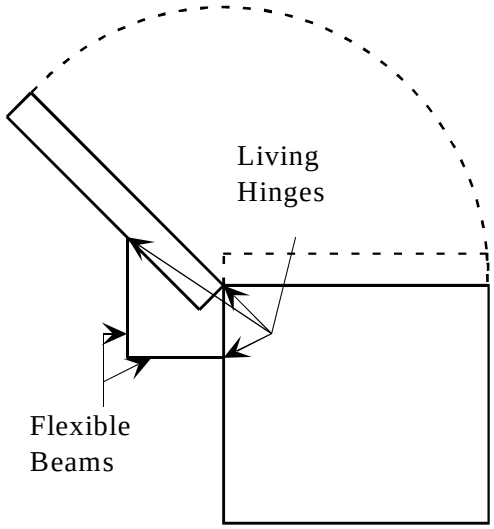

FIGURE 2-10: A schematic diagram showing a shampoo lid with a bistable closure.

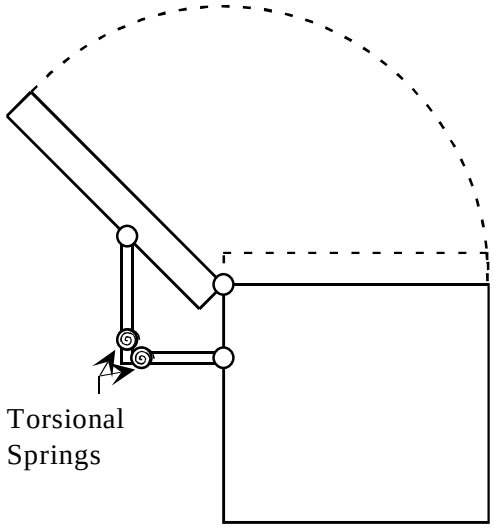

FIGURE 2-11: The pseudo-rigid-body model of the shampoo lid. The living hinges are replaced with pin joints, and the flexible beams are modeled as fixed-pinned segments.

does not allow easy conceptualization of the mechanism's motion. A different model may be created by realizing that the square connecting piece is a functionally binary pinned-pinned segment. As such, it may be modeled using a spring with a non-linear spring

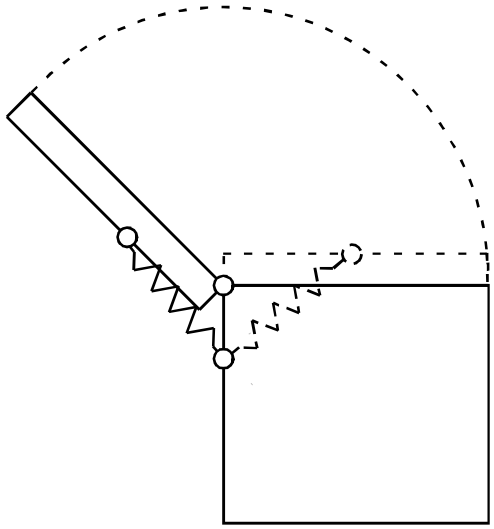

FIGURE 2-12: A modified pseudo-rigid-body model of the shampoo lid. This model makes motion of the mechanism easier to predict, although force relationships are more difficult to determine.

function, as shown in Figure 2-12. The derivation of this spring function is not straight-forward, so that the model shown in Figure 2-11 is easier to use for force-deflection data. However, the model shown in Figure 2-12 allows easy determination of the mechanism's motion. Notice that the model in Figure 2-11 is a five-bar linkage, while the model shown in Figure 2-12 is an inversion of a slider-crank mechanism.

2.2 MEMS

Micro-electro-mechanical systems (MEMS) provide a way to integrate electrical and computer circuitry with mechanical sensors or other mechanical elements. Therefore, they promise savings in cost, space, and manufacturing time for many applications. This section outlines some of the issues involved in MEMS, particularly issues associated with

MEMS fabrication. The desirability of designing bistable mechanisms for MEMS is also discussed.

2.2.1 Fabrication

Although several methods of MEMS fabrication exist, this section outlines only one. This process, called surface micromachining, is the method most similar to conventional integrated circuit processing. Surface micromachining takes place on a silicon wafer using techniques similar to those used for integrated circuit manufacturing. In this section, the fabrication of a beam which is fixed on both ends is demonstrated to illustrate the process. Such a beam might be used to test for residual compressive stress by observing the buckling of the beam. The beam's typical size would be about fifty to one hundred microns long, where 1 micron = 1μm = $1X10^{-6}$ m.

In the first step, a thin layer of silicon oxide is deposited over the silicon substrate using low pressure chemical vapor deposition (LPCVD). This oxide layer is then patterned using a process known as planar lithography. The oxide is etched away in areas where the mechanical structures will be anchored to the substrate, as shown in Figure 2-13. Next, a thin layer of polycrystalline silicon (polysilicon) is deposited using LPCVD. It is patterned to produce the structures desired, as shown in Figure 2-14. The desired structure is now completely formed, but the surrounding oxide holds it in place, preventing motion. The final step is to perform the "release etch" by etching away the oxide using hydroflouric acid. The completed beam is shown in Figure 2-15. A second or even third layer of oxide and polysilicon may also be added to produce more complex structures. In this way,

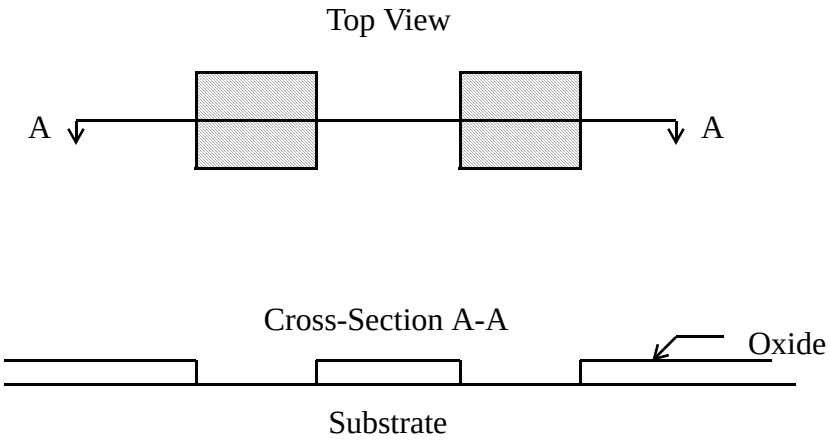

FIGURE 2-13: An early step in the surface micromachining process. The oxide has been patterned to allow a mechanical structure to be anchored to the substrate.

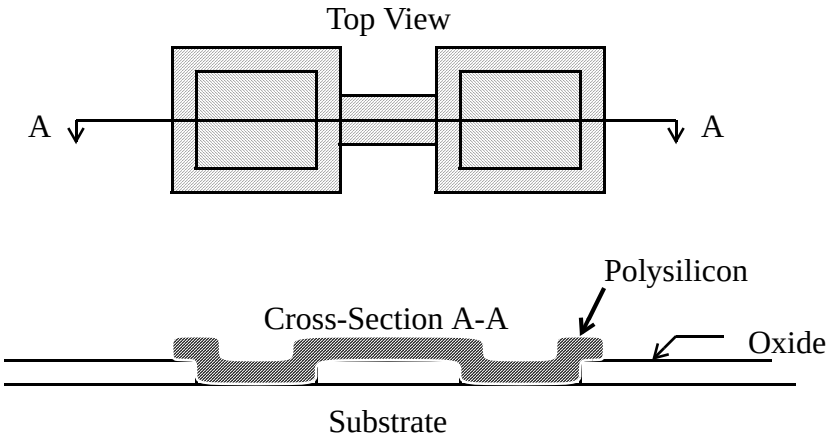

FIGURE 2-14: The fixed-fixed beam has now been patterned out of polysilicon.

mechanical motors, mechanisms, and several different types of actuators have been produced.

Several problems remain to be overcome in surface micromachining. One of the most serious is called “stiction.” While drying after the release etch, capillary action in the evaporating liquid can pull free structures down, causing them to contact the substrate. Some force, possibly Van der Waals forces, causes the structures to remain stuck to the

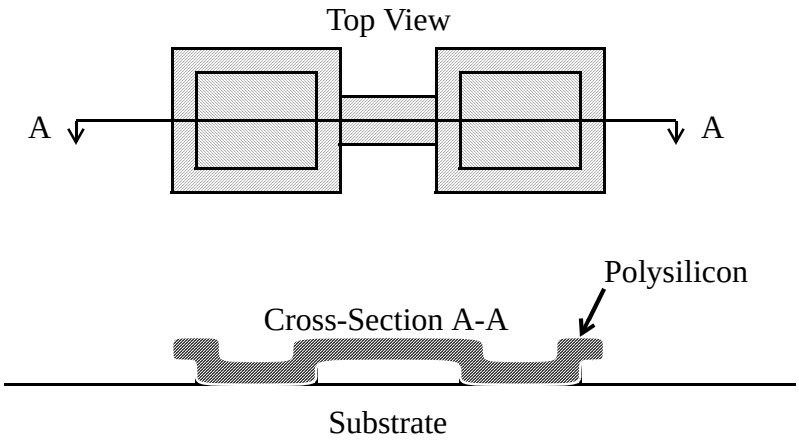

FIGURE 2-15: The completed fixed-fixed beam. The oxide under the beam has been removed by the release etch.

substrate even after drying is completed. The structures will then move only after a large force is applied to them. A similar thing happens any time a structure touches the substrate. Work is continuing to find ways to solve this problem (Abe et al., 1995).

The material involved represents another limitation to surface micromachining. Polysilicon is a very high-strength material, with an ultimate strength of about $1.2 \mathrm{X} 10^{10}$ dyne/cm^2, or almost 200 ksi (Sharpe et al., 1997). However, it is also a very brittle material, with almost no yielding before fracture. It also has a Young's modulus of about $1.6 \mathrm{X} 10^{12}$ dyne/cm^2, or about $23.2 \mathrm{X} 10^6$ psi. These properties make it almost as stiff as steel, with about the same ultimate strength as a high-strength, brittle steel. However, if deflections are desired, as in compliant mechanisms, it tends to fail catastrophically if its strength is exceeded. This means that compliant mechanisms must be carefully designed to keep stress well under the strength.

Another problem inherent with surface micromachining is the use of more than one layer of polysilicon. More layers allow more complexity in the design; however, they also

add cost and complexity to the manufacturing process, particularly if the extra layers are to be flat. If extra layers are simply deposited over lower layers, they will keep all of the topology of the underlying layers. While this fact is beneficial for some elements, it can be detrimental for others. While the layers can be planarized using a process known as chemo-mechanical polishing, this extra step is costly and allows more room for processing errors.

Because of the problems inherent with multiple layers, surface micromachining is often limited to two non-planar layers. While two layers are enough to create grounded pin or prismatic joints, floating joints are much more difficult to make. For this reason, compliant mechanisms form a vital part of many MEMS devices. Because they gain motion by bending, compliant mechanisms often can be produced using only one layer of polysilicon, allowing considerable savings in manufacturing cost. The next section reviews work that has been done in compliant MEMS.

2.2.2 A Review of Literature in Compliant MEMS

Although many MEMS researchers have used deflections to gain motion, some have specifically studied the use of deflection in MEMS. Ananthasuresh et al. (1993 and 1994) applied topological synthesis to the design of compliant MEMS. Some related work was performed by Sigmund (1996). Ananthasuresh and Kota (1996) described the principal benefits and challenges associated with compliant MEMS. Some important issues dealing with the scaling of compliant MEMS were discussed by Derderian (1996), and Opdahl (1996) specifically addressed compliant bistable MEMS. His work will be discussed in more detail later. Salmon et al. (1996) designed compliant MEMS using the pseudo-rigid-body model. Their work was expanded upon by Jensen et al. (1997). Nielson (1998) demonstrated the behavior of micro-compliant pantograph mechanisms. The fabri-

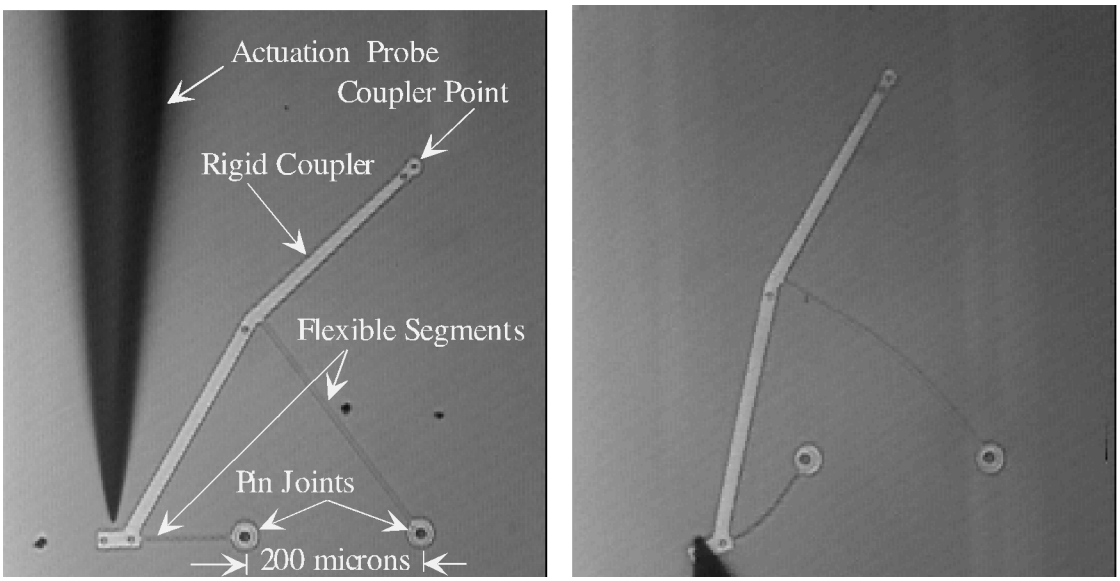

(a) (b)

FIGURE 2-16: Two photographs of a compliant straight-line mechanism. (a) shows the undeflected position; (b) shows a deflected position.

cation of novel compliant micro-mechanisms with a negative Poisson's ratio was studied by Larsen et al. (1997). The next section shows an example of a compliant mechanism fabricated using surface micromachining.

2.2.3 A Compliant MEMS Example

Figure 2-16(a) shows a microscope picture of a compliant straight-line mechanism. When the handle to this mechanism is pushed in either direction, the point on its tip moves in a straight line. This mechanism is made using a two-layer surface micromachining process. The second layer allows creation of the two grounded pin joints. The rest of the mechanism's motion comes from deflection of the two thin, flexible segments. The entire mechanism is only 400 microns tall, with 200 microns between the two pin joints. Figure 2-16(b) shows the mechanism in motion. Note the large, non-linear deflections in

the flexible segments. This mechanism traces a line over 200 μm long that is straight to within ± 3 μm. The motion of this mechanism is more complex and precise than would be possible without compliance.

2.2.4 Bistable MEMS

As mentioned earlier, bistable MEMS could perform switching or positioning operations without the need of a continual energy input. This advantage of bistable mechanisms should allow a large savings in energy for many MEMS applications. Bistable MEMS would also make applications possible which are not feasible otherwise. For example, a bistable mechanism could act as a non-volatile memory cell, allowing memory storage without the need of continual energy input. Some researchers have recognized these possible advantages, and several examples of simple bistable MEMS have been built and tested.

The first bistable micro-device was reported by Hälg (1990). In this device, a flexible beam curved out of the plane above the substrate. By pulling on it with electrostatic forces, it was forced into a second stable position curving down toward the substrate, as shown in Figure 2-17. Several such beams of varying lengths and thicknesses were fabricated and tested. Many of them remained stable in the down position even after removal of any power to the system. Not all of the devices worked so well, though. No attempt was made to define the stability of the device using stability theory, and no explanation of the forces or stresses necessary to keep the beam buckled was presented. The device was also reported to switch in only one direction, without being able to switch back into the original stable state.

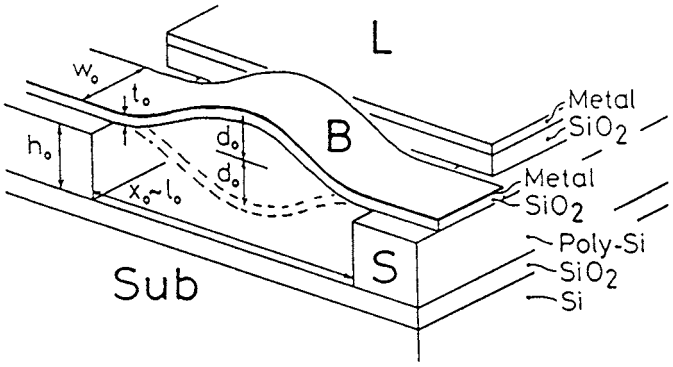

FIGURE 2-17: An early bistable micro-device (Hälg, 1990).

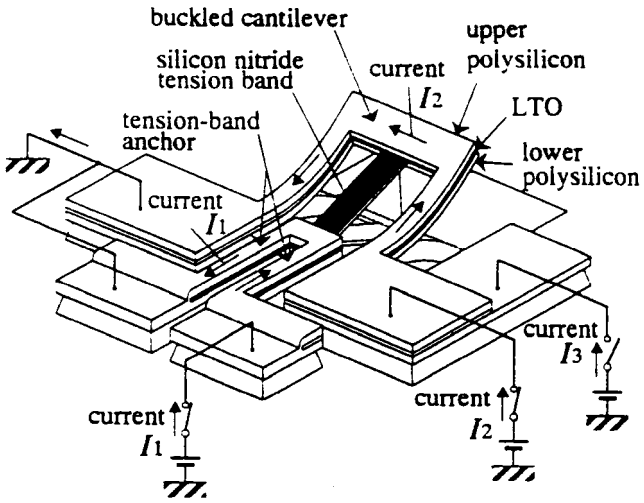

FIGURE 2-18: A bistable micro-device operating on thermal expansion to induce movement (Matoba et al., 1994).

A similar device, which was thermally rather than electrostatically operated, was reported by Matoba et al. (1994). This device is illustrated in Figure 2-18. The device relies on residual tensile stress in the silicon nitride tension band to buckle the upper and lower polysilicon cantilevers. This causes the U-shaped cantilever to buckle either up away from the substrate or down toward the substrate. Applying current to the upper or lower

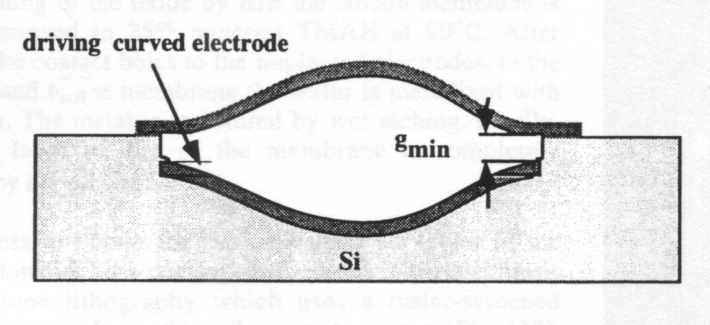

FIGURE 2-19: A bistable membrane. The buckled membrane is pulled down toward the driving curved electrode by electrostatic forces, causing it to buckle into its second stable state. It may be returned to its first state by inducing pressure under the membrane (Wagner et al., 1996).

polysilicon layers caused the layer to expand thermally, forcing the mechanism into its other stable position. A detailed analysis of the forces necessary for bistable behavior is also presented, as well as a discussion of the buckling behavior of the beams. The device is fabricated using a combination of surface and bulk micromachining.

A bistable micro-valve working, like Hälg's device, on electrostatic forces, was developed by Wagner et al. (1996). The valve consisted of two buckled membranes such as the one shown in Figure 2-19. The space under the membranes is joined by a small channel, so that the actuation of one membrane into its second stable position causes an increase in pressure under the other membrane, forcing it into its first stable position. A discussion of the size of membrane and forces necessary for bistable snapping is also presented. One such membrane arrangement was fabricated and tested, showing that the membranes did snap into two positions. The authors intended to use these membranes in a bistable valve.

These devices are all very useful, but they have one limitation. They all require some special processing to produce the necessary residual stresses to create the curved

beams. A bistable device made using ordinary surface micromachining would be cheaper and have wider application. Opdahl (1996) reported a number of attempts to make such a mechanism. His devices were all produced using the Multi-User MEMS Process at MCNC (Mehregeny and Dewa, 1993), a surface micromachining process. Although some of his mechanisms did snap once into the second stable position, none was able to snap a second time without breaking. This illustrates the largest problem facing the design of bistable MEMS: because of the large deflections usually involved, they tend to require high stresses which cause failure before the mechanism can achieve its second stable position. This is one of the issues which this research addresses.

2.3 Mechanism Type Synthesis

Type synthesis may be defined as "the process of determining possible mechanism structures to perform a given task or combination of tasks without regard to the dimensions of the components" (Olson et al., 1985). Type synthesis is performed to select a mechanism type before carrying out dimensional synthesis, which is the process of choosing mechanism dimensions to create a finished mechanism design (Hartenberg and Denavit, 1964; Erdman and Sandor, 1997). Extensive work in the area of rigid-body mechanism type synthesis has produced a large body of knowledge about many different ways to design mechanisms. Some work has also been done in compliant mechanism type synthesis. This section outlines the most important methods of rigid-body and compliant mechanism type synthesis. No attempt will be made to describe these methods in detail; instead, an overview of their use will be presented.

2.3.1 Rigid-Body Type Synthesis

Most often, type synthesis begins with an enumeration of all possible topologies which can perform the desired function (Olson et al., 1985). This list is often very large, with many topologies represented. In this step, graph theory plays an important part (Olson et al., 1985; Murphy et al., 1996). Graph theory allows the expression of any combination of mechanism links and joints in a simple, easy-to-use graphical format. Methods of representing these graphs mathematically have also been developed, allowing computer programs to generate a large list of possible mechanism topologies and compare the topologies to find any duplicates in mechanism types. Once a complete list is developed, each topology is studied using a variety of different algorithms to find topologies which are infeasible. Finally, a selection is made from the resulting list of a mechanism type which will be used to solve the synthesis problem.

2.3.2 Compliant Mechanism Type Synthesis

Compliant mechanism type synthesis follows roughly the same outline as rigid-body synthesis. However, compliance adds a great deal of complexity to the problem. This is because of the difficulty of describing the wide variety of possible compliant segments which may be used as joints. Thus, the type synthesis problem involves not only finding the proper number of rigid links, but it also involves finding which compliant joints would be best in a particular application (Her and Midha, 1987; Murphy et al., 1996). The problem becomes especially perplexing when any type of compliant segment is allowed, rather than limiting the search to well-known and well-understood segments, like the ones presented in the pseudo-rigid-body model. When the types of compliant segments are

limited, the synthesis problem is much more manageable (Murphy et al., 1994a; Murphy et al., 1994b).

In this work, no attempt is made to describe every possible kinematic linkage which could solve a particular problem. While such completeness has the advantage of covering every possible solution, it often becomes difficult to use because of the large number of possible solutions which must be considered. Additionally, bistable mechanisms require the use of compliant segments in such a way that the mechanism has two stable states. Conventional type synthesis techniques make no attempt to describe the energy states of the mechanism being designed. No method currently exists which allows the description of the general stability of mechanism topologies.

Therefore, the approach in this thesis will be to find a number of possible mechanism types which may be made bistable. The placement of compliant segments in each mechanism type will be studied to discover the appropriate mechanism configurations which result in a bistable mechanism. The type synthesis technique consists of finding a number of possible mechanism configurations, including kinematic inversions of each type, which can solve the particular problem. The mechanism configuration which will most easily solve the problem can then be chosen. In this way, the selection of a new bistable mechanism design becomes much easier.

CHAPTER 3 *A Review of Mechanism Stability*

Before identifying the mechanism configurations which result in bistable behavior, a review of the stability of mechanisms must be presented. This chapter explains some of the issues dealing with mechanism stability. In the process, a more complete definition of a bistable mechanism will be given. Examples of the analysis of bistable mechanisms are also demonstrated.

3.1 The Basic Principles of Bistable Mechanisms

This section defines stability and gives an example of the analysis of a rigid-body bistable mechanism. A review of literature in bistable mechanisms is also presented.

3.1.1 A Definition of Stability

No absolute definition of stability exists (Leipholz, 1970). Even ancient Greek researchers expressed two different definitions for stability. Aristotle defined stability based on the motion of a perturbed system, but Archimedes based his definition on the geometric state of the system after perturbation (Leipholz, 1970). Since that time, various

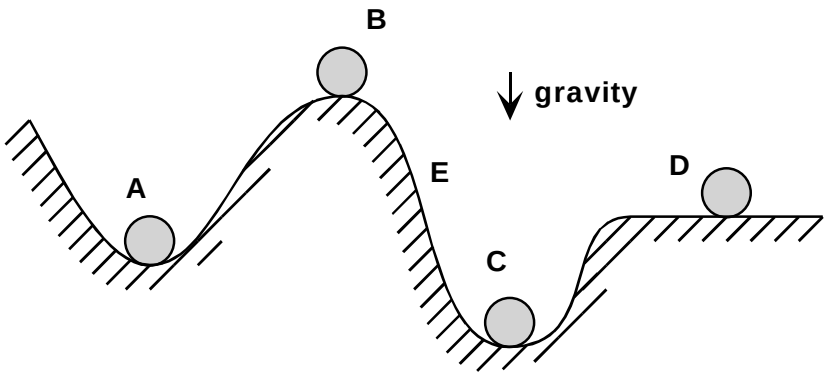

FIGURE 3-1: An illustration of the "ball-on-the-hill" analogy. Positions A and C are stable equilibrium positions. Position B is an unstable equilibrium position. Position D is neutrally stable. Position E is not an equilibrium position, and is not stable.

other definitions have also been proposed. However, no unifying theory has been presented. Instead, stability is often defined differently for each application. The definition presented here comes from the theory of elastic stability of structures (Timoshenko and Young, 1951; Timoshenko, 1961; Simitses, 1976; Ginsberg and Genin, 1984).

When a system has no acceleration, it may be said to be in a state of equilibrium. In a state of equilibrium, whether loaded or unloaded, "if . . . 'small' external disturbances are applied and the structure reacts by simply performing oscillations about the . . . equilibrium state, the equilibrium is said to be *stable"* (Simitses, 1976). However, if the small external disturbances cause the system to diverge from its equilibrium state, then the equilibrium position is *unstable*. If, on the other hand, the system reacts to the disturbances and stays in the disturbed position, then the equilibrium position is *neutral*. For each of these definitions, the external disturbances may be as small as desired (Simitses, 1976).

The stability of a system may be illustrated using the well-known "ball-on-the-hill" analogy. This analogy is illustrated in Figure 3-1. The ball is shown in a position A, which is a stable equilibrium position. If it is shifted from this position by a small amount, it will

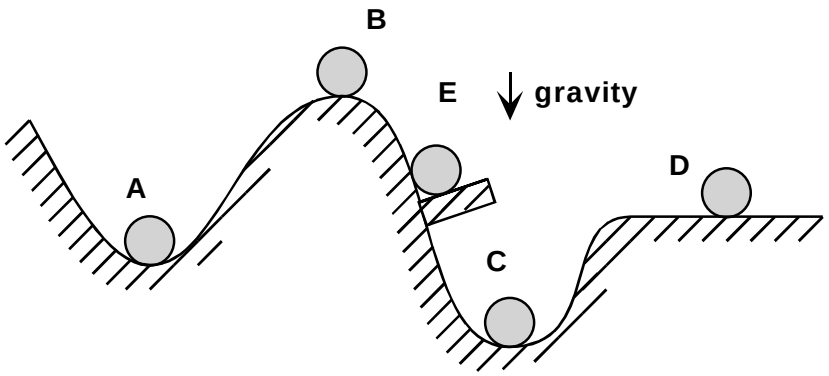

FIGURE 3-2: In this figure, a stop at position E has created a "new" stable equilibrium position. This stop could also be represented by a precisely placed force of the right magnitude.

tend to return to position A or oscillate around it. However, position B is an unstable equilibrium position. Although the ball will stay in position if placed precisely on top of the hill, it will move to a different position if any disturbance occurs. Position C is stable, while position D is neutrally stable, because any disturbance will cause the ball to move to its disturbed position only.

Because this system has two stable equilibrium positions, it is bistable. Because two local minima will always enclose a local maximum, any two stable equilibrium positions will always have an unstable position between them. Therefore, a bistable mechanism will have two stable equilibrium positions and at least one unstable equilibrium position. If the mechanism has a link which can revolve completely (a Grashof mechanism), then, because of the continuity of the rotation, it will have two stable positions and two unstable equilibrium positions. This may be illustrated by the example found in section 3.1.2 "A Bistable Mechanism Example."

Note that position E is not an equilibrium position in this configuration. However, in Figure 3-2, a stop has been placed at E to illustrate the creation of a new equilibrium

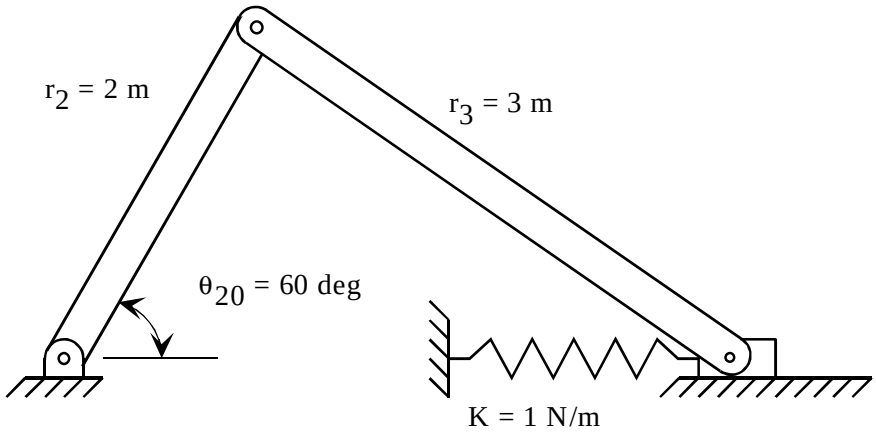

FIGURE 3-3: A bistable slider-crank. Notice that this mechanism is an inversion of the one shown in Figure 2-12.

position by the application of an external load. The stop could also be represented by a force of the proper magnitude and direction. This "new" equilibrium position is also stable.

3.1.2 A Bistable Mechanism Example

Several methods have been developed to determine the stability of a system. Ziegler (1956) described four different, related methods for determining structural stability. In this work, the energy method will be used. This method is based on the Lagrange-Dirichlet theorem, which states that "when the potential energy *U* has a minimum for an equilibrium position, the equilibrium position is stable" (Leipholz, 1970). It is used by Timoshenko and Young (1948) to establish structural stability. The method will be illustrated with an example.

Consider the bistable slider-crank in Figure 3-3. This mechanism is an inversion of the model for the shampoo cap shown in Figure 2-12. It stores energy in the spring as it moves. Because the mechanism has one degree of freedom, its motion may be determined

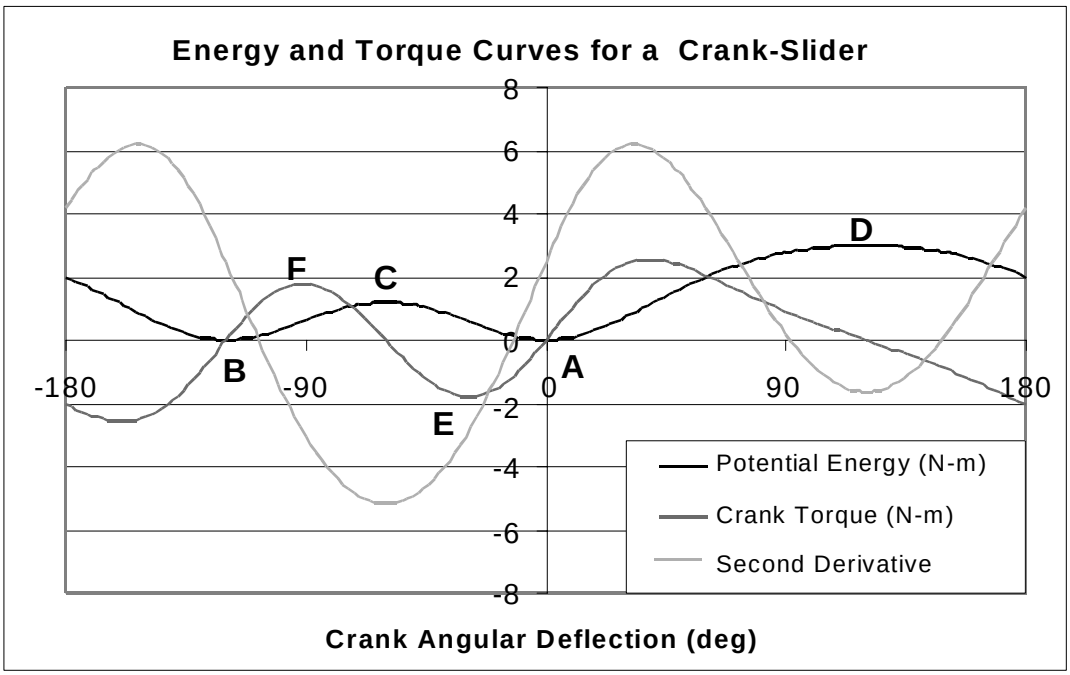

FIGURE 3-4: The energy, crank torque, and second derivative of energy as a function of crank deflection for the mechanism shown in Figure 3-3.

from the change of any variable in the mechanism, such as θ_2, θ_3, or r_1. That is, any of these variables may be the independent variable. Then, the energy stored in the spring may be calculated and plotted as a function of the independent variable. Because the energy stored in the spring is typically much more significant than any energy storage due to gravity in the mechanism, only the energy stored in the spring is considered. The energy curve in Figure 3-4 shows the spring's potential energy as a function of the deflection of the crank. Notice that the potential energy has a "well" at zero deflection (position A) and at about -120 degrees deflection (position B). These wells correspond to locations of stable equilibrium positions, as stated in the Lagrange-Dirichlet theorem. In this way, the potential energy curve is similar to the hill topography in the ball-on-the-hill analogy. The

potential energy curve also has two relative maxima; at these locations (positions C and D), the mechanism is in unstable equilibrium.

Also shown in Figure 3-4 is the curve showing the crank torque required to keep the mechanism at the specified crank angle. Notice that it is zero at all equilibrium positions on the energy curve. In fact, the torque curve is the first derivative of the energy curve with respect to the crank angle. This may be proved by considering the equation for work put into the system:

$$W = \int_{\theta_0}^{\theta} T d\theta_2 \tag{3.1}$$

by taking the derivative of this equation, it may be seen that

$$\frac{dW}{d\theta_2} = T \tag{3.2}$$

Therefore, the applied torque is equal to the first derivative of the energy with respect to crank angle.

For this reason, zeroes of the torque curve are relative maxima or minima of the energy curve. The second derivative of energy with respect to crank angle may be used to mathematically predict whether the zeroes of the torque curve are maxima or minima of the energy curve. If the second derivative is positive at the zero, it is a location of relative minimum, and is a stable equilibrium position. If the second derivative is negative, then the position is an unstable equilibrium position.

As the mechanism moves from one stable position to another, the absolute value of the torque increases until a relative maximum or minimum is reached (positions E or F). As the mechanism continues its motion, the torque required to keep it in position decreases

until the unstable equilibrium position is reached (position C). At this point, the torque changes sign. This means that the torque required to keep the mechanism at a particular deflection must be applied in the opposite direction. Unless some external body (such as a stop) applies this torque, the mechanism will "snap" into the second stable position. This snapping behavior is a characteristic of most bistable mechanisms.

Other important parameters may be found on the graph in Figure 3-4. Positions E and F represent extreme values of the crank torque. As the mechanism moves from one stable position to another, the absolute value of the torque extreme is the maximum torque that must be applied to move the mechanism from one stable position to the other. This maximum torque may be called the "critical torque" (Opdahl, 1996). If a force is used instead of a torque, the maximum force is termed the critical force. In addition, a high value of the second derivative at a stable position means that the energy curve is changing very rapidly at that point; this corresponds to steep walls on the energy curve well. Hence, the second derivative of the energy curve at a stable equilibrium position is called the stiffness of that stable position. A high stiffness means that the restoring force returning the mechanism to that position is relatively high. Depending on the application, this may or may not be a desirable attribute.

Based on the graph in Figure 3-4, the state of the mechanism in its second stable position may be determined. The second stable position is shown using dashed lines in Figure 3-5. This figure makes it obvious that the spring is undeflected in both positions. This corresponds to zero potential energy at positions A and B in Figure 3-4.

At the stable positions, no force or torque is required to keep the mechanism in position. Conversely, the mechanism cannot exert a force on any external body such as

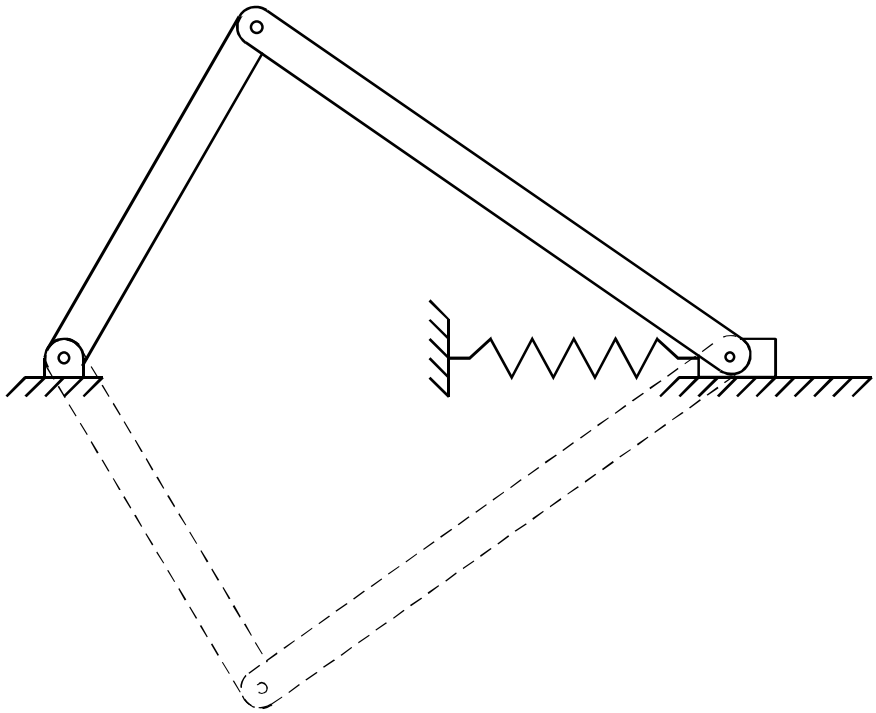

FIGURE 3-5: The two stable positions of the mechanism shown in Figure 3-3. Notice that the spring is undeflected in each position; this is why the mechanism is stable.

electrical contacts for a switch. To allow such a reaction force, the mechanism may be stopped at an intermediate position as shown in Figure 3-6. This is analogous to the stop at position E shown in Figure 3-2. At this position, the stop provides a reaction force on the crank creating a torque equal to the value predicted by the torque curve of Figure 3-4. In this way, a new stable position has been created in which the mechanism is exerting a force on the external body.

3.1.3 A Review of Past Work in Bistable Mechanisms

The basic principles of stability have been developed by several researchers. Some early work was done by Lagrange (1788) and Liapunov (1897). Timoshenko (1961) outlined how these principles could be applied to structures and mechanisms to predict

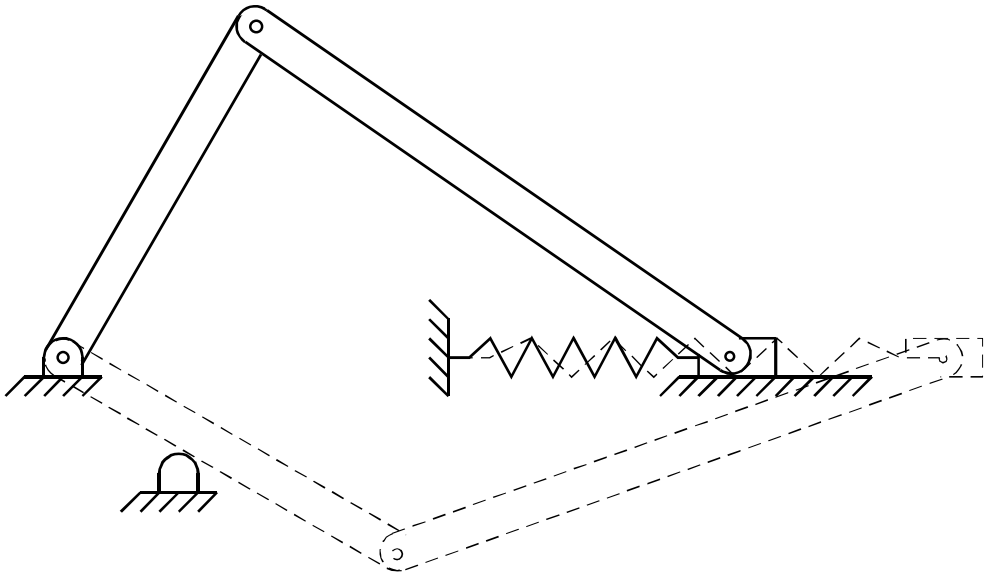

FIGURE 3-6: The mechanism is in a stopped position. This is analogous to the ball on the hill in Figure 3-2.

stability. His work focused mostly on the buckling of beams and other solid structures. This work was applied directly to mechanisms by Ginsberg and Genin (1984), and several examples of mechanism stability were presented.

Some work has also been done in the design of bistable mechanisms. Schulze (1955) derived equations for the design of snap-action toggles. His equations maximized the force required to switch the device for a given area the mechanism occupies. Artobolevsky (1975), Jensen (1991), and Chironis (1991) also presented several examples of bistable mechanisms. In addition, Howell et al. (1994b) demonstrated a method for the reliability-based design of compliant mechanisms. The example used for design was a bistable slider-crank mechanism. This paper presented some of the advantages of using compliant bistable mechanisms. The application of compliance to bistable mechanisms was expounded upon by Opdahl (1996). He identified the important elements of bistable mechanisms, classified bistable mechanisms into basic categories, and showed how the

pseudo-rigid-body model could be applied to bistable mechanism to allow the prediction of equilibrium positions, stability, and critical force or torque. He also described the fabrication and testing of some bistable MEMS.

3.2 Compliant Bistable Mechanisms

Because compliant mechanisms inherently store energy in their flexible joints, they are particularly useful as bistable mechanisms. Not only can the mechanism often be made of one piece, but no extra springs are required to allow energy storage. The analysis of such mechanisms is simplified by the use of the pseudo-rigid-body model (Opdahl, 1996; Opdahl et al., 1998). To illustrate, this section contains an example of a bistable compliant mechanism analyzed using Opdahl's method.

3.2.1 A Compliant Bistable Mechanism Example

In the mechanism shown in Figure 3-7, the compliant segment rocks back and forth as the crank turns. Because the compliant link is undeflected for two crank positions, this mechanism is bistable. Its pseudo-rigid-body model is shown in Figure 3-8. Note that the pseudo-rigid-body mechanism satisfies Grashof's criteria as a crank-rocker. Using the mechanism shown in Figure 3-8, the potential energy and crank torque curves may be calculated. These are shown in Figure 3-9.

If $\Delta\theta_2$ is defined as $\theta_2 - \theta_{20}$, these curves shown that the mechanism will be stable when $\Delta\theta_2 = -79°$, corresponding to position B in Figure 3-9. The mechanism is shown in this position in Figure 3-10. The mechanism also has an unstable position at $\Delta\theta_2 = -45°$, corresponding to position C. When moving from position A to position B, the critical

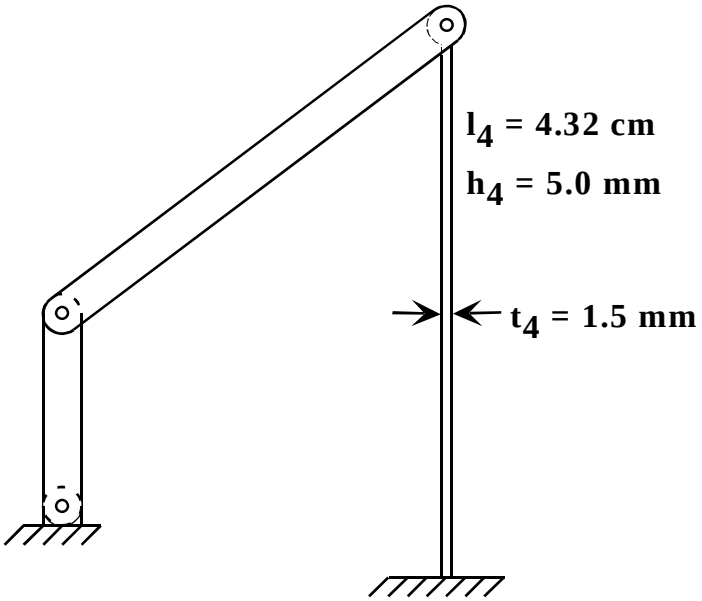

FIGURE 3-7: A partially-compliant bistable mechanism. When the short link on the left is turned, this mechanism acts as a crank-rocker.

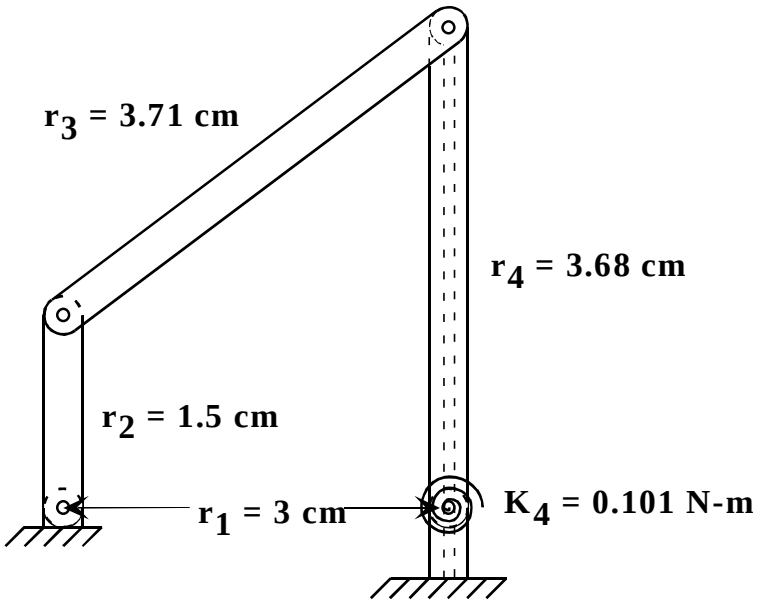

FIGURE 3-8: The pseudo-rigid-body model of the mechanism shown in Figure 3-7. The length of the pseudo-rigid joint and the value of the spring constant on the torsional spring are found using the pseudo-rigid-body model.

torque is about 0.004 N-m, as shown at D in Figure 3-9. When moving from position B to position A, the critical torque is about 0.0065 N-m, as shown at E.

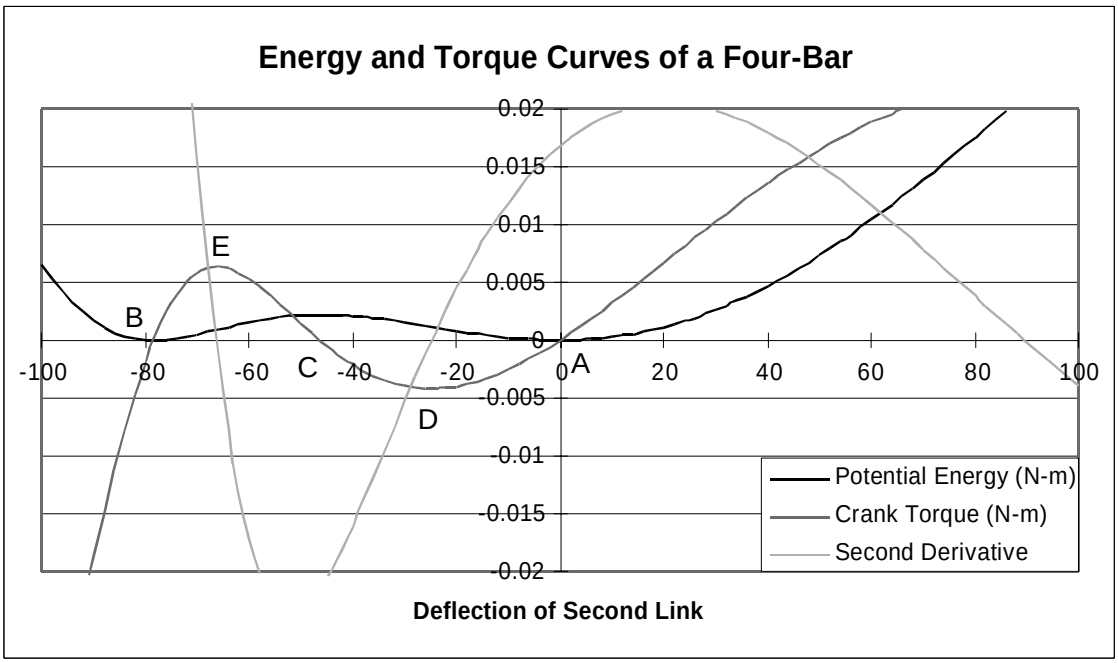

FIGURE 3-9: The energy and crank torque curves for the mechanism shown in Figure 3-7. The second derivative of energy is also shown for illustration.

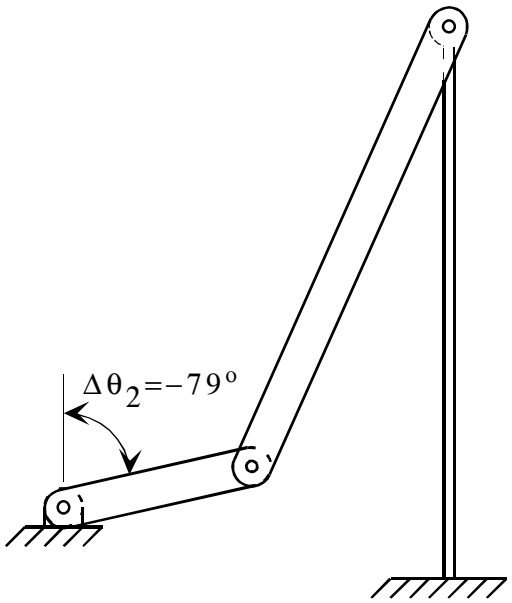

FIGURE 3-10: The mechanism shown in Figure 3-7 in its second stable position.

This mechanism, like the crank-slider in Figure 3-3, has two unstable equilibrium positions and two stable equilibrium positions. However, the energy stored in the unstable

position at $\Delta\theta_2 = -45°$ is much lower than the energy stored at the other unstable position. This is because the compliant segment has a much smaller deflection at this unstable equilibrium condition. For this reason, the mechanism would most likely be actuated by turning the crank clockwise into the second stable position shown in Figure 3-10.

CHAPTER 4 *The Classification and Analysis of Bistable Mechanisms*

As discussed in Chapter 1, the purpose of this research is to investigate the configurations of compliant mechanisms which result in bistable behavior. This knowledge will allow the development of a method of bistable mechanism synthesis which allows easy formulation of new bistable mechanism designs. This chapter performs the analysis of compliant mechanisms necessary to determine the configurations which result in bistable behavior. The information presented here permits the designer to choose the general compliant bistable mechanism class for a desired application, as well as specifying the placement of compliant segments necessary to give the mechanism two stable states. By having a good knowledge of which mechanism classes can be bistable and where compliant segments may be placed in the mechanism to make it bistable, the formulation of completely new bistable designs is greatly facilitated. This chapter sets forward classes of bistable mechanisms, and it discusses the placement of compliant segments, represented by linear or torsional springs, which will cause each mechanism class to have two stable states. The succeeding chapter provides examples of the use of this theory in finding the solution to bistable mechanism design problems.

4.1 The Stability of Compliant Mechanisms

Before bistable mechanisms can be synthesized, the relationship between their motion and energy must be well-understood. The potential energy equation allows this to be done. The potential energy equation relates the energy stored in a mechanism to the mechanism's deflection. If the mechanism has one degree of freedom, as all of the mechanisms discussed here do, then the mechanism's motion can be completely determined from one deflection variable, often called the generalized coordinate (see, for example, Howell and Midha, 1994b).

Using the pseudo-rigid-body model, the potential energy equation of a compliant mechanism can easily be found. For a small-length flexural pivot or a fixed-pinned segment, the potential energy V stored in the segment is

$$V = \frac{1}{2}K\Theta^2 \tag{4.1}$$

where K is the torsional spring constant, found using the pseudo-rigid-body model, and Θ is the pseudo-rigid-body angle, or the angle of deflection of the compliant segment. Using the linear spring model and approximating the spring function using Hooke's law, the potential energy stored in a FBPP segment is

$$V = \frac{1}{2}K_s(\Delta x)^2 \tag{4.2}$$

where Δx is the change in distance between the segment's two pin joints, and K_s is the linear spring constant. Because each compliant segment's energy storage depends only on the deflection of the segment, the total potential energy in the mechanism is simply the sum of the potential energy stored in each compliant segment (Howell and Midha, 1994b).

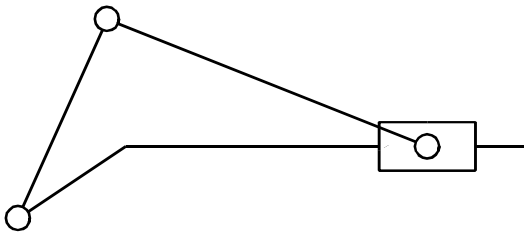

FIGURE 4-1: A basic kinematic chain of a slider-crank mechanism.

4.2 Basic Kinematic Chains and Mechanism Inversions

A rigid-body mechanism is composed of rigid links and joints which allow relative motion between the links. If none of the links is fixed to ground, the assemblage of links and joints is called a basic kinematic chain (Hartenberg and Denavit, 1964; Soni, 1974). The basic kinematic chain maintains all of the relative motion of the links, and it represents the most general form the particular configuration of links and joints can take. Figure 4-1 shows the basic kinematic chain for a slider-crank mechanism. If one of the links is then fixed, the basic kinematic chain becomes a mechanism. However, all of the relative link motions remain the same. Thus, any link can be fixed for the purpose of analysis or design without changing the displacement or energy equations of the mechanism. Different "inversions" of mechanisms are formed from the same kinematic chain by fixing different links. In the succeeding analysis, one link is always fixed to allow the mechanism to be easily described mathematically. Nevertheless, the results may be equally applied to any inversion of the mechanism.

4.3 The Method of Compliant Bistable Mechanism Analysis

In a bistable mechanism synthesis problem, a designer typically must design a mechanism to be stable at particular locations. The unstable equilibrium position and the maximum force or moment required to move the mechanism from one stable position to another may also be specified. The first step in the synthesis process is to determine the best mechanism configuration to accomplish the desired task, or, in other words, to perform type synthesis. The problem is compounded by the fact that a mechanism configuration must be chosen which will be able to meet both the motion and the stability requirements; that is, the mechanism must be stable in the desired positions as well as having the desired motion. To solve this problem, something must be known about different classes of bistable mechanisms, as well as the placement of compliant segments within each class which is necessary to have a bistable mechanism. Therefore, the remainder of this chapter will present a classification scheme for bistable mechanisms, followed by an analysis of each class to find the placement of compliant joints which is necessary to have a bistable mechanism.

4.4 The Classification of Bistable Mechanisms

This section details the classification scheme which will be used for the design and analysis of bistable mechanisms. A review of a previously-suggested scheme is given, followed by the presentation of an expanded list of bistable mechanism classes which will allow bistable mechanisms to be more easily designed and analyzed.

4.4.1 Previous Work in Bistable Mechanism Classification

Opdahl (1996) presented a classification system which allows characterization of most bistable mechanism configurations. His system consisted of four classes:

1. Snap-through buckling devices
2. Slider-crank mechanisms
3. Four-bar mechanisms
4. “Cam” type systems

Opdahl presented systems of equations for finding the important parameters of bistable mechanisms of classes two and three. These equations can be coded in a computer program, allowing a large number of bistable mechanisms to be easily classified and analyzed.

This system of classification has shown itself to be very useful in the analysis of bistable mechanisms. Therefore, it has been used as the basis for the formulation of an expanded list of bistable mechanism classes. This list is presented in the following section.

4.4.2 Bistable Mechanism Classification Scheme

The pseudo-rigid-body model allows compliant mechanisms to be analyzed as rigid-body mechanisms; therefore, the classification of compliant bistable mechanisms is most easily done using rigid-body mechanism classes. The classification scheme will then apply equally to rigid-body bistable mechanisms or to compliant bistable mechanisms. Accordingly, the following classes of one degree-of-freedom bistable mechanisms are proposed:

1. Snap-through buckled beams (note that this class must be flexible, not rigid)
2. Bistable cam mechanisms

3. Double-slider mechanisms with a pin joining the sliders
4. Double-slider mechanisms with a link joining the sliders
5. Slider-crank or slider-rocker mechanisms
6. Four-link mechanisms

These classes are not meant to be inclusive; rather, they represent a number of common classes from which to choose. Each class will be examined in more detail in the following section.

4.5 Analysis of each Mechanism Class

In this section, each mechanism class is analyzed to determine the appropriate placement of springs necessary to gain bistable behavior. In all cases, sliders and linear springs are assumed to have unlimited travel along their line of motion. In addition, all springs are assumed to have linear force-deflection characteristics. For the mechanisms discussed here, all springs are assumed to be undeflected at the same mechanism position; thus, this position corresponds to a stable position, often called the first stable position.

4.5.1 Snap-Through Buckled Beams

This class is one of the easiest classes to use; however, its motion is very limited. A snap-through buckled beam is simply a buckled beam, like the one illustrated in Figure 4-2(a), which can snap into a second stable position, as shown in Figure 4-2(b). The analysis of such beams is based on classical structural mechanics, as explained by Timoshenko and Young (1951) and others (such as Simitses, 1976). Several examples of this type of device

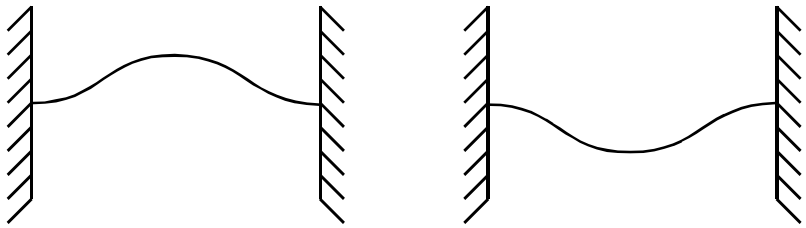

FIGURE 4-2: A snap-through buckled beam in its two stable positions. While this example shows a fixed-fixed beam, it may also be either pinned at either end or free at one end.

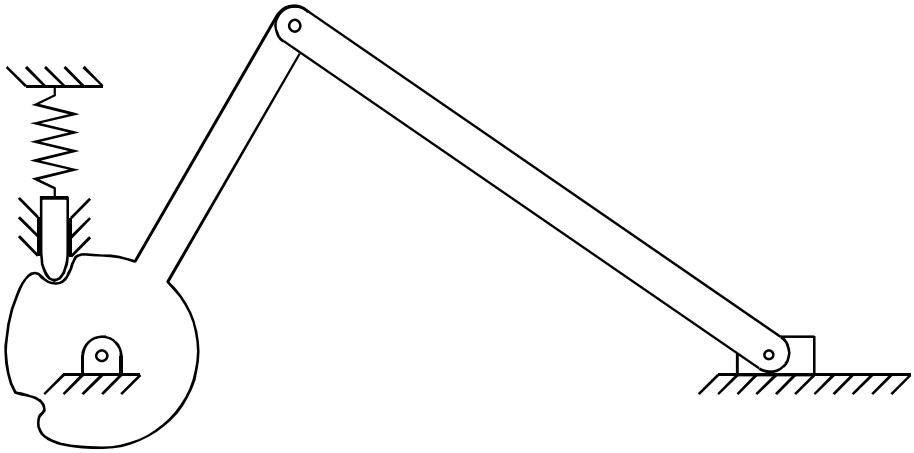

FIGURE 4-3: A bistable cam mechanism.

have been presented (Hälg, 1990; Matoba et al., 1994; Wagner et al., 1996). This is the only class listed above which can not be realized using rigid-body mechanisms.

4.5.2 Bistable Cam Mechanisms

If a spring-loaded follower goes through two local minima of potential energy as it travels around the cam, then a bistable mechanism results, as illustrated in Figure 4-3. The actual mechanism may be of any class, either rigid or compliant. If the mechanism is compliant, care should be taken so that the energy stored in the compliant segments is not greater than the energy stored in the spring-loaded follower. The principles of cam design are well-

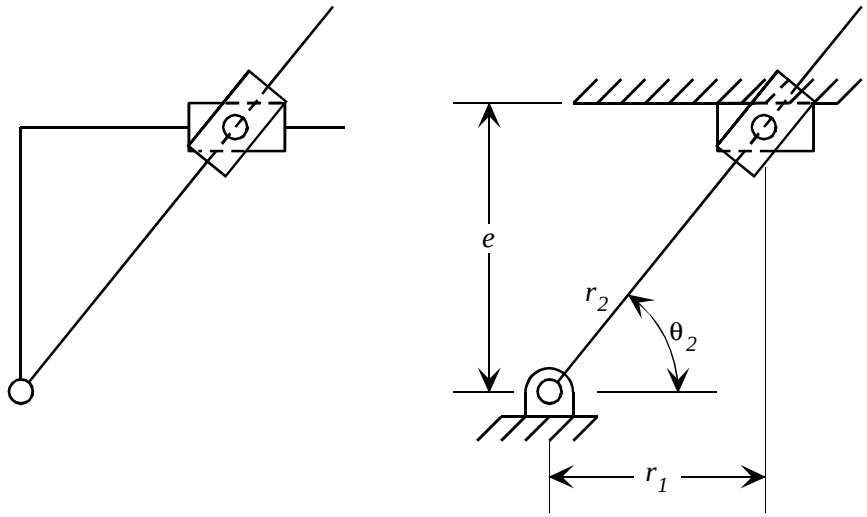

(a) (b)

FIGURE 4-4: The basic kinematic chain of a double-slider mechanism. By fixing one link, the mechanism in (b) results. In this mechanism class, the two sliders are joined by a pin joint.

documented, and bistable cams allow the stable positions to be easily placed anywhere in the mechanism's motion. Multiple stable positions may even be created using this method. However, cam designs do not take advantage of the beneficial aspects of compliant mechanisms, especially the integration of the mechanism's motion and energy storage into one member.

4.5.3 Double-Slider Mechanisms with a Pin Joining the Sliders

This class consists of mechanisms with four joints, two of which are prismatic joints. The two sliders are joined by a pin joint, as shown by the basic kinematic chain in Figure 4-4(a). When one link is fixed, the mechanism shown in Figure 4-4(b) is formed. This mechanism's motion may be easily analyzed. Using θ_2 as the generalized coordinate,

$$r_2 = \frac{e}{\sin\theta_2} \tag{4.3}$$

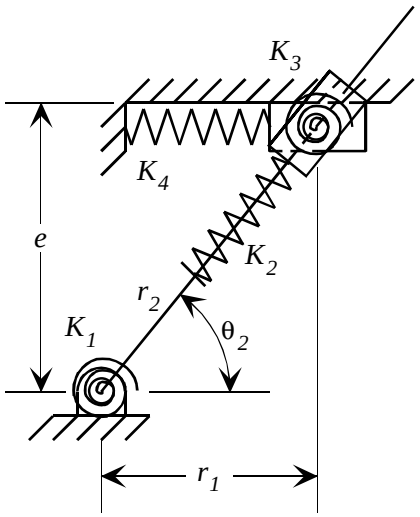

FIGURE 4-5: A model of a fully compliant double-slider mechanism. Each compliant segment is modeled by a joint with a spring attached to it.

and

$$r_1 = \frac{e}{\tan\theta_2} \tag{4.4}$$

where r_2 is the distance from the fixed pin joint to the pin joint joining the sliders, r_1 is the horizontal distance between the pin joints, and e and θ_2 are defined in Figure 4-4. If a compliant segment is added in place of each joint, the mechanism may be modeled as shown in Figure 4-5, where a spring has been placed at each joint.

4.5.3.1 Analysis of the Energy Equation- The energy equation is found by adding the energy storage terms for each spring:

$$V = \frac{1}{2}(K_1\psi_1^2 + K_2\psi_2^2 + K_3\psi_3^2 + K_4\psi_4^2) \tag{4.5}$$

where the K's are the spring constants as noted in the figure, and the ψ's are the deflections of each spring, given by

$$\begin{aligned} \psi_1 &= \theta_2 - \theta_{20} \\ \psi_2 &= r_2 - r_{20} \\ \psi_3 &= \theta_2 - \theta_{20} \\ \psi_4 &= r_1 - r_{10} \end{aligned} \tag{4.6}$$

where a "0" subscript indicates the initial, undeflected position. To find the minima of the energy equation, take the derivative and set it equal to zero:

$$\frac{dV}{d\theta_2} = 0 = K_1\psi_1 + K_2\psi_2\frac{d\psi_2}{d\theta_2} + K_3\psi_3 + K_4\psi_4\frac{d\psi_4}{d\theta_2} \tag{4.7}$$

After substituting and rearranging, the equation becomes

$$0 = (K_1 + K_3)(\theta_2 - \theta_{20}) - \frac{e^2}{\sin^2\theta_2}\left[K_2\cos\theta_2\left(\frac{1}{\sin\theta_2} - \frac{1}{\sin\theta_{20}}\right) + K_4\left(\frac{1}{\tan\theta_2} - \frac{1}{\tan\theta_{20}}\right)\right] \tag{4.8}$$

The solutions to this equation represent the positions of minima or maxima in the potential energy equation. For given values of the spring constants, this equation must have three solutions in θ_2 for the mechanism to be bistable: two minima (stable positions) and one maximum (unstable position between the stable positions). In particular, by setting all of the spring constants to zero except for one, it is possible to find the spring locations necessary for bistable behavior. For example, if $K_1 \neq 0$, while $K_2 = K_3 = K_4 = 0$, then

$$0 = K_1(\theta_2 - \theta_{20}) \tag{4.9}$$

which gives only one solution corresponding to the stable, undeflected position. Similarly, if K_3 or K_4 are chosen to be exclusively non-zero, the equation gives just one solution. However, if K_2 is exclusively non-zero, then the equation becomes

$$0 = K_2\cos\theta_2\left(\frac{1}{\sin\theta_2} - \frac{1}{\sin\theta_{20}}\right) \tag{4.10}$$

This equation has three solutions on the range from 0 to π radians:

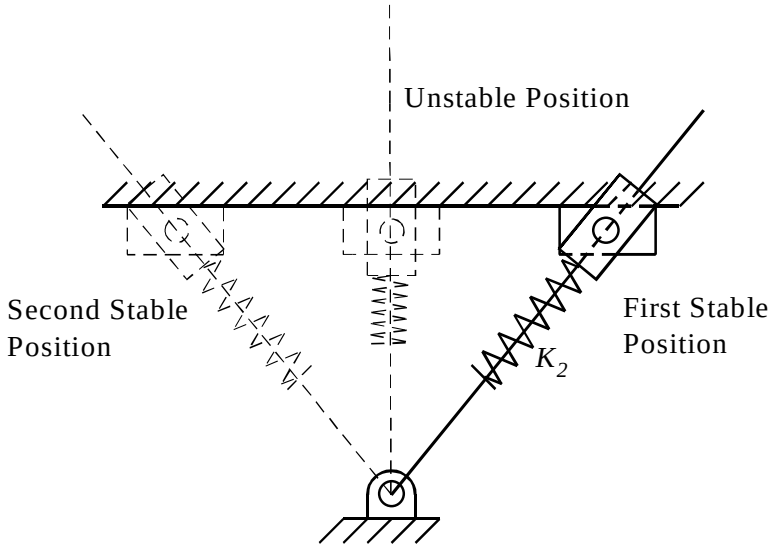

FIGURE 4-6: A bistable double-slider mechanism with a pin joint joining the sliders. The unstable and second stable positions are shown in dashed lines.

$$\theta_2 = \theta_{20}$$
$$\theta_2 = \frac{\pi}{2} \qquad (4.11)$$
$$\theta_2 = \pi - \theta_{20}$$

where

$$\theta_{20} \neq \frac{\pi}{2} \qquad (4.12)$$

The first solution to Eq. (4.11) corresponds to the undeflected stable position, the second solution corresponds to the unstable equilibrium position, and the third solution corresponds to the second stable position.

4.5.3.2 Results of the Analysis- Therefore, for this class of double-slider mechanisms, a spring must be placed between the rotating bar and its slider for the mechanism to be bistable, as illustrated in Figure 4-6. If this is the only spring in the mechanism, bistable behavior is guaranteed; if other springs (K_1, K_3, or K_4) are present, then Eq. (4.8) must be

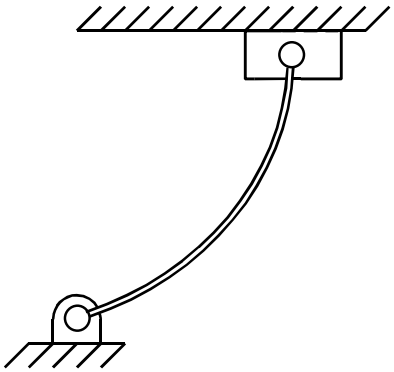

FIGURE 4-7: A compliant mechanism whose pseudo-rigid-body model is a double-slider with the sliders joined by a pin joint.

solved to determine whether the mechanism is bistable. A bistable compliant mechanism may be constructed as illustrated in Figure 4-7, where the spring and slider have been replaced by a FBPP segment. This figure represents only one possible compliant configuration.

4.5.4 Double-Slider Mechanisms with a Link Joining the Sliders

The basic kinematic chain for this type of mechanism is shown in Figure 4-8(a). By fixing the link between the two prismatic joints, the mechanism in Figure 4-8(b) is formed. In this figure, x_2 and x_4 are measured from the undeflected state. Choosing θ_3 as the generalized coordinate, the displacement equations are

$$x_2 = \frac{r_3[\sin(\theta_1 - \theta_{30}) + \sin(\theta_3 - \theta_1)]}{\sin\theta_1} \tag{4.13}$$

$$x_4 = \frac{r_3(\sin\theta_3 - \sin\theta_{30})}{\sin\theta_1} \tag{4.14}$$

If all joints are replaced with compliant segments, the mechanism may be modeled as shown in Figure 4-9.

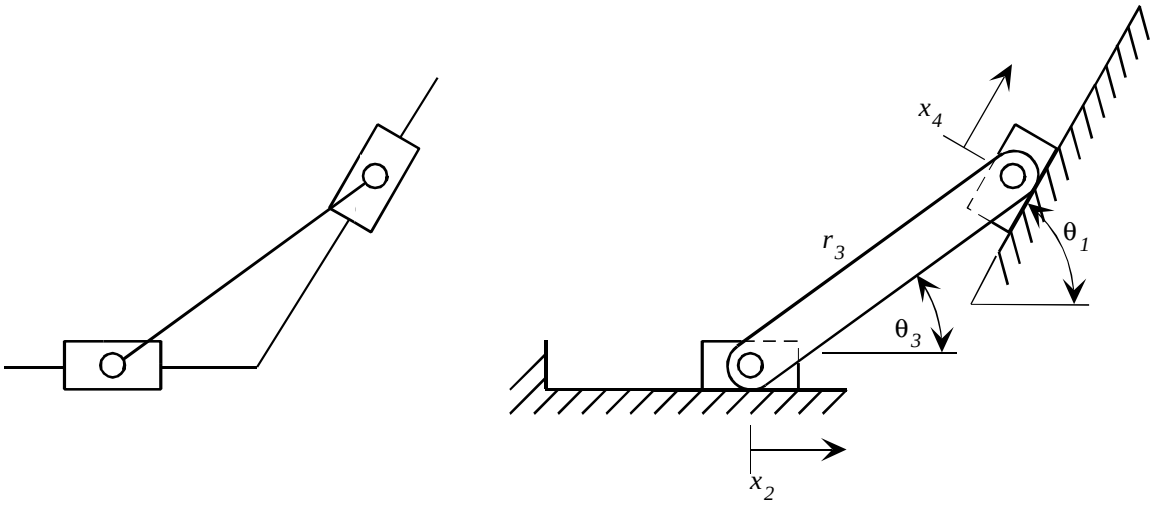

(a) (b)

FIGURE 4-8: A double-slider mechanism with the two sliders joined by a link. The basic kinematic chain is shown in (a), with the mechanism in (b) formed by fixing the link between the slider joints.

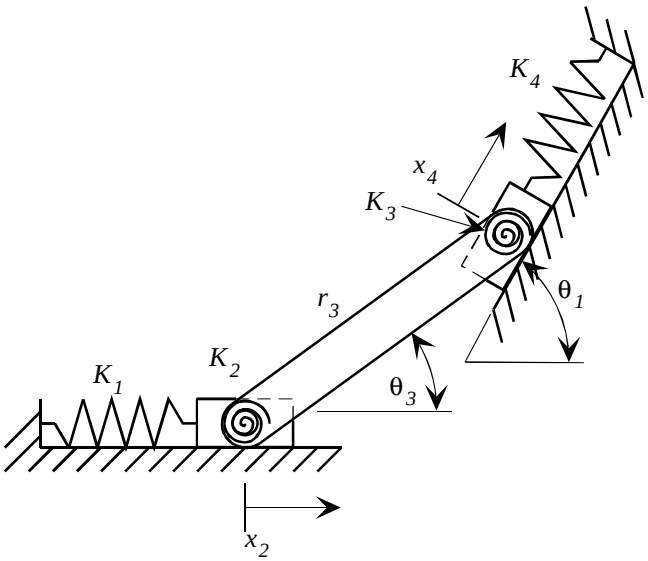

FIGURE 4-9: A model of a compliant double-slider mechanism with the two sliders joined by a link. All compliant segments are modeled as a link attached to a spring.

4.5.4.1 Analysis of the Energy Equation- The energy equation for this mechanism is the same as Eq. (4.5), with

$$\begin{aligned} \psi_1 &= x_2 \\ \psi_2 &= \theta_3 - \theta_{30} \\ \psi_3 &= \theta_3 - \theta_{30} \\ \psi_4 &= x_4 \end{aligned} \tag{4.15}$$

The first derivative is

$$\frac{dV}{d\theta_3} = 0 = K_1 x_2 \frac{dx_2}{d\theta_3} + (K_2 + K_3)(\theta_3 - \theta_{30}) + K_4 x_4 \frac{dx_4}{d\theta_3} \tag{4.16}$$

Using the method of determining the necessary springs outlined above, it is apparent that K_2 and K_3 can not be necessary for the mechanism to be bistable because only one solution results if either of them are exclusively non-zero. However, if K_1 is exclusively non-zero, then

$$0 = K_1 x_2 \frac{dx_2}{d\theta_3} = K_1 \left(\frac{r_3}{\sin\theta_1} \right)^2 [\sin(\theta_1 - \theta_{30}) - \sin(\theta_3 - \theta_1)] \cos(\theta_3 - \theta_1) \tag{4.17}$$

The solutions to this equation are

$$\begin{aligned} \theta_3 &= \theta_{30} \\ \theta_3 &= \theta_1 \pm \frac{\pi}{2} \\ \theta_3 &= 2\theta_1 - \pi - \theta_{30} \end{aligned} \tag{4.18}$$

where

$$\theta_{30} \neq \theta_1 \pm \frac{\pi}{2} \tag{4.19}$$

Once again, the first and third solutions correspond to stable positions. The second solution actually represents two different mechanism positions, each of which corresponds to an unstable position. This is because the link can rotate through a complete revolution. For an unstable position to be between the two stable positions, there must be an unstable

position in each direction of rotation, so that the mechanism has two stable positions and two unstable positions.

If K_4 is exclusively non-zero, then Eq. (4.16) becomes

$$0 = K_4 x_4 \frac{dx_4}{d\theta_3} = K_4 \left(\frac{r_3}{\sin\theta_1} \right)^2 (\sin\theta_3 - \sin\theta_{30}) \cos\theta_3 \tag{4.20}$$

with solutions

$$\begin{aligned} \theta_3 &= \theta_{30} \\ \theta_3 &= \pm\frac{\pi}{2} \\ \theta_3 &= \pi - \theta_{30} \end{aligned} \tag{4.21}$$

where

$$\theta_{30} \neq \pm\frac{\pi}{2} \tag{4.22}$$

These solutions also correspond to stable, unstable, and stable positions, respectively.

4.5.4.2 Results of the Analysis- Therefore, for a double-slider mechanism with a link joining the sliders, the mechanism will be bistable if a spring is placed between either of the sliders and the ground link, as shown in Figure 4-10. In the figure, one of the two possible springs is shown. A mechanism with a spring at the other position would have similar motion, though. This figure also shows one of the unstable positions and the second stable position. An equivalent compliant mechanism is shown in Figure 4-11. As before, if more than one spring is used in the mechanism, then Eq. (4.16) must be evaluated. This case will be discussed in more depth later, in section 4.6, “Analysis of Mechanisms with More than One Spring.”

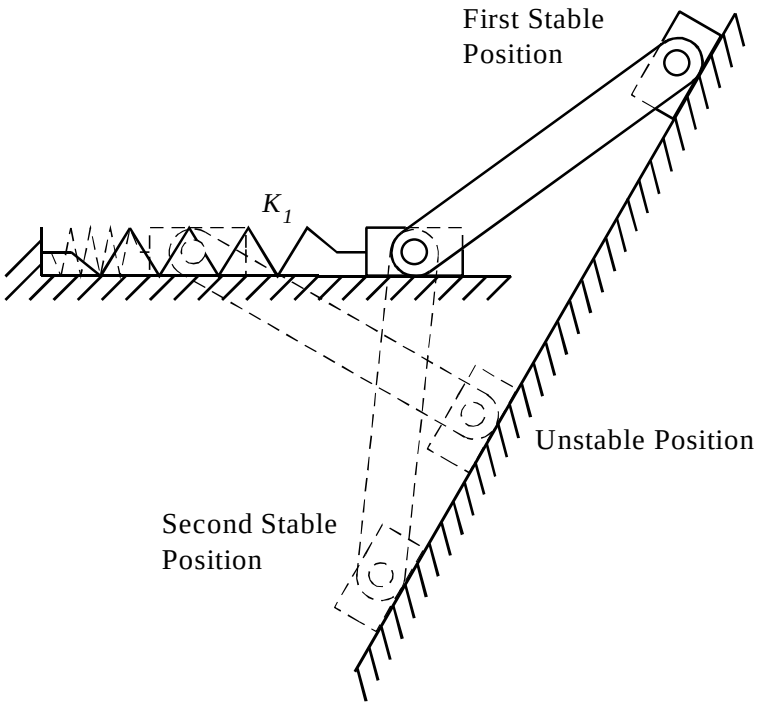

FIGURE 4-10: A bistable double-slider mechanism with a link joining the sliders. The second stable position and one of the unstable positions are shown. If the mechanism has a spring at position 4 instead of position 1, the motion will be similar.

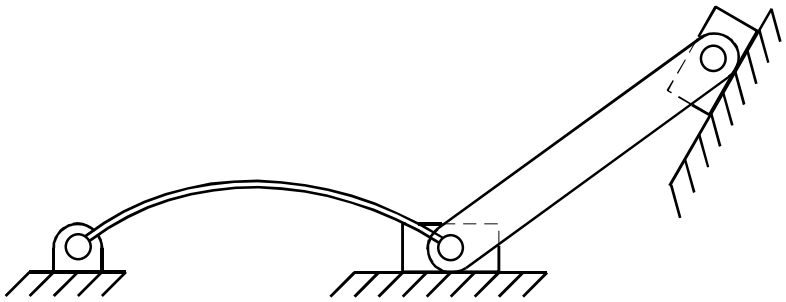

FIGURE 4-11: A compliant mechanism whose pseudo-rigid-body model is shown in Figure 4-10.

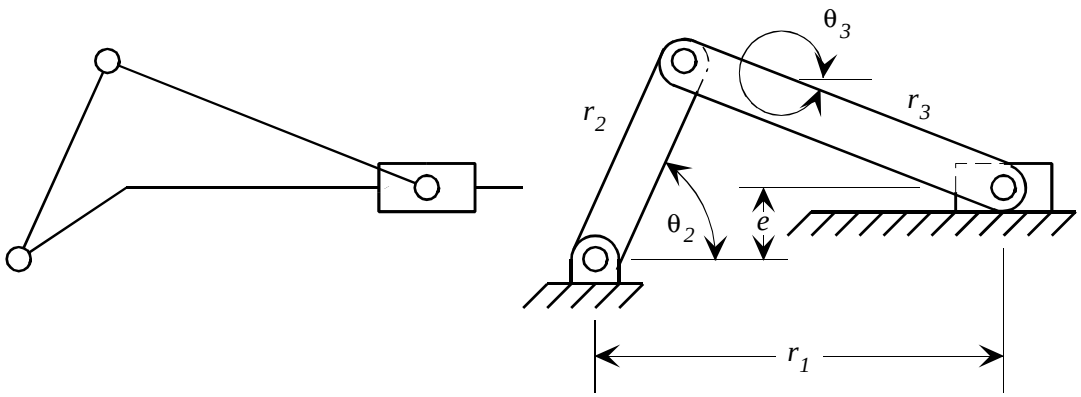

FIGURE 4-12: The basic kinematic chain of a general slider-crank or slider-rocker mechanism and the mechanism that results when one link is fixed. If $r_3 - r_2 \geq e$, then the mechanism is a slider-crank; otherwise, it is a slider-rocker.

4.5.5 Slider-Crank or Slider-Rocker Mechanisms

The basic kinematic chain of a general slider-crank mechanism is shown in Figure 4-12(a). By fixing the long sliding link, the mechanism shown in Figure 4-12(b) results. For this mechanism, if

$$r_3 - r_2 > e \tag{4.23}$$

then the mechanism is a slider-crank. If the two sides in Eq. (4.23) are equal, then the mechanism is a change-point slider-crank, and if the left side is less than the right side, then the mechanism is a slider-rocker. In addition, r_2 is arbitrarily chosen as the shortest link. This may be done without loss of generality because the case where $r_2 > r_3$ is merely a kinematic inversion of the case where $r_2 < r_3$. Also, e is constrained to be positive or zero. A negative value for e represents a rotation of the mechanism of 180°. Choosing θ_2 as the generalized coordinate, the displacement equations are

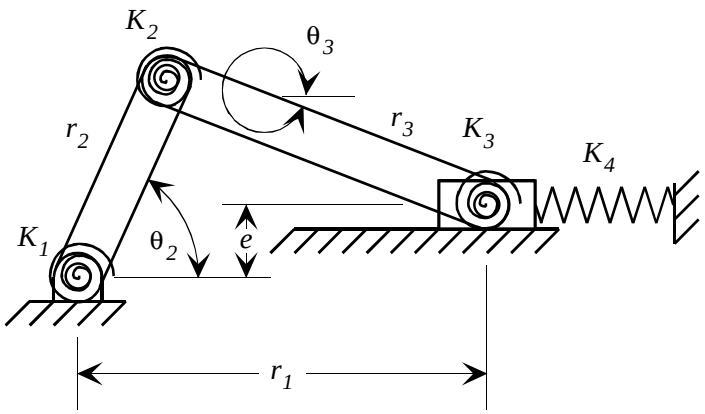

FIGURE 4-13: The model of a compliant slider-crank or slider-rocker mechanism. Each joint and spring combination models a compliant segment.

$$\theta_3 = \sin^{-1}\left(\frac{e - r_2 \sin\theta_2}{r_3}\right) \tag{4.24}$$

$$r_1 = r_2\cos\theta_2 + r_3\cos\theta_3 \tag{4.25}$$

If a compliant segment is added in place of each joint, the mechanism may be modeled as shown in Figure 4-13.

4.5.5.1 Analysis of the Energy Equation- The energy equation is the same as Eq. (4.5) with

$$\begin{aligned} \psi_1 &= \theta_2 - \theta_{20} \\ \psi_2 &= \theta_2 - \theta_{20} - (\theta_3 - \theta_{30}) \\ \psi_3 &= \theta_3 - \theta_{30} \\ \psi_4 &= r_1 - r_{10} \end{aligned} \tag{4.26}$$

The first derivative of energy is

$$\frac{dV}{d\theta_2} = 0 = K_1\psi_1 + K_2\psi_2\frac{d\psi_2}{d\theta_2} + K_3\psi_3\frac{d\psi_3}{d\theta_2} + K_4\psi_4\frac{d\psi_4}{d\theta_2} \tag{4.27}$$

The terms may be considered one at a time to determine which spring locations result in bistable behavior.

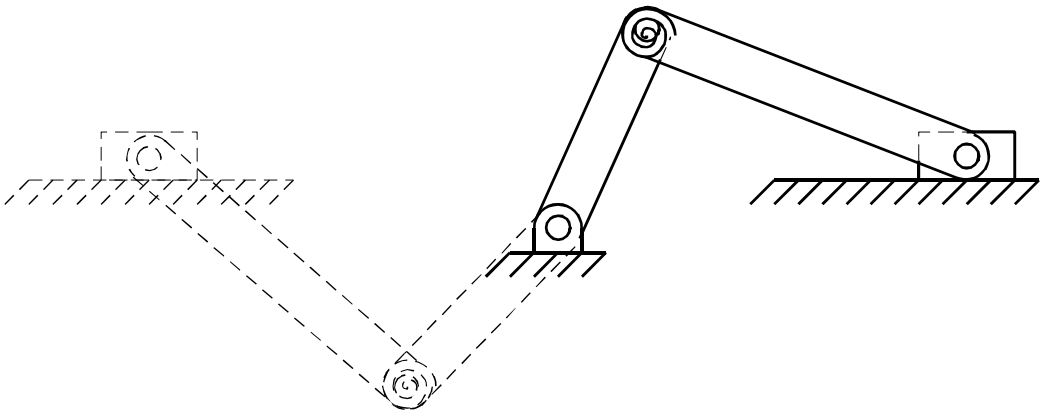

FIGURE 4-14: An illustration of the two positions for which a spring at position two is undeflected.

4.5.5.2 Analysis for $K_1 \neq 0$- This analysis shows that if K_1 is exclusively non-zero, the mechanism will only have one stable position because only one solution results. This result will be looked at more closely later.

4.5.5.3 Analysis for $K_2 \neq 0$- If K_2 is exclusively non-zero, then Eq. (4.27) becomes

$$0 = K_2[\theta_2 - \theta_3 - (\theta_{20} - \theta_{30})]\left(1 + \frac{r_2 \cos\theta_2}{r_3\sqrt{1 - \left(\frac{e - r_2 \sin\theta_2}{r_3}\right)^2}}\right) \tag{4.28}$$

The first part of this equation represents the change in the angle between the second and third links. Mathematically, it becomes very complex, and the solutions are difficult to interpret properly. However, by considering the motion of the mechanism, it may be seen that the mechanism can take two positions for any given angle between these two links. This is illustrated in Figure 4-14. Therefore, the first part of this equation has two physically realizable solutions, corresponding to two stable positions.

The second part of the equation represents the first derivative of ψ_2 with respect to θ_2. Algebraic and trigonometric manipulation lead to the solution

$$\theta_2 = \sin^{-1}\left(\frac{e^2 + r_2^2 - r_3^2}{2er_2}\right) \tag{4.29}$$

Initially, it seems that this solution leads to two potential values for θ_2, as the arcsin function has two solutions on the region from 0 to 2π. Closer examination shows that real solutions are only possible for a slider-rocker mechanism, though. This result comes from the inequality which must be satisfied for the mechanism to be a slider-crank:

$$r_3 \geq e + r_2 \tag{4.30}$$

Then, both sides may be squared to give

$$r_3^2 \geq e^2 + 2er_2 + r_2^2 \tag{4.31}$$

which may be written as

$$r_3^2 = e^2 + 2er_2 + r_2^2 + \varepsilon \tag{4.32}$$

where ε is an arbitrary constant greater than or equal to zero. Substituting Eq. (4.32) into Eq. (4.29) gives

$$\theta_2 = -\sin^{-1}\left(1 + \frac{\varepsilon}{2er_2}\right) \tag{4.33}$$

which is physically impossible, as the arcsin function only accepts arguments from -1 to 1. The only feasible solution to this equation occurs when $\varepsilon = 0$, signifying a change-point slider-crank. In this case, the solution is

$$\theta_2 = \frac{3\pi}{2} \tag{4.34}$$

which corresponds to the change-point position.

On the other hand, for a slider-rocker mechanism,

$$r_3 < e + r_2 \tag{4.35}$$

Squaring both sides gives

$$r_3^2 = e^2 + 2er_2 + r_2^2 - \varepsilon \tag{4.36}$$

where, ε is a non-negative constant. Substitution into Eq. (4.29) gives

$$\theta_2 = \sin^{-1}\left(-1 + \frac{\varepsilon}{2er_2}\right) \tag{4.37}$$

In addition, by considering the inequality necessary for the assembly of the mechanism:

$$r_3 > |e - r_2| \tag{4.38}$$

it can be shown that

$$\theta_2 = \sin^{-1}\left(1 - \frac{\varepsilon}{2er_2}\right) \tag{4.39}$$

indicating that the argument for the arcsin function for a slider-rocker is between 1 and -1, showing that this solution is feasible.

4.5.5.4 Result for $K_2 \neq 0$ - Therefore, for a slider-crank mechanism, a spring placed at position 2 will not result in a bistable mechanism because the mechanism cannot reach an unstable position to toggle between stable positions. However, for a change-point slider-crank or a slider-rocker, a spring place at position 2 will result in bistable behavior, unless the undeflected state corresponds to the unstable position. An example mechanism with the spring in this location is shown in Figure 4-15. Figure 4-16 shows a sample compliant mechanism with a compliant segment at position 2.

4.5.5.5 Analysis for $K_3 \neq 0$- If K_3 is exclusively non-zero, then Eq. (4.27) becomes

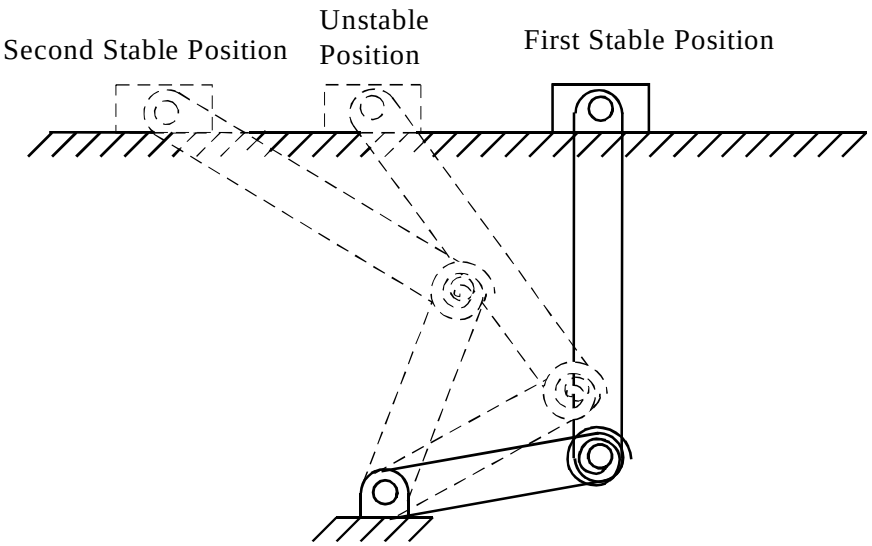

FIGURE 4-15: A bistable slider-rocker with a spring placed at position 2.

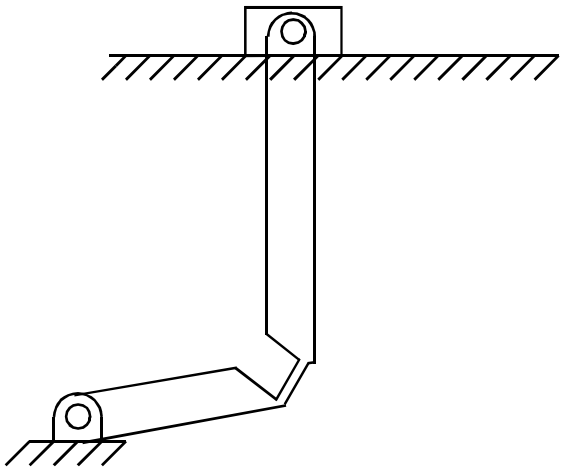

FIGURE 4-16: A compliant bistable slider-rocker with a compliant segment at position 2.

$$0 = -K_3(\theta_3 - \theta_{30})\frac{r_2\cos\theta_2}{r_3\cos\theta_3} \tag{4.40}$$

This equation has four solutions on the range from 0 to π. The four solutions, found by substituting Eq. (4.24), are

$$\begin{aligned} \theta_2 &= \theta_{20} \\ \theta_2 &= \frac{\pi}{2} \\ \theta_2 &= \pi - \theta_{20} \\ \theta_2 &= \frac{3\pi}{2} \end{aligned} \tag{4.41}$$

where

$$\begin{aligned} \theta_{20} &\neq \frac{\pi}{2} \\ \theta_{20} &\neq \frac{3\pi}{2} \end{aligned} \tag{4.42}$$

As before, the first and third solutions are stable; the second is an unstable position. The fourth solution also represents an unstable position. This is because link two has full rotation for a slider-crank; it must have an unstable position between the stable positions in both directions of travel. If the mechanism is a slider-rocker, then the fourth solution is not physically possible, and travel between stable positions is only possible in one direction. Note also that the unstable positions represent the maximum deflection of the spring placed at position three.

4.5.5.6 Results for $K_3 \neq 0$- Therefore, a spring placed exclusively at position 3 will cause the mechanism to be bistable unless its undeflected state corresponds to one of the two unstable states indicated in Eq. (4.41). A bistable mechanism with a spring at position 3 is shown in Figure 4-17. Figure 4-18 illustrates one way that this mechanism could be made compliant.

4.5.5.7 Analysis for $K_4 \neq 0$- If K_4 is chosen to be exclusively non-zero, Eq. (4.27) becomes

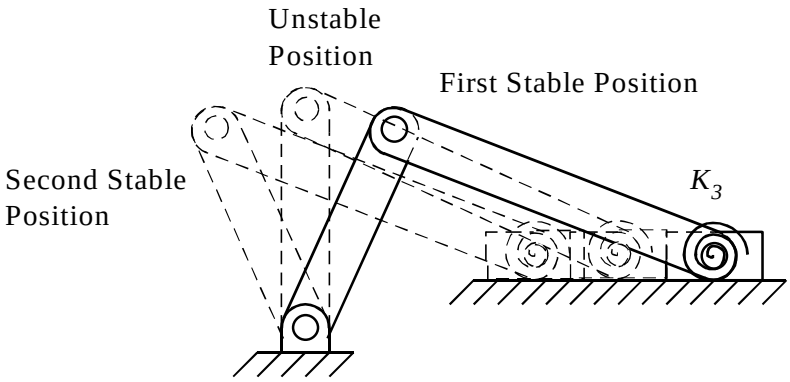

FIGURE 4-17: A bistable slider-crank with a spring at position 3. The second stable position and one of the unstable positions are shown in dashed lines.

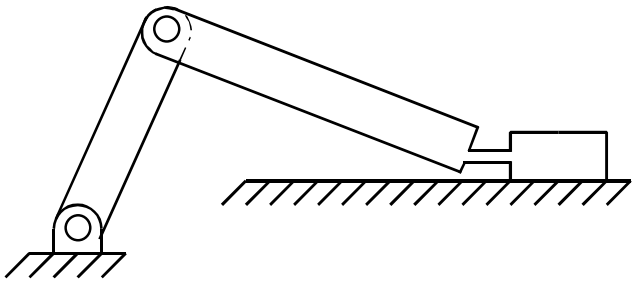

FIGURE 4-18: A compliant bistable mechanism. Figure 4-17 shows a model of this mechanism.

$$0 = K_4(r_1 - r_{10})(r_2\cos\theta_2\tan\theta_3 - r_2\sin\theta_2) \tag{4.43}$$

As with K_2, the solution in terms of θ_2 to the first part of this equation, $r_1 - r_{10} = 0$, is long and difficult to interpret. However, consideration of the mechanism's motion indicates that the mechanism will have two different positions where $r_1 = r_{10}$. These two positions are shown in Figure 4-19. If θ_{20} is the upper position shown in solid lines, then the lower position is

$$\theta_2 = 2\sin^{-1}\left(\frac{e}{r_2 + r_3}\right) - \theta_{20} \tag{4.44}$$

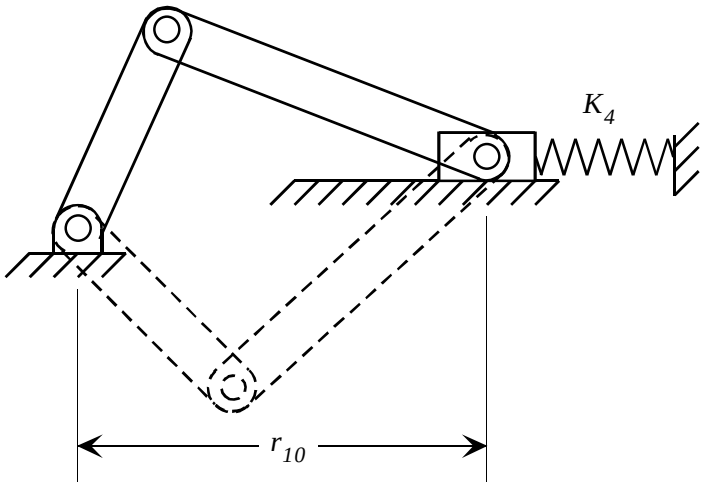

FIGURE 4-19: The two positions a slider-crank or -rocker mechanism can take if $r_1 = r_{10}$.

The second part of Eq. (4.44) may be solved to give

$$\begin{aligned} \theta_2 &= \theta_3 \\ \theta_2 &= \theta_3 - \pi \end{aligned} \tag{4.45}$$

as long as

$$\begin{aligned} \theta_{20} &\neq \theta_{30} \\ \theta_{20} &\neq \theta_{30} - \pi \end{aligned} \tag{4.46}$$

Eq. (4.45) will be satisfied when

$$\begin{aligned} \theta_2 &= \sin^{-1}\left(\frac{e}{r_2 + r_3}\right) \\ \theta_2 &= \pi + \sin^{-1}\left(\frac{e}{r_3 - r_2}\right) \end{aligned} \tag{4.47}$$

These two solutions correspond to the limit positions of the slider, which are unstable equilibrium positions, while the two solutions found earlier for the first part of Eq. (4.43) correspond to stable equilibrium positions. A slider-crank mechanism will be able to move over either unstable position to the second stable position. A slider-rocker, on the other

hand, will only be able to reach the first unstable position within its range of motion. This may be proven using the inequality required for a slider-rocker:

$$r_3 < e + r_2 \tag{4.48}$$

which may be written

$$r_3 = e + r_2 - \varepsilon \tag{4.49}$$

where ε is some number greater than zero. Substitution gives

$$\theta_2 = \pi + \sin^{-1}\left(\frac{e}{e-\varepsilon}\right) \tag{4.50}$$

The argument of the arcsin function is greater than one, meaning that this solution is not physically realizable for a slider-rocker mechanism.

4.5.5.8 Results for $K_4 \neq 0$- Based on this analysis, the mechanism will be bistable if a spring is place exclusively between the slider and ground, unless the undeflected spring position is already at one of the limit positions specified in Eq. (4.47). Such a mechanism is illustrated in Figure 4-20, with one unstable position and the second stable position shown in dashed lines. A compliant equivalent could be achieved by replacing the spring with a FBPP segment.

4.5.5.9 Return to the Analysis for $K_1 \neq 0$- One more aspect of the bistable analysis of the slider-rocker mechanism remains to be studied. A slider-crank or slider-rocker mechanism with given link lengths r_2, r_3, and e can take on two different positions for a given θ_2. This means that the preceding analysis, based on θ_2 as the generalized variable, fails to adequately predict stable positions resulting from a spring place at position 1. A more

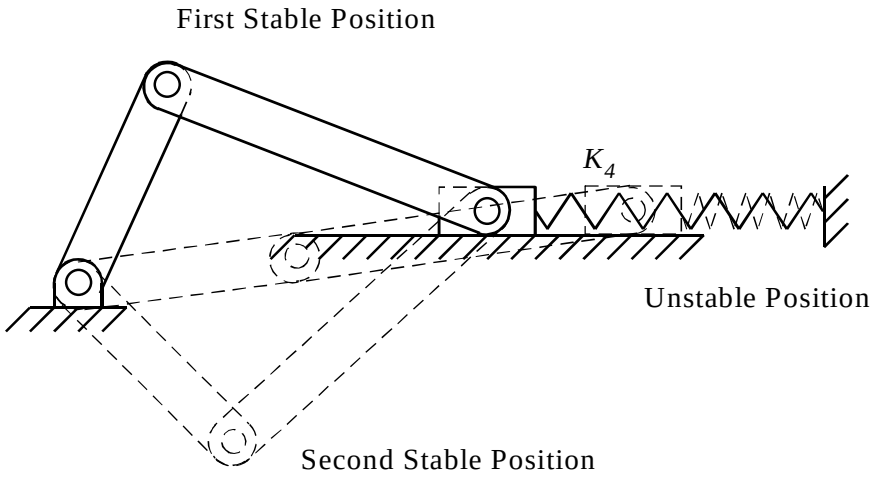

FIGURE 4-20: A bistable slider-crank with the two stable positions and one unstable position shown. In this case, the spring is placed in position 4.

thorough analysis of this spring location requires the use of a different generalized coordinate. θ_3 is chosen for use here. The first derivative of energy with respect to θ_3 is

$$\frac{dV}{d\theta_3} = 0 = K_1\psi_1\frac{d\psi_1}{d\theta_3} + K_2\psi_2\frac{d\psi_2}{d\theta_3} + K_3\psi_3 + K_4\psi_4\frac{d\psi_4}{d\theta_3} \tag{4.51}$$

Note that this analysis fails to predict stable positions associated with K_3, just as the preceding analysis failed to predict stable positions associated with K_1. If K_1 is exclusively non-zero, Eq. (4.51) becomes

$$0 = K_1(\theta_2 - \theta_{20})\frac{d\theta_2}{d\theta_3} \tag{4.52}$$

θ_2 may be given in terms of θ_3 by

$$\theta_2 = \sin^{-1}\left(\frac{e - r_3\sin\theta_3}{r_2}\right) \tag{4.53}$$

The solution to the first term of Eq. (4.52), $\theta_2 - \theta_{20} = 0$, is

$$\begin{aligned} \theta_3 &= \theta_{30} \\ \theta_3 &= \pi - \theta_{30} \end{aligned} \tag{4.54}$$

The solution to the second term (the derivative term) may be found from

$$\frac{d\theta_2}{d\theta_3} = -\frac{r_3 \cos\theta_3}{r_2 \cos\theta_2} \tag{4.55}$$

By setting this equal to zero, the solution is found to be

$$\theta_3 = \frac{\pi}{2} \text{ or } \frac{3\pi}{2} \tag{4.56}$$

where

$$\theta_{30} \neq \frac{\pi}{2} \tag{4.57}$$

Also, from the geometry of the mechanism, for θ_3 to be equal to $3\pi/2$,

$$\theta_2 = \sin^{-1}\left(\frac{e + r_3}{r_2}\right) \tag{4.58}$$

Because $r_3 \geq r_2$, the argument of this arcsin function is greater than one, indicating that this solution is not possible. Also, for θ_3 to be equal to $\pi/2$,

$$\theta_2 = \sin^{-1}\left(\frac{e - r_3}{r_2}\right) \tag{4.59}$$

For a slider-crank, $e < r_3 - r_2$, so this solution is also not possible.

4.5.5.10 Results for $K_1 \neq 0$- Therefore, while a slider-crank with a spring at position one may be assembled in two different stable positions, it can not move between those positions after assembly. A slider-rocker or change-point slider-crank can move between these positions in one direction; consequently, a slider-rocker or change-point slider-crank will be bistable if a spring is placed at position one. A bistable slider-rocker mechanism with a

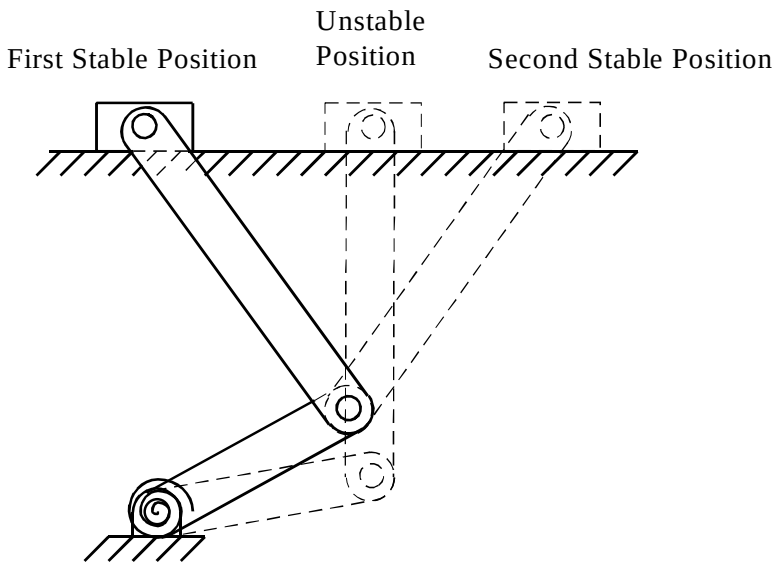

FIGURE 4-21: A bistable slider-rocker with a spring at position 1. The unstable position and second stable position are also shown.

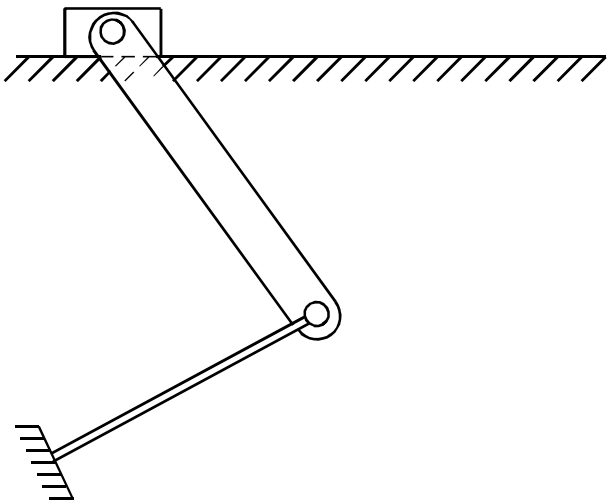

FIGURE 4-22: A compliant mechanism based on the model shown in Figure 4-21.

spring at position 1 is shown in Figure 4-21. One possible compliant mechanism that is based on this model is shown in Figure 4-22.

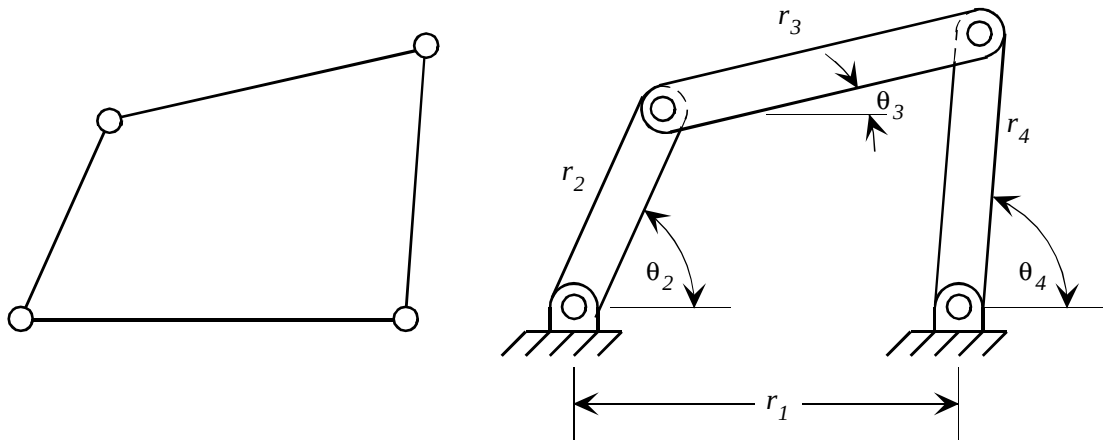

FIGURE 4-23: A general four-link mechanism. The basic kinematic chain is shown in (a), and the mechanism is shown in (b).

4.5.6 Four-Link Mechanisms

A general four-link mechanism's basic kinematic chain is shown in Figure 4-23(a). By fixing any link, the mechanism may be formed, as shown in Figure 4-23(b). This mechanism may be further classified according to Grashof's criterion (Grashof, 1883; Paul, 1979a; Barker, 1985) as a Grashof or non-Grashof mechanism. In a Grashof mechanism, the shortest link can rotate through a full revolution with respect to either link connected to it. In a non-Grashof mechanism, no link can rotate through a full revolution with respect to any other links. Grashof's criterion is mathematically stated as

$$s + l \leq p + q \tag{4.60}$$

where s is the length of the shortest link, l is the length of the longest link, and p and q are the lengths of the intermediate links. If the mechanism's link lengths satisfy this inequality, it is a Grashof mechanism; if they do not, the mechanism is non-Grashof. If the sum of the lengths of the longest and shortest links is equal to the sum of the lengths of the other two

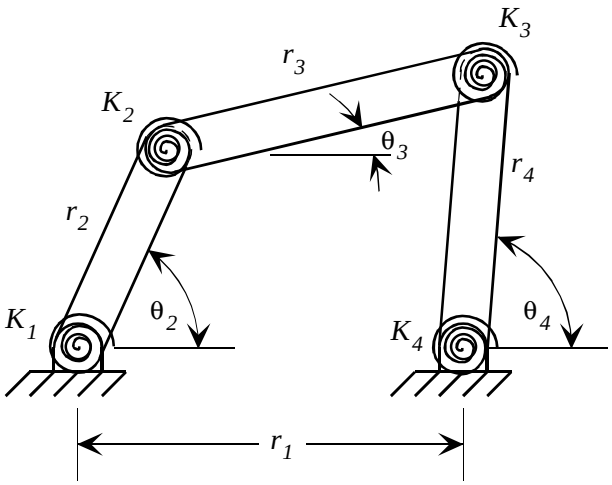

FIGURE 4-24: A four-link mechanism with a spring at each joint.

links, the mechanism is a special case of a Grashof mechanism known as a change-point mechanism.

4.5.6.1 Analysis of the Energy Equation- The model of a fully compliant four-link mechanism is shown in Figure 4-24. For any four-link mechanism, the energy equation is the same as Eq. (4.5), where

$$\begin{aligned} \psi_1 &= \theta_2 - \theta_{20} \\ \psi_2 &= \theta_2 - \theta_{20} - (\theta_3 - \theta_{30}) \\ \psi_3 &= \theta_4 - \theta_{40} - (\theta_3 - \theta_{30}) \\ \psi_4 &= \theta_4 - \theta_{40} \end{aligned} \tag{4.61}$$

Choosing θ_2 as the generalized coordinate, the first derivative is

$$\frac{dV}{d\theta_2} = 0 = K_1\psi_1 + K_2\psi_2\left(1 - \frac{d\theta_3}{d\theta_2}\right) + K_3\psi_3\left(\frac{d\theta_4}{d\theta_2} - \frac{d\theta_3}{d\theta_2}\right) + K_4\psi_4\frac{d\theta_4}{d\theta_2} \tag{4.62}$$

Because this mechanism may be inverted so that any of its links is ground, only one spring position needs to be analyzed, and the results may then be applied to any of the four spring

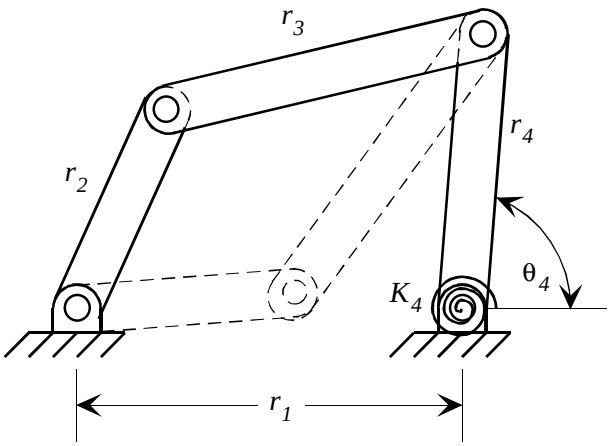

FIGURE 4-25: The two different positions a four-link mechanism may take for a given angle θ_4.

positions. Position 4 is chosen because the equations are somewhat simpler, and no problem is encountered because of the choice of θ_2 as the generalized coordinate. If K_4 is exclusively non-zero, Eq. (4.62) becomes

$$0 = K_4(\theta_4 - \theta_{40})\frac{d\theta_4}{d\theta_2} \tag{4.63}$$

The first part of this equation, $\theta_4 - \theta_{40} = 0$, provides two solutions corresponding to the two ways that the mechanism can be assembled. That is, for any given link lengths r_1, r_2, r_3, and r_4, and the angle of the fourth link, θ_4, two different mechanism positions may be found, as shown in Figure 4-25. The exact positions may be found by solving the Freudenstein equations (Freudenstein, 1955):

$$\begin{aligned} r_2\cos\theta_2 + r_3\cos\theta_3 &= r_1 + r_4\cos\theta_{40} \\ r_2\sin\theta_2 + r_3\sin\theta_3 &= r_4\sin\theta_{40} \end{aligned} \tag{4.64}$$

For the purpose of this analysis, though, it is sufficient to know that these two solutions to the first part of Eq. (4.63) exist. The second part of Eq. (4.63), the derivative, may be written

$$\frac{d\theta_4}{d\theta_2} = \frac{r_2 \sin(\theta_3 - \theta_2)}{r_4 \sin(\theta_3 - \theta_4)} = 0 \tag{4.65}$$

If $\sin(\theta_3 - \theta_4) \neq 0$, then this equation has two solutions:

$$\begin{aligned} \theta_2 &= \theta_3 \\ \theta_2 &= \theta_3 + \pi \end{aligned} \tag{4.66}$$

Therefore, the derivative term will be zero when links two and three are collinear, unless the denominator of Eq. (4.65) is also zero at this point. However, if the denominator is zero, it implies that links three and four are also collinear, which indicates that the mechanism is a change-point mechanism. This case will be examined separately later.

4.5.6.2 Interpretation of Solutions- The analysis presented above has shown that four solutions exist to the first derivative of the energy equation for a spring placed at any link of a four-link mechanism. The first two solutions, which may be given by the Freudenstein equations in Eq. (4.64), are stable positions of the mechanism, while the two solutions in Eq. (4.66) are unstable positions. While the two stable positions are possible for any configuration of link lengths and one torsional spring, the unstable positions can not be reached in some configurations. In other words, a mechanism can always be assembled in either stable position, but it may not be able to toggle between the stable positions after assembly. For a mechanism to reach the point where $\theta_2 = \theta_3$, two inequalities must be satisfied, as shown in Figure 4-26. These are

FIGURE 4-26: A graphical representation near the limits required for θ_2 to be equal to θ_3.

$$\begin{aligned} r_1 + r_4 &> r_2 + r_3 \\ |r_1 - r_4| &< r_2 + r_3 \end{aligned} \tag{4.67}$$

Similarly, if θ_2 and θ_3 differ by π radians, the following two conditions must be met:

$$\begin{aligned} r_1 + r_4 &> |r_2 - r_3| \\ |r_1 - r_4| &< |r_2 - r_3| \end{aligned} \tag{4.68}$$

The second condition of Eq. (4.67) and the first condition of Eq. (4.68) can both be proved at the same time for any four-link mechanism by showing that the difference of the lengths of any two links is less than the sum of the lengths of the other two links. This may be done by considering the inequality which must be satisfied for a mechanism to be assembled. For four given link lengths, the sum of the lengths of the three shortest links must be greater than the length of the longest link. Mathematically, this means

$$s + p + q > l \tag{4.69}$$

Algebra gives the three inequalities

$$\begin{aligned} l - q &< s + p \\ l - p &< s + q \\ l - s &< p + q \end{aligned} \tag{4.70}$$

In addition, by defining l as the length of the longest link, the following inequalities result:

$$\begin{aligned} p - s &< l + q \\ q - s &< l + p \\ |p - q| &< l + s \end{aligned} \tag{4.71}$$

These six inequalities prove that the difference of any two link lengths is less than the sum of the other two links for any four-link mechanism, so that the second condition of Eq. (4.67) and the first condition of Eq. (4.68) are satisfied. Therefore, for the mechanism to be considered bistable, it must be able to satisfy at least one of the other two inequalities in Eq. (4.67) or (4.68), showing that it is able to reach one of the two unstable positions to toggle into the other stable position. To determine which mechanism configurations are bistable, every possible configuration of link lengths for Grashof and non-Grashof mechanisms will be considered.

4.5.6.3 General Approach to the Proof for any Four-Link Mechanism- Before presenting proofs for each mechanism configuration's ability to reach an unstable position, three useful relations will be derived. For the first one, begin with the relation

$$l > q \tag{4.72}$$

By adding p to both sides,

$$l + p > q + p \tag{4.73}$$

But p is greater than s, so

$$l + p > q + s \tag{4.74}$$

Which is also equivalent to

$$l + q > p + s \tag{4.75}$$

The third useful relation starts by subtracting s from both sides of Eq. (4.72),

$$l - s > q - s \tag{4.76}$$

The difference between q and s will always be greater than the difference between q and p, so

$$l - s > |q - p| \tag{4.77}$$

Eq. (4.74), (4.75), and (4.77) will be used extensively in the determination of which mechanism configurations can reach the unstable positions.

The material presented up to this point proves that for a spring placed at any of the four positions, a four-link mechanism may be assembled in one of two stable positions. However, it will only be able to toggle between the two positions if one of the two unstable positions can be reached. These unstable positions correspond to the positions where the two links opposite the spring are collinear, or, in other words, when they have the same angle or their angles differ by π radians. For the mechanism to reach the unstable position where the two opposite links are at the same angle, the following inequality must be met:

$$r_{a1} + r_{a2} > r_{o1} + r_{o2} \tag{4.78}$$

where r_{a1} and r_{a2} are the lengths of the two links adjacent to the spring, and r_{o1} and r_{o2} are the lengths of the two links opposite the spring. This is condition one for a four-link bistable mechanism. Similarly, for the mechanism to reach the unstable position where the two opposite links' angles differ by π radians, the following inequality must be satisfied:

$$\left|r_{a1} - r_{a2}\right| < \left|r_{o1} - r_{o2}\right| \tag{4.79}$$

This is condition two for a four-link bistable mechanism. For a complete analysis of which spring positions result in a bistable mechanism, each spring position must be examined to determine if either or both of conditions one and two are satisfied. If both are satisfied, then that spring position results in a bistable mechanism which can reach its two stable positions by rotation in either direction. If exactly one is satisfied, the that position gives a bistable mechanism which can reach its two stable positions by toggling through just one of the two unstable states. If neither is satisfied, then that spring position does not result in a bistable mechanism.

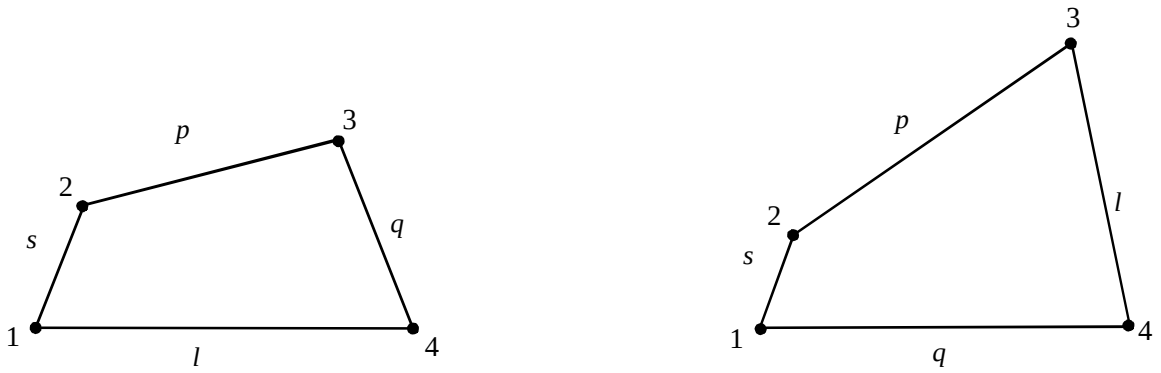

FIGURE 4-27: The two basic kinematic chains which a four-link mechanism may form. In (a), the shortest and longest links are adjacent, and in (b) they are opposite each other. The four spring positions are labeled.

4.5.6.4 Proof for a Grashof Mechanism- The cases of Grashof and non-Grashof mechanisms will be investigated separately. In both cases, though, the mechanism can form one of two basic kinematic chains, or basic ways that the mechanism can be formed. These are illustrated in Figure 4-27. In Figure 4-27(a), the shortest and longest links are adjacent, and in Figure 4-27(b) they are opposite. For a Grashof mechanism of the type shown in Figure 4-27(a) with a spring placed at position 1,

$$s + l < p + q \tag{4.80}$$

which violates condition one. Similarly, by Eq. (4.77), the second condition is also violated. For a Grashof mechanism of the type shown in Figure 4-27(b) with a spring at position 1,

$$q - s > l - p \tag{4.81}$$

which violates condition two. By Eq. (4.74) condition one is violated. Hence, a Grashof mechanism with a spring at position 1 will not be bistable for either basic kinematic chain.

TABLE 4-1: Each of the eight spring positions in Figure 4-27 are analyzed to determine whether they meet conditions one and two for a Grashof mechanism. The inequality proving that the condition is met or not met is shown, along with the source of the inequality (Grash. = Grashof's law, otherwise, the equation number is given).

Spring Position	Condition One met?	Proof	Source of Proof	Condition Two met?	Proof	Source of Proof
1a	No	$s+l<p+q$	Grash.	No	$l-s>\|q-p\|$	(4.77)
1b	No	$q+s<l+p$	(4.74)	No	$q-s>l-p$	Grash.
2a	No	$p+s<l+q$	(4.75)	No	$p-s<l-q$	Grash.
2b	No	$p+s>l+q$	(4.75)	No	$p-s>l-q$	Grash.
3a	Yes	$p+q>l+s$	Grash.	Yes	$\|q-p\|<l-s$	(4.77)
3b	Yes	$l+p>q+s$	(4.74)	Yes	$l-p<q-s$	Grash.
4a	Yes	$l+q>p+s$	(4.75)	Yes	$l-q<p-s$	Grash.
4b	Yes	$l+q>p+s$	(4.75)	Yes	$l-q<p-s$	Grash.

By following the same method, each spring position can be analyzed to determine whether it results in a bistable mechanism. The results for Grashof mechanisms are shown in Table 4-1. In this table, spring position 1a means position 1 in Figure 4-27(a), position 1b means position 1 in Figure 4-27(b), and so on. The table shows that for either basic kinematic chain, the mechanism will be bistable if the spring is placed at position 3. This means that a Grashof mechanism will be bistable if a spring is placed at one of the two joints which are not adjacent to the shortest link, regardless of the position of the longest link. In addition, any Grashof mechanism that satisfies one condition satisfies the other, meaning that the mechanism can rotate through either unstable position to toggle into the second stable position.

TABLE 4-2: Each of the eight spring positions in Figure 4-27 are analyzed to determine whether they meet conditions one and two for a non-Grashof mechanism. The inequality proving that the condition is met or not met is shown, along with the source of the inequality (Grash. = Grashof's law, otherwise, the equation number is given).

Spring Position	Condition One met?	Proof	Source of Proof	Condition Two met?	Proof	Source of Proof
1a	Yes	$s+l>p+q$	Grash.	No	$l-s>\|q-p\|$	(4.77)
1b	No	$q+s<l+p$	(4.74)	Yes	$q-s<l-p$	Grash.
2a	No	$p+s<l+q$	(4.75)	Yes	$p-s<l-q$	Grash.
2b	No	$p+s<l+q$	(4.75)	Yes	$p-s<l-q$	Grash.
3a	No	$p+q<l+s$	Grash.	Yes	$\|q-p\|<l-s$	(4.77)
3b	Yes	$l+p>q+s$	(4.74)	No	$l-p>q-s$	Grash.
4a	Yes	$l+q>p+s$	(4.75)	No	$l-q>p-s$	Grash.
4b	Yes	$l+q>p+s$	(4.75)	No	$l-q>p-s$	Grash.

4.5.6.5 Proof for a Non-Grashof Mechanism- For a non-Grashof mechanism, the same kinematic chains can be used. If a spring is placed at position 1a, following the nomenclature used earlier, then Grashof's law gives the inequality

$$s + l > p + q \tag{4.82}$$

which proves that the non-Grashof mechanism satisfies condition one. However, by Eq. (4.77), condition two is not satisfied. If a spring is placed at position 1b, then Eq. (4.74) proves that condition one is not met. Also, Grashof's law gives

$$q - s < l - p \tag{4.83}$$

which proves that condition two is met. Results for all other spring positions are shown in Table 4-2. Exactly one of the two conditions is satisfied for every possible spring position. This means that a spring placed at any of the four positions will cause a non-Grashof mechanism to be bistable. While it will always be able to reach the unstable position if

deflected in one direction, it will not be able to reach the unstable position in the other direction.

Another interesting note that the table shows is which direction a given mechanism will be able to toggle. Notice that springs placed at 1b, 2a, 2b, and 3a result in mechanisms which only meet condition two, meaning that angles of the two links opposite the spring must differ by π radians. The other spring locations - 1a, 3b, 4a, and 4b - result in mechanisms which require the two opposite links to reach the same angle. A close look at Figure 4-27 reveals that each of these positions which satisfy condition 1 is adjacent to the longest link, while each position which satisfies condition 2 is not adjacent to the longest link. This information is valuable in some design problems because meeting condition two requires the two opposite links to be able to cross each other. In situations where the two links are coplanar, as is often the case with surface micromachined MEMS, this is usually not possible.

4.5.6.6 Proof for a Change-Point Mechanism- The last case to consider is the change-point mechanism. As noted previously, the derivative term in Eq. (4.65) goes to zero over zero when links 2 and 3 are collinear. This is because the position where all links are collinear in a change-point mechanism is a singular position - at this point, the mechanism can move into two different positions. If it moves one way, then $|\theta_4 - \theta_{40}|$ becomes larger; if it moves the other way, then $|\theta_4 - \theta_{40}|$ becomes smaller. Thus, movement in one direction means that the derivative of θ_4 changes sign; in the other direction, its sign remains the same. However, if its sign changes, then the singular position represents a relative maximum in potential energy. This is true regardless of which link is shortest or longest because the

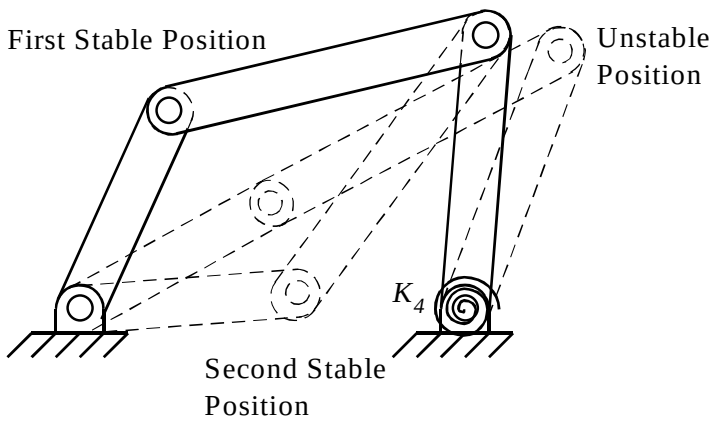

FIGURE 4-28: A bistable four-link mechanism showing the two stable positions and one unstable position.

change-point position is always possible for a change-point mechanism (Paul, 1979a). Thus, for a change-point mechanism, a spring placed at any of the four locations will result in a mechanism with bistable behavior. The spring will tend to force the mechanism into the right position when it reaches its change-point.

4.5.6.7 Results for a Four-Link Mechanism- In summary, a Grashof four-link mechanism will be bistable if a spring is placed at either position opposite the shortest link. A change-point or non-Grashof four-link mechanism will be bistable if a spring is placed at any of the four positions. An example of a four-link bistable mechanism with a spring at position 4 is shown in Figure 4-28. For a compliant equivalent, the spring would be replaced by either a small-length flexural pivot or a fixed-pinned segment.

4.6 Analysis of Mechanisms with More than One Spring

The analysis presented above finds the locations of springs which, if used exclusively, will guarantee bistable behavior. Other springs may be present in the mechanism,

though. In fact, this may even be desirable. If only one spring is in the mechanism, it will always have zero potential energy at both stable positions. In some design problems, a mechanism may be desired with a stable position that is "cocked." In other works, a stable position may be desired which requires very little energy to move out of to the unstable position, after which the mechanism releases considerably more energy in returning to the first stable position. For a full analysis of the location of the unstable and stable positions when multiple springs are present, the potential energy equation must be solved for each configuration involving more than one spring. However, the designer should have some idea of the effect extra springs will have on the stability of the mechanism.

Because each spring adds its potential energy to the energy of the whole, the energy equation of each spring may be analyzed individually, and some idea of their sum may be arrived at. For a spring placed at a location where bistable behavior results, as presented in the preceding analysis, the potential energy curve starts at zero at the undeflected position. The potential energy then increases to a maximum at the unstable position, after which it decreases back to zero at the stable position. For a spring placed at a location which does not give bistable behavior, the energy curve will also start at zero at the undeflected state, but then it will increase continually as the generalized coordinate changes. Cases with two springs are analyzed here, but the results may be generalized to any number of springs.

4.6.1 Analysis for One Bistable Spring and One Non-bistable Spring Location

Consider a case of a mechanism with one spring placed at a position which will give bistable behavior, called spring one, and another spring placed at a position which does not give bistable behavior, called spring two. The total potential energy will start at zero in the undeflected state, and it will increase until the unstable position of spring one is reached.

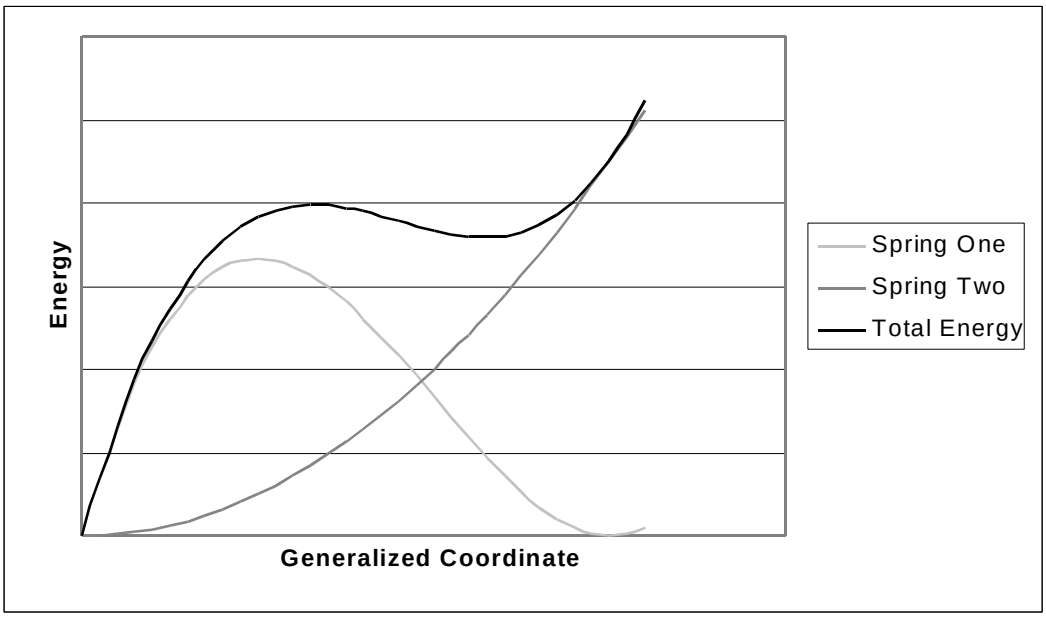

FIGURE 4-29: An example showing the sum of potential energy due to one spring which causes bistable behavior and another that does not. In this case, the sum of energy also has two relative minima because spring one's curve decreases more rapidly than spring two's curve increases.

After this point, if the potential energy due to spring one is decreasing more rapidly than the potential energy due to spring two is increasing, then the total potential energy will also decrease, and a minimum will be reached at some point, as illustrated in Figure 4-29. Thus, a bistable mechanism results. On the other hand, if the potential energy due to spring one is decreasing more slowly than the potential energy due to spring two is increasing, the total potential energy will continue to increase, and the mechanism will not be bistable, as Figure 4-30 shows. The rate of increase or decrease due to each spring depends on the geometry of the mechanism as well as the stiffness of the springs.

While the mechanism geometry is case-specific, the relative stiffness of the springs can give the designer some information even if the geometry is not considered. This may

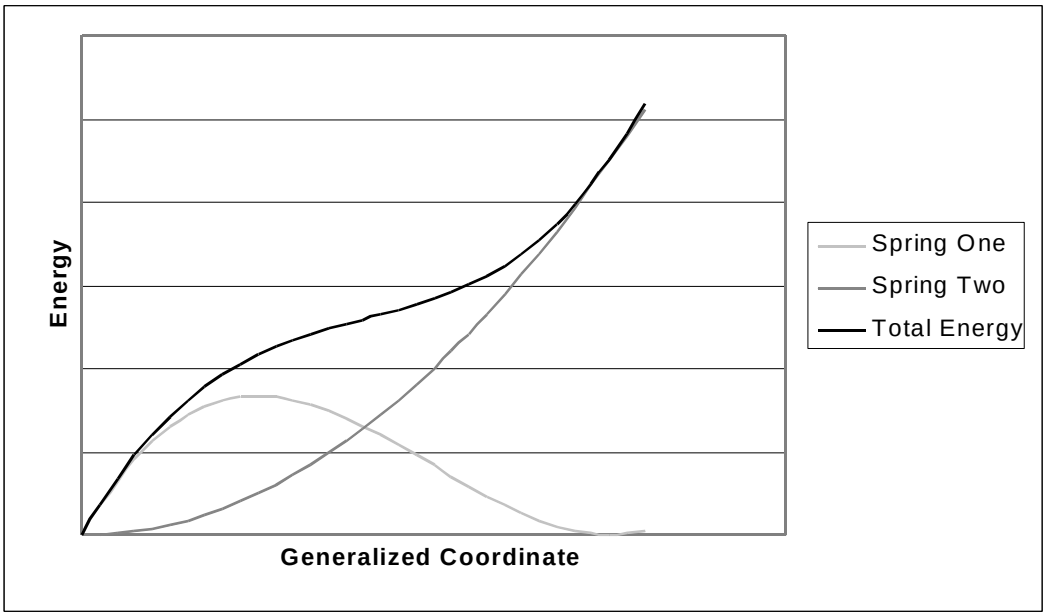

FIGURE 4-30: The sum of potential energy in this case continually increases because spring two's energy curve increases more rapidly than spring one's curve decreases.

be seen by considering the equation for the rate of increase of potential energy in a spring, either torsional or linear:

$$\frac{dV}{d\phi} = K\psi\frac{d\psi}{d\phi} \tag{4.84}$$

where ϕ is the generalized coordinate. In this equation, the spring deflection ψ and its derivative depend on the mechanism geometry. Thus, the increase or decrease of potential energy in the spring depends entirely on mechanism geometry, as expected. However, the spring constant *K* will scale this increase or decrease. Thus, if spring one in the hypothetical mechanism considered above has a very high spring constant relative to spring two, its potential energy curve will dominate, and the mechanism will be bistable. If spring two is much stiffer than spring one, though, the mechanism will probably not be bistable.

4.6.2 Analysis for Two Bistable Spring Locations

Similarly, if spring two is placed at a position which causes bistable behavior, its energy curve will add with spring one's energy curve. In particular, if the energy stored in spring one is decreasing over any part of the mechanism motion when the energy in spring two is also decreasing, then the total energy will decrease, and the mechanism will be bistable. However, if this is not the case, then the two springs will interact in the same way as discussed above.

4.7 Summary of Spring Locations Resulting in Bistable Behavior

Figure 4-31 shows each of the four mechanism classes analyzed here. For each class, the springs which can be placed at each shown are numbered for easy reference. Table 4-3 summarizes the spring locations for each class which will result in a bistable mechanism if used exclusively. The other two classes, snap-through buckled beams and bistable cam mechanisms, do not require any special information concerning the placement of springs.

The information contained in Table 4-3 gives the designer the knowledge needed for the formulation of bistable mechanism designs. It allows the determination of the mechanism classes and configurations which will lead to a valid bistable design, so that a wide variety of desired behaviors may be easily synthesized. The next chapter demonstrates the use of this theory in the solution of specific design problems.

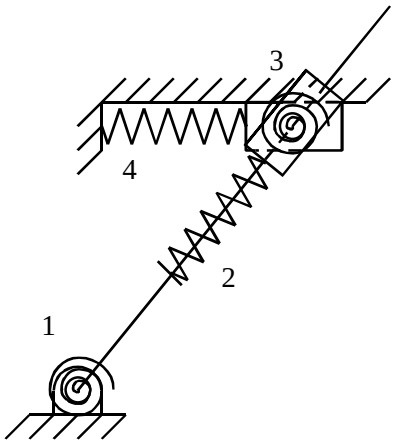

Double Slider with a Pin Joint joining the Sliders

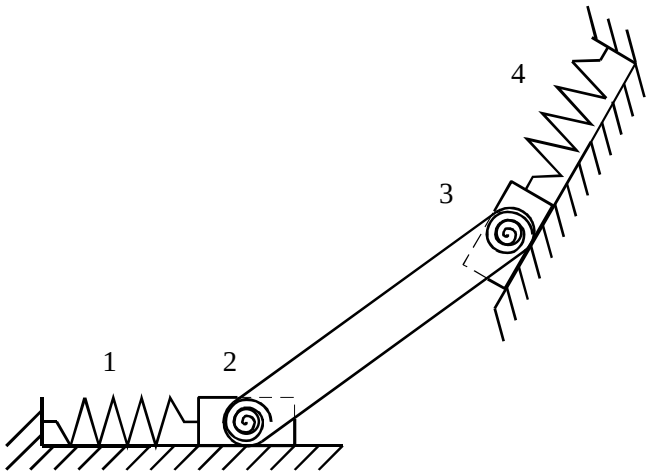

Double Slider with a Link joining the Sliders

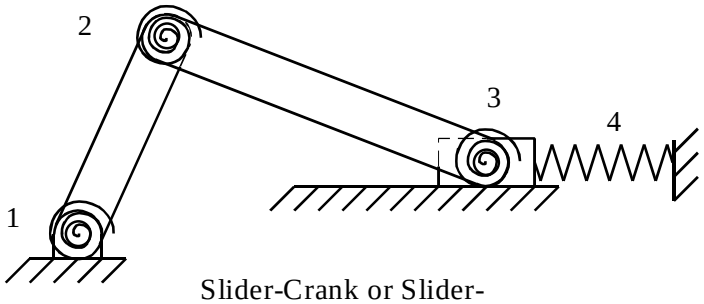

Slider-Crank or Slider-Rocker Mechansim

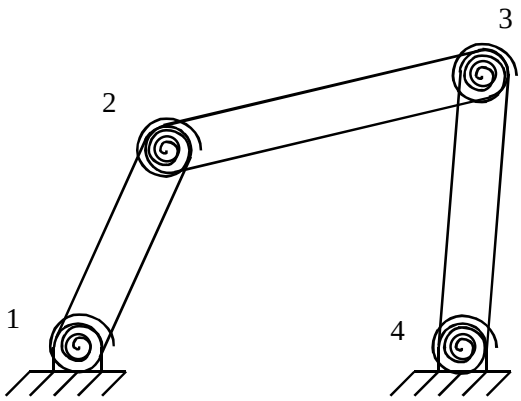

Four-Link Mechanism

FIGURE 4-31: Each of the four mechanism classes analyzed. The location of each spring is numbered for easy reference.

TABLE 4-3: The spring locations necessary for each class to cause bistable behavior in the mechanism.

Mechanism Class	Location of Springs for Bistable Mechanism
Double-Slider (pin joint joining)	2
Double-Slider (link joining)	1 or 4
Slider-Crank	3 or 4
Change-Point Slider-Crank	1, 2, 3, or 4
Slider-Rocker	1, 2, 3, or 4
Grashof Four-Link Mechanism	Either location opposite the shortest link
Change-Point Four-Link Mechanism	1, 2, 3, or 4
Non-Grashof Four-Link Mechanism	1, 2, 3, or 4

CHAPTER 5 *Bistable Mechanism Type Synthesis*

5.1 Method of Type Synthesis

The theory presented in the preceding chapter leads to an easy method of bistable mechanism type synthesis. When faced with a bistable mechanism design problem, a designer can consider each class of mechanisms discussed in Chapter 4 to determine whether that class can meet the motion requirements in the design problem. For example, motion along a line often requires a slider joint, leading to the selection of one of the classes which uses a slider. Then, for the classes which can meet the motion requirements, a bistable configuration can be found be adding a spring at one of the locations specified in Table 4-3 on page 90. It is usually helpful to consider many possible designs, including kinematic inversions of each class, and then choosing an appropriate mechanism configuration (class and spring location) to best meet the design specifications. The method will be demonstrated using three examples.

5.2 Design Examples Using Bistable Mechanism Type Synthesis

To illustrate the type synthesis of bistable mechanisms, several examples will be presented. These examples demonstrate the flexibility and ease of determining appropriate mechanism configurations for bistable mechanisms.

5.2.1 Example 1: Bistable CD Ejection Actuator

5.2.1.1 Problem Statement- A bistable mechanism is desired to eject compact discs or similar media from a case. The mechanism must move in a straight line, while pushing the CD, with 3.0 cm between the first stable position and the unstable position, and 3.0 cm between the unstable position and the second stable position, for a total ejection distance of 6.0 cm. The maximum force that must be applied to the actuator is 0.5 N.

5.2.1.2 Solution- The first step in the design process is to determine the mechanism class that can best meet the problem specifications. Because the mechanism must eject the CD in a straight line, a slider link is chosen to push the CD. Thus, three mechanism classes may be used: either type of double-slider mechanism or a slider-crank or slider-rocker mechanism. Figure 5-1 shows four possible mechanisms that could meet the design specifications. In each case, one of the joints has a spring attached to it; with the spring positions given by Table 4-3 on page 90. Note that spring position four is not used for the slider-crank mechanism because that configuration would require the slider to be in the same place in both stable positions.

While any of these mechanisms could be used for the CD ejection actuator, the double-slider with the sliders joined by a pin joint is chosen because it is easy to analyze. In addition, if the spring is replaced by a FBPP segment, then the segment's curvature could

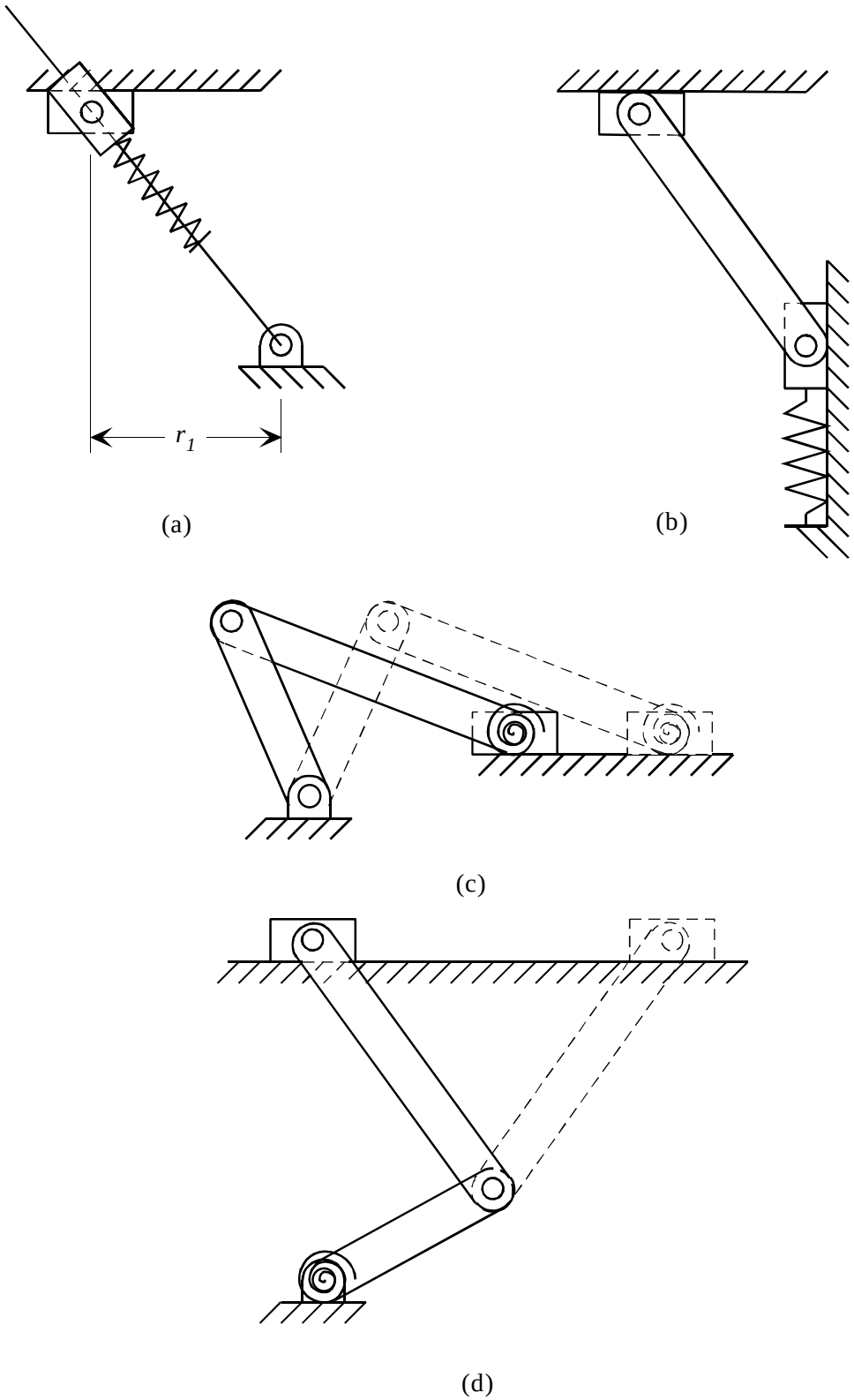

FIGURE 5-1: Possible mechanisms that could be used to make a bistable CD ejection actuator. (a) and (b) are the two types of double-slider mechanisms; (c) and (d) are a slider-crank and slider-rocker mechanism, respectively.

be made to match the curvature of the CD, making an attractive mechanism. The dimensions of the mechanism must be chosen to give the desired distance between the stable and unstable positions, as outlined above. The unstable position will occur when the rotating bar is vertical; thus, r_{10} is chosen to be 3.0 cm. The position of the fixed pin joint must also be specified; it is chosen to lie just outside the edge of the CD, allowing the semi-circular FBPP segment to wrap around the outside of the CD. The horizontal slider is simulated by reflecting the entire mechanism about the line of the slider's path. Finally, the pin joints are approximated with very small, thin flexural hinges, known as living hinges. Because these hinges have very low stiffness, they have very little effect on the mechanism's stability.

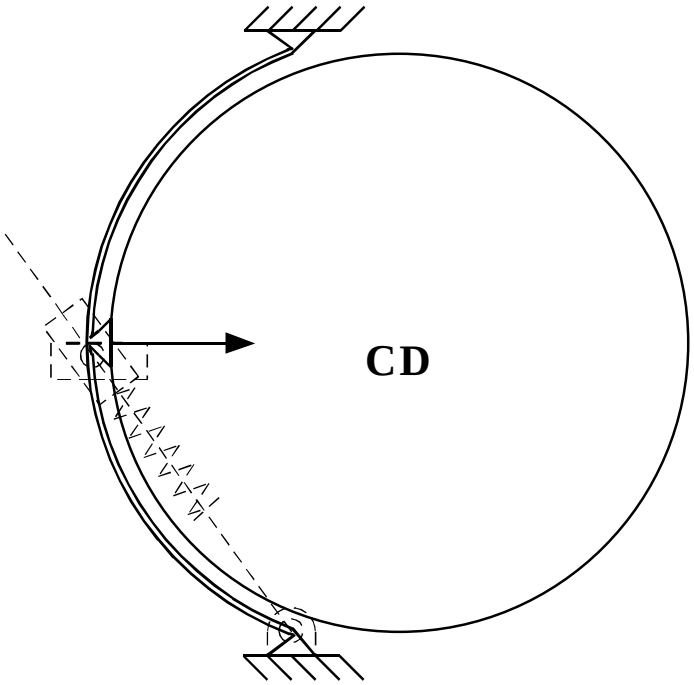

FIGURE 5-2: The resulting compliant bistable mechanism, based on the double-slider with a pin joint joining the sliders. A pseudo-rigid-body model mechanism is shown in dashed lines.

The resulting fully-compliant mechanism design is shown in Figure 5-2. This mechanism is a working compliant mechanism designed at BYU (Hilton and Beal, 1997).

The final step in the design process is to choose an appropriate material to allow the FBPP segment and the living hinges to have adequate deflections before failure. The dimensions of the FBPP segment's cross-section can then be found using the pseudo-rigid-body model to give the appropriate actuation force.

5.2.2 Example 2: Bistable Electrical Switch

5.2.2.1 Problem Statement- A bistable electrical switch is desired with a rotating lever used to toggle the mechanism between states. The lever must rotate through a ninety-degree

deflection between the two stable states, and the unstable state should lie midway between the two stable states. The maximum actuation moment is 0.04 N-m.

5.2.2.2 Solution- Because the rotating lever must be pinned to ground, this mechanism could be designed using a double-slider connected by a pin joint, a slider-crank or slider-rocker, or a four-bar mechanism. A slider-crank or slider-rocker mechanism is chosen here. Figure 5-3 shows five different configurations of this class which could be used to solve this problem. This figure illustrates how mechanism inversions can be used to create many different types of possible configurations. Specifically, for Figure 5-3(c-e), link two is taken as the ground link, and the spring is placed at positions 4, 3, and 2, respectively.

Figure 5-3(c) is chosen as the most likely candidate for this design problem because of its simplicity, allowing it to be constructed with only one link and one slider. In addition, by replacing the spring and slider with a FBPP segment, and by using living hinges in place of pin joints, the mechanism can be made fully compliant. The curvature of the FBPP segment must also be chosen so that it does not cross the rotating member in the second stable position. The mechanism design is shown in Figure 5-4. The relative link lengths and the geometry of the cross-section of the FBPP segment may now be chosen to meet the design criteria (the placement of the stable positions and the maximum moment required).

5.2.3 Example 3: A Bistable Micro-Device

5.2.3.1 Problem Statement- As mentioned in the first chapter, one of the reasons for developing this method of compliant bistable mechanism type synthesis is to determine possible designs for compliant bistable micro-mechanisms. These mechanisms should not exceed

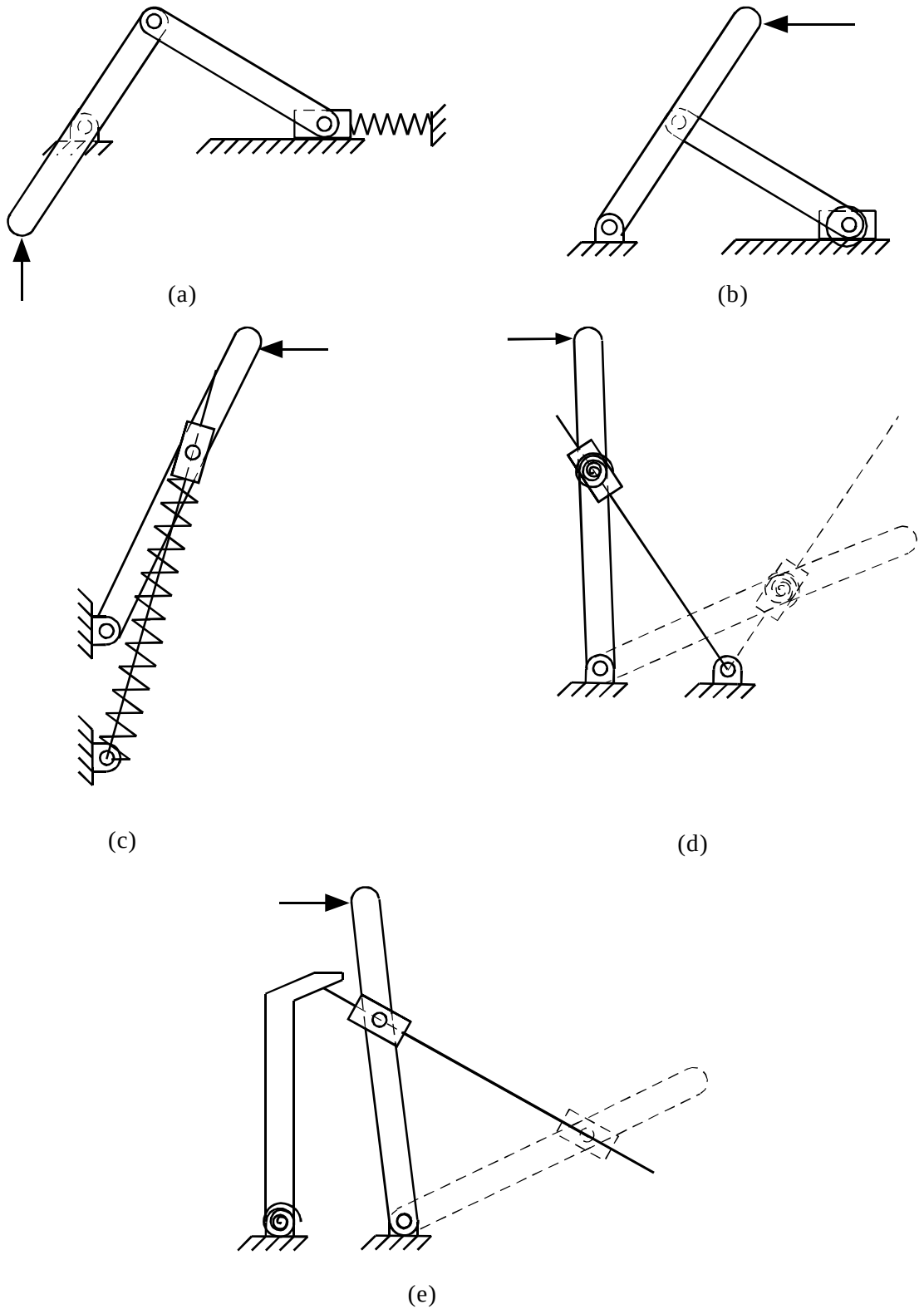

FIGURE 5-3: Five different possible configurations of the slider-crank or slider-rocker class which could meet the design specifications. The second positions of (d) and (e) are included to aid in visualization.

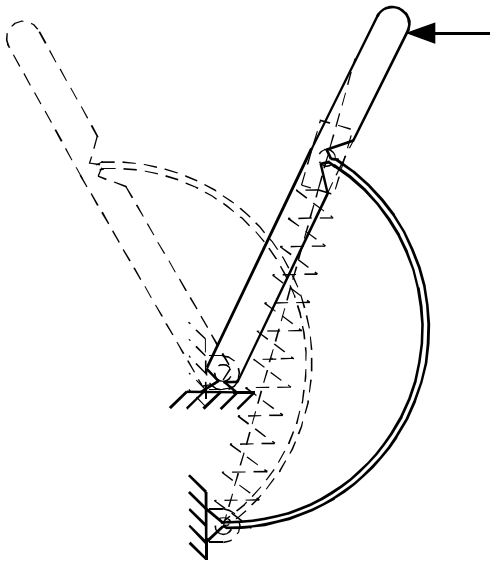

FIGURE 5-4: The conceptual design for the bistable electrical switch. Electrical contacts may be placed at the two stable positions. The pseudo-rigid-body model is shown for reference.

the strength limit of polysilicon (about 1.2×10^{10} dyn/cm^2) throughout their range of motion. Because of fabrication constraints, pin joints may be constructed only if they are fixed to the substrate, and conventional slider joints often have very high friction during motion.

5.2.3.2 Solution One - A Snap-Through Buckled Beam- A snap-through buckled beam could be used to solve this problem. In fact, the three bistable micro-devices which have been presented in published literature all use some form of bistable buckled beam (Hälg, 1990; Matoba et al., 1994; Wagner et al., 1996). The disadvantages of this approach to the problem were mentioned in Chapter 2. They include lack of flexibility in the stable positions which can be achieved and lack of freedom of motion due to being limited to out-of-plane deflection. However, it is possible to create a snap-through buckled beam design which does not require out-of-plane deflection. This may be done by using a curved beam

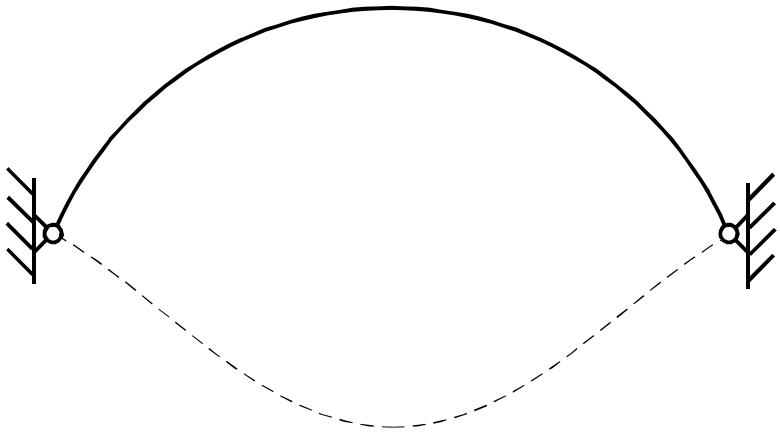

FIGURE 5-5: A functionally binary pinned-pinned segment which is pinned to ground on both ends. It will snap into the second stable position shown if a moment is applied to one of the pin joints, or if it is pushed by a force.

which is either fixed or pinned at the ends. The beam will be stable in the initial position and in a second position where it is curved in the opposite direction, much as Figure 4-2 shows. The stress in the beam will be lower if it is pinned on both ends. The resulting mechanism is really just a FBPP segment which is pinned to the substrate at both ends, as shown in Figure 5-5. A moment can then be applied to one pin, or a force can be applied anywhere along the segment's length, to snap it into its second stable position. This mechanism configuration has been studied in more detail, and the design and fabrication of actual devices is discussed in Appendix A.

5.2.3.3 Solution Two - A Four-Link Mechanism- While a snapping FBPP segment is simple, it does not allow very much flexibility in design. Therefore, the other mechanism classes should also be considered. Because slider joints have low reliability in MEMS, a four-link mechanism is chosen as the basic mechanism class. In addition, two fixed pin joints should be used because stress in the mechanism is a concern, and the rotation at the

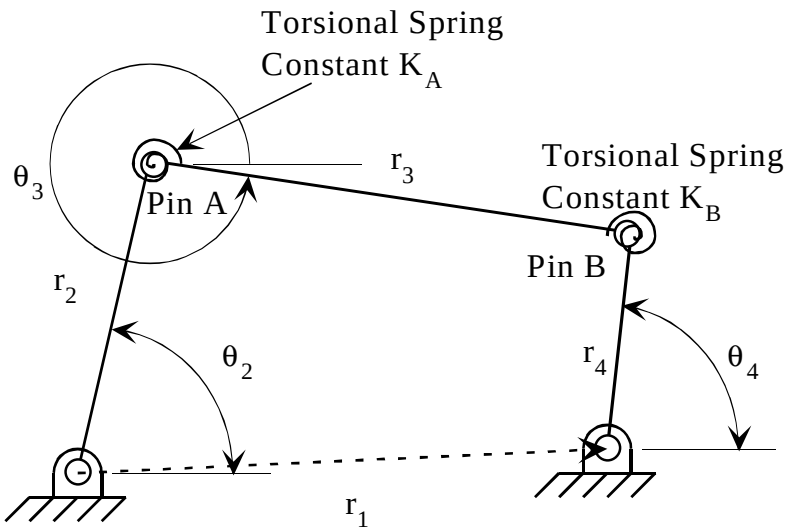

FIGURE 5-6: A model of the four-link mechanism class chosen for the bistable micro-mechanism.

pin joint helps to relieve stress. The resulting mechanism is a four-link mechanism with springs placed at positions 2 and 3. A model for this mechanism is shown in Figure 5-6. This mechanism will be more rigorously defined and classified in Chapter 6, but some additional points about the type synthesis of the mechanism will be discussed here.

If the mechanism is a Grashof mechanism, then it is best to choose the shortest link as the ground link. This is because a spring placed next to the shortest link will not cause the mechanism to have bistable behavior. Thus, the basic form of a Grashof micro-bistable mechanism will be a double-crank mechanism (Paul, 1979a). Of course, for a non-Grashof mechanism any link may be the ground link.

In addition, the two springs will require motion in opposite directions for either of them to have a bistable energy curve. This is because each spring goes bistable when the two links opposite it are collinear; however, if the two links opposite one spring are collinear, the two links opposite the other spring will not be, unless the mechanism is a

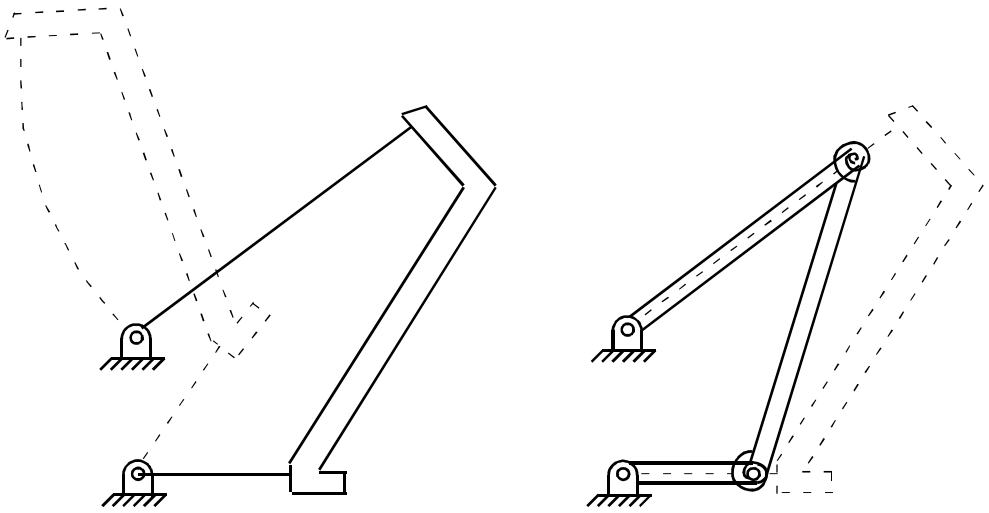

(a) (b)

FIGURE 5-7: An example of a bistable compliant micro-mechanism whose pseudo-rigid-body model is a four-link mechanism. (a) shows the mechanism in its two stable positions and (b) shows the pseudo-rigid-body model.

change-point mechanism. Change-point mechanisms are not feasible, though, because all of the links are made from one layer of polysilicon, so that they cannot overlap. For the same reason, it is desirable for the unstable position to occur when the two links opposite the spring have the same angle, rather than when they differ by π radians. Therefore, the mechanism designed should have one dominant spring with a relatively high stiffness compared to the other spring. In addition, the spring should have an unstable position when the two links opposite it have the same angle.

Figure 5-7 shows a mechanism design which meets all of these criteria. The mechanism's pseudo-rigid-body model is also shown. This mechanism is a non-Grashof mechanism, with link three being the longest link. Because both springs are adjacent to the longest link, each requires the two links opposite it to be at the same angle in its unstable position. Thus, if each spring were considered separately, each one would require motion

in the opposite direction of the other spring to result in bistable behavior. However, the spring on the shorter link has a much higher spring stiffness, causing its potential energy curve to dominate in the mechanism's total potential energy curve. For this reason, the mechanism is bistable in the two positions shown in Figure 5-7(a). Note that in the second position, the short compliant link is nearly undeflected. This example micro-mechanism has been fabricated and tested, and the results are given, along with those of several such mechanisms, in Chapter 6.

CHAPTER 6 *Design of Bistable MEMS Based on the Four-Link Mechanism Class*

This chapter presents work on the development of in-plane bistable MEMS based on the four-link mechanism class. Because of their ability to stay in position without power input and regardless of external disturbances, bistable mechanisms can allow MEMS systems to be built with increased energy efficiency and improved accuracy and precision in positioning. The energy efficiency effect may be especially critical in autonomous applications which must produce or store their own energy, such as devices which use micro-batteries as a power source. Bistable MEMS could also be used as mechanical switches, non-volatile memory, or micro-valves, as well as micro-positioners with two repeatable positions. The mechanisms presented here demonstrate the design and fabrication of planar bistable MEMS and establish the repeatability of their stable positions.

Previous examples of bistable MEMS relied on buckling of beams or membranes to obtain bistable behavior, as discussed in Chapter 1. The advantage of this method is that it is simple and requires less complex analysis. Trial and error approaches may even be used to find a working design of this type. However, lack of variety of possible motion, need for special fabrication, and reliance on residual stresses are all disadvantages of the

buckling approach. The method used in this chapter to design bistable devices, which is based on the choice of mechanism class and spring locations explained in section 5.2.3.3, "Solution Two - A Four-Link Mechanism," provides more freedom and flexibility, allowing the designer to change the location of equilibrium points, the actuation force, and device stresses. Moreover, the mechanism designs require only simple and well-known surface micromachining processes for their fabrication.

Based on the analysis of mechanism class and spring locations presented in Chapter 5, mechanisms with a pseudo-rigid-body model resembling a four-link mechanism were chosen for design. Each mechanism was to have two pin joints and two compliant segments. This class of bistable MEMS is defined more rigorously in this chapter, and it is given the name of "Young[1]" mechanisms to allow easy reference. It is believed that this mechanism class will play a substantial role in the development of working bistable MEMS applications.

The examples of bistable MEMS presented in this chapter demonstrate how bistable mechanisms may be designed to create more complex motion than has previously been possible for bistable micro-machines. In addition, testing has demonstrated the repeatability of the devices' equilibrium positions. The mechanisms will be presented by considering the general mechanism class used in these designs and describing the testing performed to characterize their bistable behavior.

1. Descriptive titles or acronyms were considered too unwieldy to use conveniently. Instead, the name "Young" was chosen because of the author's affiliation with Brigham Young University.

6.1 Definition of Young Mechanisms

To design compliant bistable planar MEMS, a specific class of mechanisms was defined, known as Young mechanisms. A Young mechanism is one that:

- Has two revolute joints, and, therefore, two links, where a link is defined as the continuum between two rigid-body joints (Midha et al., 1994)
- Has two compliant segments, both part of the same link
- Has a pseudo-rigid-body model which resembles a four-bar mechanism.

The first and second conditions, taken together, imply that the two pin joints are connected with one completely rigid link, while the other link consists of two compliant segments and one or more rigid segments. A general pseudo-rigid-body model of a Young mechanism is

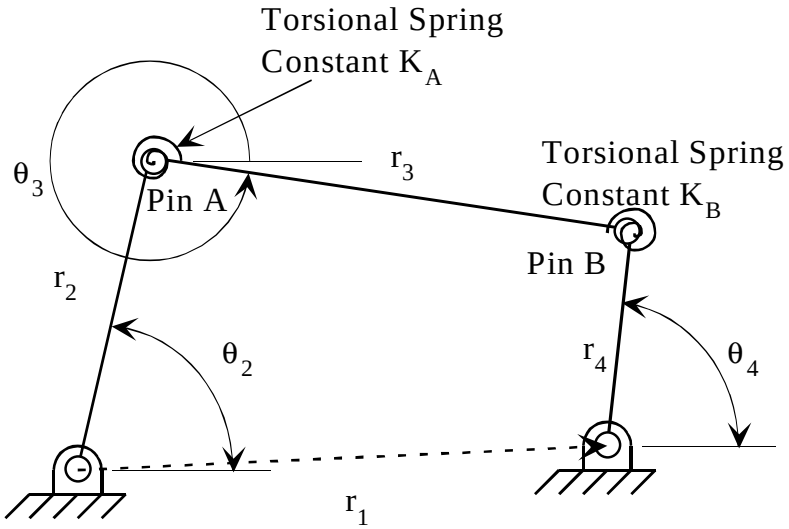

FIGURE 6-1: The generic model used to design bistable mechanisms. Pin A and Pin B represent compliant segments according to the pseudo-rigid-body model, with torsional spring constants K_A and K_B.

shown in Figure 6-1. In this model, the two revolute joints are connected to ground, while Pin A and Pin B represent compliant segments modeled by the pseudo-rigid-body model.

Young mechanisms make sense for MEMS for several reasons, as was explained previously in Chapter 5. For example, pin joints connected to the substrate (ground) can easily be fabricated with two layers of polysilicon, but true pin joints connecting two moving links require more layers. Also, the two pin joints help the mechanism to achieve larger motion, in general, by reducing the stress in the compliant segments. In addition, the two compliant segments give the mechanism the energy storage elements it needs for bistable behavior. Figure 6-2(a) illustrates an example of a Young mechanism, and Figure 6-2(b) shows its pseudo-rigid-body model.

Three main classes of Young mechanisms may be defined, depending on the type of compliant segments used. These are:

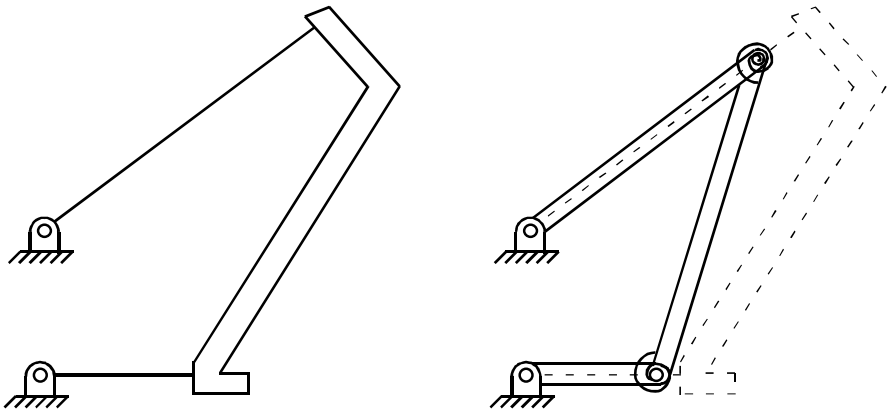

(a) (b)

FIGURE 6-2: A compliant bistable mechanism (a) with its corresponding pseudo-rigid-body model (b). This mechanism is a Class I bistable Young micro-mechanism fabricated as part of this study (mechanism 3-I, see Table 6-1).

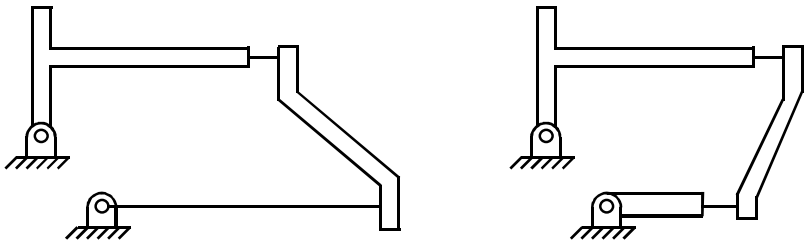

(a) (b)

FIGURE 6-3: Young mechanism Classes II and III. Class II, shown in (a) has one small-length flexural pivot and one fixed-pinned segment. Class III, shown in (b) has two small-length flexural pivots.

- Class I: Both compliant segments are fixed-pinned segments. The mechanism shown in Figure 6-2 is a Class I mechanism.
- Class II: One compliant segment is a fixed-pinned segment, and the other is a small-length flexural pivot. An example mechanism of this class is shown in Figure 6-3(a)
- Class III: Both compliant segments are small-length flexural pivots. An example mechanism is shown in Figure 6-3(b).

Classes I and II have been used in this study for bistable MEMS. No mechanisms of Class III were designed because the stresses for the small-length flexural pivots usually exceeded the strength of polysilicon.

A unique Young mechanism of Class I may be described using the seven parameters r_1, r_2, r_4, θ_{20}, θ_{40}, I_2, and I_4, where each parameter is defined as:

- r_1 - the distance between the centers of the pin joints.
- r_2 -the length of the largest side-link of the pseudo-rigid-body model. The length l_2 of the associated compliant fixed-pinned segment may be found from the equation

$$l_2 = \frac{r_2}{\gamma} \tag{6.1}$$

  where γ is given by the pseudo-rigid-body model.
- r_4 - the length of the shortest side-link of the pseudo-rigid-body model. The length l_4 of the associated compliant fixed-pinned segment may be found using the same method used to find l_2.
- θ_{20} - the initial value of θ_2 (defined in Figure 6-1) at the undeflected position.
- θ_{40} - the initial value of θ_4 (defined in Figure 6-1) at the undeflected position. An alternate approach to define the mechanism would be to specify the value of r_3 rather than one of the two initial angles. However, while r_3 describes the length of the third link in the pseudo-rigid-body model, it has little physical significance in the actual compliant mechanism. In addition, if only one angle is specified, the mechanism could take either the leading or the lagging form based on the link lengths, so that the definition of the mechanism would be less precise.

- I_2 - the area moment of inertia of the flexible segment associated with link 2. For a rectangular cross-section, like those used in each mechanism presented here,

$$I = \frac{ht^3}{12} \tag{6.2}$$

  where h is the height of the beam (out of the plane of motion) and t is the segment's thickness (within the plane of motion).
- I_4 - the area moment of inertia of the flexible segment associated with link 4. It is given by Eq. (6.2).

Given these parameters and the material's Young's modulus, the values of the torsional spring constants may be calculated from the equations

$$K_A = \gamma K_\Theta \frac{EI_2}{l_2} \tag{6.3}$$

$$K_B = \gamma K_\Theta \frac{EI_4}{l_4} \tag{6.4}$$

where γ and K_Θ are given by the pseudo-rigid-body model.

Similar parameters are required to define mechanisms of Class II, but an additional variable is needed to define the length of the small-length flexural pivot. The parameters defining a Class II mechanism are:

- r_1, r_4, θ_{20}, θ_{40}, I_4 - same as for Class I.
- r_2 - the length of pseudo-link 2, defined as the distance from the pin joint to the center of the small-length flexural pivot. No associated value of l_2 may be defined.
- I_2 - the area moment of inertia of the small-length flexural pivot, given by Eq. (6.2).
- l_s - length of the small-length flexural pivot.

Spring constant K_B is the same as for Class I, but K_A must be found from the equation

$$K_A = \frac{EI_2}{l_s} \tag{6.5}$$

6.1.1 The Design of Bistable Young Mechanisms

To design bistable Young mechanisms, equations must be used which relate the motion and potential energy of the mechanism. The motion of the model shown in Figure 6-1 may be found as a function of θ_2 using rigid-body kinematics. Equations and a description of the process used to analyze the motion of this mechanism may be found in any kinematics textbook (for example, Paul, 1979b; Erdman and Sandor, 1997). The potential energy equation may be found by summing the energy stored in the two torsional springs:

$$V = \frac{1}{2}(K_A\psi_A^2 + K_B\psi_B^2) \tag{6.6}$$

where V is the potential energy, K_A and K_B are the torsional spring constants, and ψ_A and ψ_B are the relative deflections of the torsional springs. These are given by

$$\begin{aligned} \psi_A &= (\theta_2 - \theta_{20}) - (\theta_3 - \theta_{30}) \\ \psi_B &= (\theta_4 - \theta_{40}) - (\theta_3 - \theta_{30}) \end{aligned} \tag{6.7}$$

where the "0" subscript denotes the initial (undeflected) value of each angle. The minima of Eq. (6.6) may be found by locating zeroes of the first derivative of V where the second derivative is positive. The first derivative of V with respect to θ_2 is

$$\frac{dV}{d\theta_2} = K_A\psi_A(1 - h_{32}) + K_B\psi_B(h_{42} - h_{32}) \tag{6.8}$$

where h_{32} and h_{42} are the kinematic coefficients (Paul, 1979b)

$$h_{32} = \frac{d\theta_3}{d\theta_2} = \frac{r_2 \sin(\theta_4 - \theta_2)}{r_3 \sin(\theta_3 - \theta_4)} \tag{6.9}$$

and

$$h_{42} = \frac{d\theta_4}{d\theta_2} = \frac{r_2 \sin(\theta_3 - \theta_2)}{r_4 \sin(\theta_4 - \theta_3)} \tag{6.10}$$

The second derivative of potential energy is

$$\frac{d^2V}{d\theta_2^2} = K_A(1 - 2h_{32} + h_{32}^2 - \psi_A h'_{32}) + K_B[h_{42}^2 - 2h_{42}h_{32} + h_{32}^2 + \psi_B(h'_{42} - h'_{32})] \tag{6.11}$$

where

$$h'_{32} = \frac{dh_{32}}{d\theta_2} = \frac{r_2}{r_3}\left[\frac{\cos(\theta_4 - \theta_2)}{\sin(\theta_3 - \theta_4)}(h_{42} - 1) - \frac{\sin(\theta_4 - \theta_2)\cos(\theta_3 - \theta_4)}{\sin^2(\theta_3 - \theta_4)}(h_{32} - h_{42})\right] \tag{6.12}$$

$$h'_{42} = \frac{dh_{42}}{d\theta_2} = \frac{r_2}{r_4}\left[\frac{\cos(\theta_3 - \theta_2)}{\sin(\theta_4 - \theta_3)}(h_{32} - 1) - \frac{\sin(\theta_3 - \theta_2)\cos(\theta_4 - \theta_3)}{\sin^2(\theta_4 - \theta_3)}(h_{42} - h_{32})\right] \tag{6.13}$$

Any value of θ_2 for which Eq. (6.8) is zero and Eq. (6.11) is positive identifies a relative minimum of potential energy, and, thus, a stable equilibrium position.

The maximum nominal stress in the compliant segment during motion is another important quantity to consider. Compliant mechanism theory can be used to find this stress from the maximum angular deflection of each segment, $\psi_{A,max}$ and $\psi_{B,max}$. For either compliant segment, the maximum nominal stress may be approximated with the classical stress equation

$$\sigma_{0max} = \frac{M_{max}c}{I} \tag{6.14}$$

where M_{max} may be approximated, using the pseudo-rigid-body model, as the product of K and ψ_{max}. Assuming a rectangular cross-section,

$$\sigma_{0max} = \frac{6K\psi_{max}}{ht^2} \tag{6.15}$$

where h is the height of the compliant beam (the dimension out of the plane of motion) and t is its thickness (the dimension within the plane of motion). This nominal stress is the stress calculated without taking stress concentrations into account. It may be used by comparing the nominal stress in the segment to the nominal stress at fracture of previously-tested devices with similar stress concentrations.

To design the mechanisms presented in this paper, the seven (Class I) or eight (Class II) parameters described above were varied to find mechanism configurations with two stable positions, as determined by the potential energy equation, without exceeding the polysilicon strength during motion. To avoid fracture, a maximum strain, equal to the ratio of ultimate strength to Young's modulus, S_{UT}/E, was specified to be 1.05×10^{-2}. This value was determined from prior experience in the design of compliant micro-mechanisms.

This design process was used to design a total of fifteen bistable micro-mechanism configurations, seven of Class I and eight of Class II. Each mechanism was identified by a number from one to fifteen. The defining parameters for all fifteen mechanism configurations are listed in Table 6-1. Each mechanism's class is designated by the roman numeral following the mechanism's identifying number. Each mechanism is shown in a microscope image in Appendix D. To illustrate the design process, one of these mechanisms, mechanism number 5-II, will be studied in more detail.

6.1.2 A Bistable MEMS Example

Mechanism 5 is a Class II mechanism, with one small-length flexural pivot and one fixed-pinned segment, as illustrated Figure 6-4(a). The design parameters for this mechanism are listed in Table 6-1. These parameters define the pseudo-rigid-body model shown in Figure 6-4(b). Using the design parameters listed in Table 6-1, the potential energy curve through the mechanism's motion may be generated using Eq. (6.6). This curve is shown as a function of θ_2 in Figure 6-5. The two relative minima on this curve represent the two stable positions of the mechanism. These minima occur at $\theta_2 = \theta_{20} = 83\ ^\circ$ and $\theta_2 = 7\ ^\circ$. Therefore, the angular deflection of the second link between

TABLE 6-1: Design parameters for the fifteen mechanisms. Each mechanism's class is given by the roman numeral following the dash in the mechanism number.

Mech. No.	r_1, μm	r_2, μm	r_4, μm	θ_{20}	θ_{40}	I_2, μm^4	I_4, μm^4	l_s, μm
1-I	120	480	108	130°	40°	4.5	4.5	
2-I	120	216	120	130°	90°	4.5	4.5	
3-I	120	236	109	130°	90°	4.5	4.5	
4-II	100	295	364	83°	53°	7.88	4.5	26
5-II	100	250	250	83°	53°	4.5	4.5	26
6-II	100	200	300	70°	46°	7.88	4.5	33
7-II	100	300	400	90°	45°	7.88	4.5	30
8-II	100	300	400	90°	45°	4.5	4.5	30
9-I	120	360	78	140°	50°	4.5	4.5	
10-I	100	404	144	130°	58°	4.5	4.5	
11-I	100	404	128	130°	58°	4.5	4.5	
12-II	100	80	200	40°	15°	7.88	4.5	9
13-II	100	80	200	40°	15°	7.88	4.5	9
14-II	100	130	200	30°	15°	4.5	4.5	13
15-I	100	250	120	120°	200°	4.5	4.5	

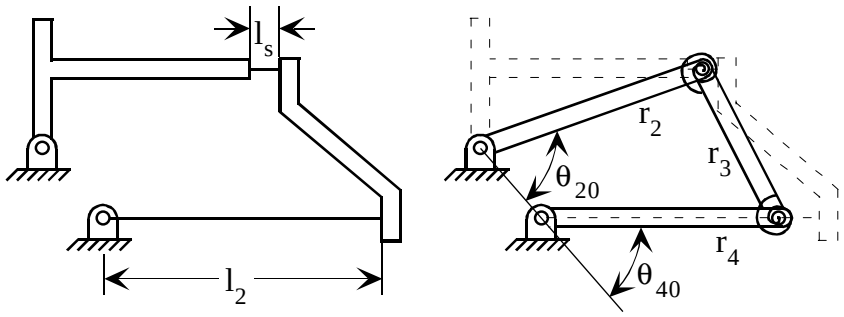

(a) (b)

FIGURE 6-4: An illustration of mechanism 5-II (a) with its pseudo-rigid-body model (b).

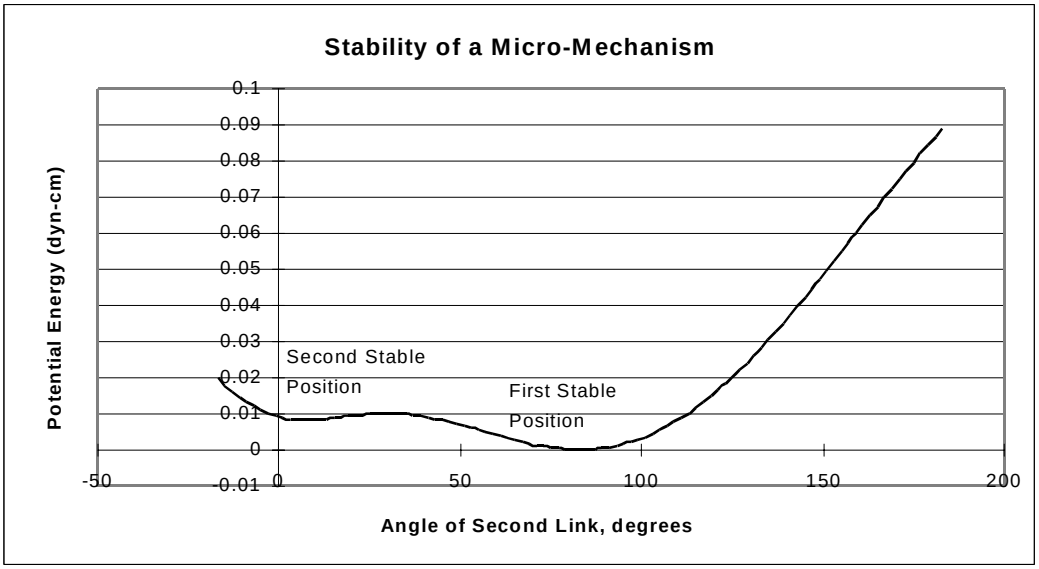

FIGURE 6-5: The potential energy curve of mechanism five as a function of θ_2.

the two stable positions is approximately 76°. At each point, the first derivative of potential energy, given in Eq. (6.8), is zero, and the second derivative, given in Eq. (6.11), is positive. The maximum strain in each compliant segment to Young's modulus may be calculated using Eq. (6.15). This strain is 1.02×10^{-2} for the small-length flexural pivot and 5.74×10^{-3} for the fixed-pinned segment. As stated earlier, fracture is expected when the ultimate strain is reached at 1.05×10^{-2}.

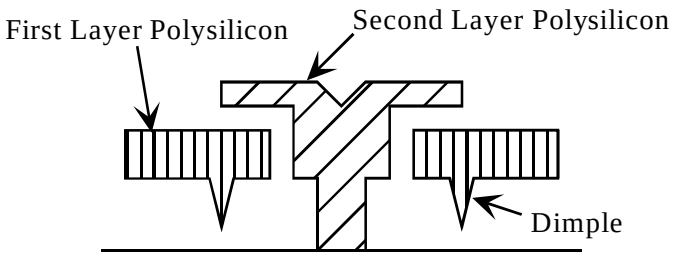

FIGURE 6-6: A cross-section of the pin joints fixed to the substrate. A disk is formed from the first layer of polysilicon, with a post formed from the second layer of polysilicon.

6.2 Mechanism Fabrication and Testing

Each of the fifteen mechanism configurations was fabricated using the Multi-User MEMS Process (MUMPS) at MCNC. This process allows the designer to use two released layers of polysilicon. For all cases, the mechanisms were fabricated from the first layer, with a thickness of 2.0 μm. In addition, the "stacked polysilicon" method described by Comtois and Bright (1995) was used to make some of the small-length flexural pivots as thick as both layers, or 3.5 μm thick. The pin joints fixed to ground were fabricated as shown in Figure 6-6, with a disk formed from the first layer of polysilicon and a post formed from the second layer. The mechanisms were released at the BYU Integrated Microelectronics Laboratory and were tested by displacing them with probes. Figure 6-7 shows a scanning electron microscope (SEM) photograph of an example mechanism from Class I (mechanism 3-I) and another from Class II (mechanism 5-II).

Eleven of the mechanism configurations fabricated demonstrated bistable behavior by snapping between the two stable states. Figure 6-8 shows an SEM image of mechanism 3-I in the second stable position, and Figure 6-9 shows an SEM image of mechanism 5-II

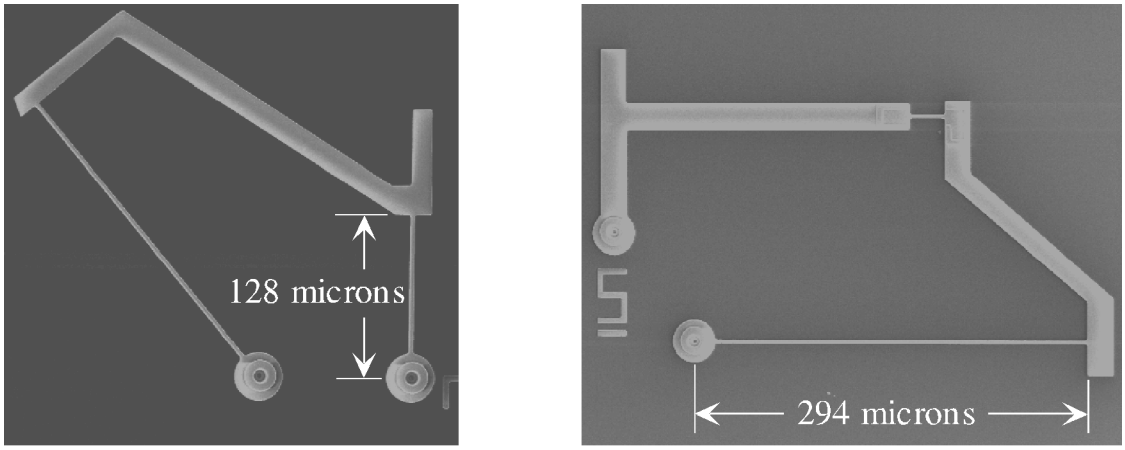

(a) (b)

FIGURE 6-7: Scanning electron microscope (SEM) photographs of two bistable micro-mechanisms. One dimension is given to provide an idea of the mechanism's scale.

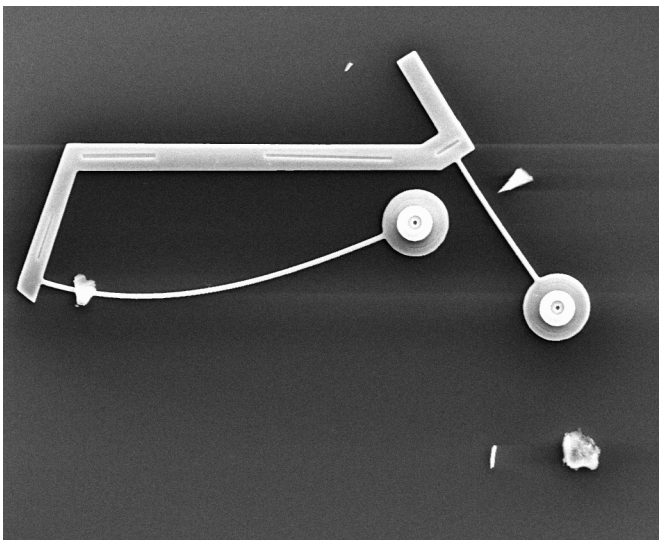

FIGURE 6-8: Mechanism 3-I in its second stable position.

in the second stable position. In the figures, note the large, non-linear deflections in the compliant segments. Note also that one of the compliant segments is still deflected in the second stable position, indicating that some energy is stored in that state. Despite this stored energy, the mechanism is at a local minimum of potential energy. In other words, while the second stable position does not represent an absolute minimum of potential

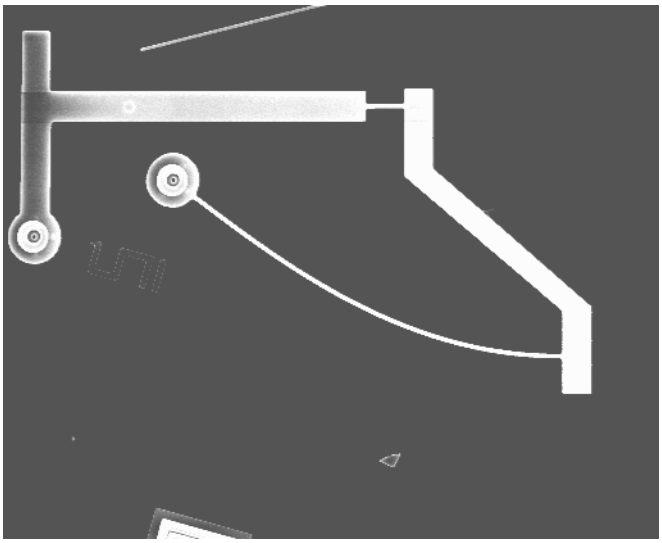

FIGURE 6-9: Mechanism 5-II in its second stable positions.

energy (i.e., the potential energy is not zero), it is a local minimum because any small deviation from that position requires more energy to be put into the mechanism. Figure 6-5 illustrates this point for mechanism 5-II. The pictures showing the second stable position were taken by displacing the mechanisms until they reached their unstable states, after which they snapped into the positions shown. This successful snapping behavior represents the first time planar MEMS have shown bistable behavior without buckling.

The repeatability of each stable position was measured by recording the angle between a reference line and a rigid part of each mechanism. For example, on mechanisms of Class II, the angle ABC, shown in Figure 1, was measured when the mechanism was in each stable position. This measurement allows determination of the change in θ_2 for the two stable positions. For mechanisms of Class I, the angle between the line joining the pin joints and the rigid coupler link was measured. This angle allows determination of the change in θ_3 for the two stable positions.

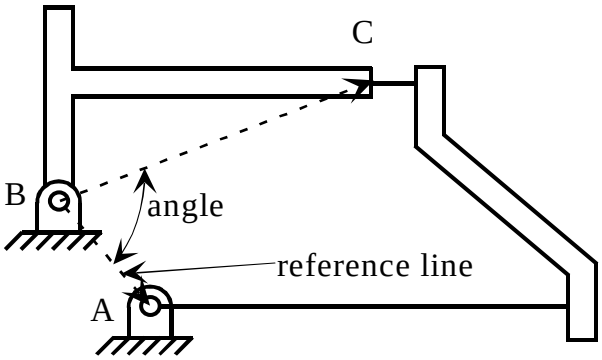

FIGURE 1: The angle measured to determine the repeatability of Class II mechanisms' stable positions

The angle was measured in each case over several cycles of snapping. The measurement was made using computer analysis of video images. The standard deviation of the angles measured in each position was then used as an indication of the variation in position for that stable state. Of the eleven configurations which successfully snapped between positions, only eight snapped enough times before fracture to make a good measurement of the variability in the stable position. The standard deviations of the angles for these eight mechanism configurations are listed in Table 1, along with the difference

TABLE 1: The standard deviation of angles measured at stable positions. Position 1 is the undeflected stable position; Position 2 is the other stable position.

Mechanism	*Mean Angular Difference*	*Samples at Pos. 1*	*St. Dev., Pos. 1*	*Samples at Pos. 2*	*St. Dev., Pos. 2*	*Predicted Angular Difference*
2-I	0.849 rad	3	0.053 rad	4	0.099 rad	0.958 rad
3-I	0.909 rad	7	0.038 rad	6	0.098 rad	1.09 rad
5-II	1.30 rad	8	0.020 rad	7	0.0079 rad	1.36 rad
10-I	1.10 rad	7	0.074 rad	3	0.079 rad	1.33 rad
11-I	1.18 rad	6	0.034 rad	6	0.025 rad	1.36 rad
12-II	0.457 rad	10	0.068 rad	10	0.027 rad	0.349 rad
13-II	0.449 rad	18	0.056 rad	20	0.043 rad	0.349 rad
14-II	0.308 rad	12	0.064 rad	14	0.061 rad	0.332 rad

between the means of the angles measured at each position. The difference in the means is presented to allow comparison between the angular difference between stable states and the variation of position at each stable state. The predicted angular difference between the stable positions is also shown. Many of the mechanisms showed a very low standard deviation, indicating a high level of repeatability in the stable positions. However, in most cases, the measured angular difference is less than the predicted angular difference. This is because friction between the mechanism and the substrate exceeds the restoring force for small deviations around the stable position.

While many of the mechanisms showed good bistable behavior, several of the mechanisms either failed to snap or else fractured after snapping once or twice. This is most likely due to high frictional forces caused by rubbing against the substrate. The frictional forces could overcome the mechanism's restoring force, causing the mechanism not to snap into a stable position. Methods of decreasing the friction between the mechanism and the substrate have been studied to improve the performance of these mechanisms. These methods are further explained in Appendix B.

CHAPTER 7 *Conclusions and Recommendations*

The purpose of this thesis has been to identify the compliant mechanism configurations which result in bistable behavior. This analysis allowed the development of a method of type synthesis of bistable mechanisms, and the application of this method to the design of bistable MEMS has been demonstrated. This method of type synthesis has shown itself to be easily applied to a variety of bistable mechanism synthesis problems, including the design of bistable MEMS. This chapter gives a brief summary of the work presented in this thesis, and it offers some recommendations for future research opportunities in this area.

7.1 Conclusions

The theory developed in this thesis consists of the classification scheme and analysis of mechanism configurations which result in a bistable mechanism. The classification scheme performs a double function: it allows existing bistable mechanisms to be grouped together in meaningful ways for analysis, and it gives the designer sets of easy-to-use choices when facing a synthesis problem. In addition, most of the mechanism classes discussed here can be realized using either compliant or rigid-body mechanisms.

The real power behind the research reported here lies in the method of type synthesis developed as a result of the analysis. Each class presented in the classification scheme has been rigorously analyzed to determine the spring locations which cause bistable behavior. In this analysis, it was assumed that all the springs in the mechanism were undeflected at the same position. This condition will be discussed further in the Recommendations section. Based on the successful completion of the analysis, the method of type synthesis was developed and explained.

Several example problems were presented to demonstrate the method of bistable type synthesis. These problems demonstrate how easily the method may be applied to specific design problems. The ease of use of the method is particularly striking when compared with the laborious trial-and-error solutions required in the past. The design of bistable MEMS was particularly studied, and a basic model of the mechanism class to be used in bistable MEMS was developed.

This basic model was then studied in more detail to facilitate the design of working bistable MEMS. A specific class of mechanisms was derived, called Young mechanisms. This class is really a sub-class of the four-link mechanism class. Young mechanisms are compliant mechanisms consisting of two links, where a link is defined as the continuum between rigid-body joints (Midha et al., 1994). In addition, one of the links contains two compliant segments and one or more rigid segments, and the mechanism's pseudo-rigid-body model resembles a four-link mechanism. Young mechanisms were further divided into three sub-classes depending on the types of compliant segments used.

Using the Young mechanism class, fifteen bistable MEMS were designed. After fabrication using the MUMPS process, the fifteen bistable MEMS were tested by pushing

on them with probes. Several of the mechanisms successfully snapped into two stable positions, representing the first time that bistable MEMS have been realized without requiring the buckling of beams. The repeatability of the stable positions was measured using motion analysis software, and a high degree a repeatability in positions was found. It is expected that this successful demonstration of bistable micro-mechanisms will lead to a variety of MEMS incorporating bistable behavior.

7.2 Recommendations

Several areas of research remain to be explored in the type synthesis of bistable mechanisms and the development of bistable MEMS. This section outlines some of these future research opportunities.

7.2.1 Mechanisms with Multiple Degrees of Freedom

All of the mechanism classes studied in this thesis had one degree of freedom, meaning that only one input was needed to completely describe the state of the mechanism. However, it is conceivable and possibly even desirable to characterize the stability and energy states of mechanisms whose pseudo-rigid-body models have multiple degrees of freedom. For example, the shampoo lid mechanism shown in Figure 2-10, on page 18, may be modeled as the five-bar mechanism shown in Figure 2-11, on page 18. Kinematically, this five-bar mechanism has two degrees of freedom, requiring two inputs to determine the mechanism's state. A knowledge of this mechanism's motion reveals that only one input is given, though - the top is flipped open or shut. Most likely, the mechanism is seeking the lowest energy state that it can take for a given deflection of the top. In other words, with

only one input specified, the mechanism is free to move to its lowest energy state for that value of the input. This idea could be studied in more detail by finding the energy surface that results from varying the two inputs. Then, stable states would be represented by local minima of the energy surface, but unstable states could also represent a potential energy minimum for one input and a maximum for the other - or, in other words, a saddle point. This idea could then be generalized to mechanisms with higher degrees of freedom, possibly allowing a mechanism with very complex motion but requiring only one specified input. Therefore, it is recommended that the energy equations of mechanisms with multiple degrees of freedom be studied in more depth.

7.2.2 Higher-Order Chains

In addition to multiple degree-of-freedom mechanisms, this thesis has not addressed mechanism types consisting of more than four kinematic pairs (or joints). For example, six-bar mechanisms may be constructed with seven joints to form a mechanism with one degree of freedom. The motion and energy analysis of such mechanisms are outside the scope of this research. However, because the motion of six-bar or higher order mechanisms is more complex than any of the motions studied here, it may be profitable to study these mechanisms to allow easy synthesis of bistable mechanisms with more complex motion.

7.2.3 Compliant Mechanisms in which Not All Joints Are Undeflected at One Stable Position

One of the conditions on the analysis presented in this thesis is that all the compliant joints in the mechanism are undeflected at the same mechanism position, corresponding to

what has been called the first stable position. This condition applies especially to compliant MEMS because assembly of micro-mechanisms is not feasible, requiring all joints to be fabricated in a particular mechanism position. This is not a requirement of macro-mechanisms, though. Such mechanisms may have two or more compliant segments which are assembled in such a way that they are not undeflected at the same mechanism location. In such a case, the analysis presented in section 4.6, "Analysis of Mechanisms with More than One Spring," becomes invalid. Instead, the interactions of any combination of springs in the mechanism would have to be studied individually. It is possible that such an analysis may uncover a case where the potential energy of each spring adds in such a way that two or more stable positions result. It is also possible that the analysis would find a way to create a compliant mechanism with an energy curve which is flat over a large range of motion. This would mean that all forces in the mechanism are balanced, so that a large region of neutral stability results. Such a result would have valuable applications. Consequently, it is recommended that future research be done in this area.

7.2.4 Characterization of Frequency Response of Bistable Mechanisms

The theory presented in this thesis establishes the steady-state stability of bistable mechanisms. However, full characterization of these mechanisms requires theory to be developed to allow the prediction of the frequency response of these mechanisms. This work is especially vital for MEMS, where a very fast response to inputs will be required for any working systems.

7.2.5 On-Chip Actuation of Bistable MEMS

The examples of bistable MEMS in this thesis were all actuated using probe tips. While this was sufficient for showing that bistable MEMS were feasible, it obviously falls far short of desirability. Not only would on-chip actuation move these mechanisms one step closer to real applications, but it would also contribute to the reliability of the mechanisms. This is because on-chip actuation should have less variation than pushing on the mechanisms with probe tips, which introduces such sources of variation as human error, quality of the probe tip, and so on.

Studies on the on-chip actuation of bistable mechanisms are already underway at Brigham Young University. Several methods have been designed, such as rotary comb drives, large arrays of linear comb drives, and thermal actuators. The results of these actuation designs are still under investigation.

7.2.6 Development of Particular Applications for Bistable MEMS

While bistable MEMS have great possibilities for future MEMS applications, a working micro-system incorporating a bistable device such as those presented here has yet to be demonstrated. For example, a working micro-switch or micro-valve is a feasible next step in the research. Such a device would allow the demonstration and characterization of the advantages of bistable MEMS. Some work has been started at Brigham Young University in this area.

List of References

Abe, T., Messner, W.C., and Reed, M.L., 1995, "Effective Methods to Prevent Stiction During Post-Release-Etch Processing," *Proceedings of IEEE Micro Electro Mechanical Systems 1995*, 95CH35754, pp. 94-99.

Ananthasuresh, G.K., Kota, S., and Gianchandani, Y., 1993, "Systematic Synthesis of Microcompliant Mechanisms - Preliminary Results," *Proceeding of the Third National Applied Mechanisms and Robotics Conference*, Cincinnati, Ohio, Paper No. AMR-93-082.

Ananthasuresh, G.K., 1994, "A New Design Paradigm for Micro-Electro-Mechanical Systems & Investigations on the Compliant Mechanism Synthesis," Ph.D. Dissertation, University of Michigan, Ann Arbor, Michigan, 1994.

Ananthasuresh, G.K., Kota, S., and Gianchandani, Y., 1994, "A Methodical Approach to the Design of Compliant Micromechanisms," *Solid-State Sensor and Actuator Workshop*, Hilton Head Island, South Carolina, pp. 189-192.

Ananthasuresh, G.K. and Kota, S., 1996, "The Role of Compliance in the Design of MEMS," *Proceedings of the 1996 ASME Design Engineering Technical Conferences*, 96-DETC/MECH-1309.

Artobolevsky, I.I., 1975, *Mechanisms in Modern Engineering Design*, MIR Publishers, Moscow, Vol. I.

Barker, C.R., 1985, "A Complete Classification of Planar Four-Bar Linkages," *Mechanism and Machine Theory*, Vol. 20, No. 6, pp. 535-554.

Bisshopp, K.E. and Drucker, D.C., 1945, "Large Deflection of Cantilever Beams," *Quarterly of Applied Mathematics*, Vol. 3, No. 3, pp. 272-275.

Burns, R.H., 1964, "The Kinetostatic Synthesis of Flexible Link Mechanisms," Ph.D. Dissertation, Yale University, New Haven, Connecticut.

Burns, R.H. and Crossley, F.R.E., 1966, "Structural Permutations of Flexible Link Mechanisms," ASME Paper No. 66-MECH-5.

Burns, R.H. and Crossley, F.R.E., 1968, "Kinetostatic Synthesis of Flexible Link Mechanisms," ASME Paper No. 68-MECH-36.

Chironis, N.P., 1991, *Mechanisms and Mechanical Devices Sourcebook*, McGraw-Hill, Inc., New York.

Comtois, J.H. and Bright, V.M., 1995, “Design Techniques for Surface-Micromachining MEMS Processes,” *SPIE*, Vol. 2639, pp. 211-222.

Derderian, J.M., Howell, L.L., Murphy, M.D., Lyon, S.M., and Pack, S.D., 1996, “Compliant Parallel-Guiding Mechanisms,” *Proceedings of the 1996 ASME Design Engineering Technical Conferences*, 96-DETC/MECH-1208.

Derderian, J.M., 1996, “The Pseudo-Rigid-Body-Model Concept and Its Application to Micro Compliant Mechanisms,” M.S. Thesis, Brigham Young University, Provo, Utah.

Edwards, B.T., 1996, “Functionally Binary Pinned-Pinned Segments,” M.S. Thesis, Brigham Young University, Provo, Utah.

Erdman, A.G. and Sandor, G.N., 1997, *Mechanism Design: Analysis and Synthesis*, Vol. 1, 3rd Ed., Prentice Hall, New Jersey.

Euler, L., 1744, *Methodus Inveniendi Leneas Curvas Maximi Minimive Peoprietate Gavdentes*, Lausanne and Beneva (in Latin); (in English) see Isis vol. 20, Bruges, Belgium, November 1933.

Frecker, M., Kota, S., Fonseca, J., and Kikuchi, N., 1995, “A Systematic Synthesis Method for the Design of Distributed Compliant Mechanisms,” *AMR ‘95 - The Fourth National Applied Mechanisms and Robotics Conference*, Cincinnati, OH, Vol. 2, #062, December, 1995.

Frecker, M.I., Kikuchi, N., and Kota, S., 1996, “Optimal Synthesis of Compliant Mechanisms to Meet Structural and Kinematic Requirements - Preliminary Results,” *Proceedings of the 1996 ASME Design Engineering Technical Conferences*, 96-DETC/DAC-1497.

Frecker, M.I., Kota, S., and Kikuchi, N., 1997, “Use of Penalty Function in Topological Synthesis and Optimization of Strain Energy Density of Compliant Mechanisms,” *Proceedings of the 1997 ASME Design Engineering Technical Conferences*, DETC97/DAC-3760.

Freudenstein, F., 1955, “Approximate Synthesis of Four-Bar Linkages,” *Trans. ASME*, Vol. 77, No. 6, pp. 853-861.

Frisch-Fay, R., 1962, *Flexible Bars*, Butterworth, Washington, D.C.

Ginsberg, J.H. and Genin, J, 1984, *Statics and Dynamics, Combined Version*, John Wiley & Sons, New York.

Gorski, W., 1976, "A Review of Literature and a Bibliography on Finite Elastic Deflections of Bars," *Transactions of the Institute of Engineers, Australia, Civil Engineering Transactions*, Vol. 18, No. 2, pp. 74-85.

Grashof, F., 1883, *Theoretische Mashinenlehre*, Leipzig, pp. 113-118.

Hälg, B., 1990, "On A Nonvolatile Memory Cell Based on Micro-electro-mechanics," *IEEE Micro Electro Mechanical Systems 1990*, pp. 172-176.

Harrisberger, L., 1961, *Mechanization of Motion*, John Wiley & Sons, Inc., New York, New York.

Hartenberg, R.S. and Denavit, J., 1964, *Kinematic Synthesis of Linkages*, McGraw-Hill Book Company, New York, New York.

Her, I. and Midha, A., 1987, "A Compliance Number Concept for Compliant Mechanisms, and Type Synthesis," *Journal of Mechanisms, Transmissions, and Automation in Design*, Trans. ASME, Vol. 109, No. 3, pp. 348-355.

Her, I., Midha, A., and Salamon, B.A., 1992, "A Methodology for Compliant Mechanisms Design: Part II - Shooting Method and Application," *Advances in Design Automation*, (Ed.:D.A. Hoeltzel), DE-Vol. 44-2, 18th ASME Design Automation Conference, pp. 39-45.

Hill, T.C., Midha, A., 1990, "A Graphical User-Driven Newton-Raphson Technique for use in the Analysis and Design of Compliant Mechanisms," *Journal of Mechanical Design*, Trans. ASME, Vol. 112, No. 1, pp. 123-130.

Hilton, L. and Beal, V.S., 1997, "Storage Case for Disk-Shaped Media Having a Bistable Ejection Mechanism Utilizing Compliant Device Technology," U.S Patent No. 5,590,768, granted Jan. 7, 1997.

Howell, L.L. and Midha, A., 1994a, "A Method for the Design of Compliant Mechanisms with Small-Length Flexural Pivots," *ASME Journal of Mechanical Design*, Vol. 116, No. 1, pp. 280-290.

Howell, L.L. and Midha, A., 1994b, "The Development of Force-Deflection Relationships for Compliant Mechanisms," *Machine Elements and Machine Dynamics*, DE-Vol. 71, 23rd ASME Biennial Mechanisms Conference, pp. 501-508.

Howell, L.L., Midha, A., and Murphy, M.D., 1994a, "Dimensional Synthesis of Compliant Constant-Force Slider Mechanisms," *Machine Elements and Machine Dynamics*, DE-Vol. 71, 23rd ASME Biennial Mechanisms Conference, pp. 509-515.

Howell, L.L, Rao, S.S., and Midha, A., 1994b, “The Reliability-Based Optimal Design of a Bistable Compliant Mechanism,” *ASME Journal of Mechanical Design*, Vol. 117, No. 1, pp. 156-165.

Howell, L.L. and Midha, A., 1995a, “Parametric Deflection Approximations for End-Loaded, Large-Deflection Beams in Compliant Mechanisms,” *ASME Journal of Mechanical Design*, Vol. 117, No. 1, pp. 156-165.

Howell, L.L. and Midha, A., 1995b, “Determination of the Degrees of Freedom of Compliant Mechanisms Using the Pseudo-Rigid-Body Model Concept,” *Proceedings of the Ninth World Congress on the Theory of Machines and Mechanisms*, Milano, Italy, Vol. 2, pp. 1537-1541.

Howell, L.L, Midha, A., and Norton, T.W., 1996, “Evaluation of Equivalent Spring Stiffness for Use in a Pseudo-Rigid-Body Model of Large-Deflection Compliant Mechanisms,” *ASME Journal of Mechanical Design*, Vol. 118, No. 1, pp. 126-131.

Howell, L.L. and Midha, A., 1996a, “Parametric Deflection Approximations for Initially Curved, Large-Deflection Beams in Compliant Mechanisms,” *Proceedings of the 1996 ASME Design Engineering Technical Conferences*, 96-DETC/MECH-1215.

Howell, L.L. and Midha, A., 1996b, “A Loop-Closure Theory for the Analysis and Synthesis of Compliant Mechanisms,” *Journal of Mechanical Design*, March 1996, Vol. 118, pp. 121-125.

Jensen, P.W., 1991, *Classical and Modern Mechanisms for Engineers and Inventors*, Marcel Dekken, Inc., New York.

Jensen, B.D., Howell, L.L, Gunyan, D.B., and Salmon, L.G., 1997, “The Design and Analysis of Compliant MEMS Using the Pseudo-Rigid-Body Model,” *Microelectromechanical Systems (MEMS) 1997*, 1997 ASME International Mechanical Engineering Congress and Exposition, November 16-21, 1997, Dallas, TX, DSC-Vol. 62, pp. 119-126.

Jensen, B.D., Howell, L.L., and Salmon, L.G., 1998, “Introduction of Two-Link, In-Plane, Bistable Compliant MEMS,” *Proceedings of the 1998 ASME Design Engineering Technical Conferences*, DETC98/MECH-5837.

Kimbrell, J.T., 1991, *Kinematics Analysis and Synthesis*, McGraw-Hill, Inc., New York, New York.

Lagrange, J.L., 1788, *Mecanique Analytique*, Vol. 1, Pt.1, Sec. 3, Art 5, published 1853 by Mallet-Bachelier, Paris.

Larsen, U. D., Sigmund, O. and Bouwstra, S., 1997, “Design and Fabrication of Compliant Mechanisms and Material Structures with Negative Poisson's Ratio,” *Journal of Microelectromechanical Systems*, Vol. 6, No. 2, pp. 99-106.

Leipholz, H., 1970, *Stability Theory,* Academic Press, New York and London.

Liapunov, A.M., 1897, *Jour. de Math*, Ser. 5, Vol. 3, p. 81.

Lyon, S.M., Evans, M.S., Erickson, P.A., and Howell, L.L, 1997, "Dynamic Response of Compliant Mechanisms Using the Pseudo-Rigid-Body Model," *Proceedings of the 1997 ASME Design Engineering Technical Conferences,* DETC97/VIB-4177.

Mallik, A.K., Ghosh, A., and Dittrich, G., 1994, *Kinematic Analysis and Synthesis of Mechanisms,* CRC Press, Inc., Florida.

Matoba, H., Ishikawa, T., Kim, C., and Muller, R.S., 1994, "A Bistable Snapping Mechanism," *IEEE Micro Electro Mechanical Systems 1994*, pp. 45-50.

Mehregany, M. and Dewa, A.S., 1993, *Case Western Reserve University - MCNC Short Course Handbook: Introduction to Microelectromechanical Systems and the Multiuser MEMS Processes*, Electronics Design Center and Department of Electrical Engineering and Applied Physics, Case Western Reserve University, Cleveland, Ohio.

Mettlach, G.A. and Midha, A., 1996, "Using Burmester Theory in the Design of Compliant Mechanisms," *Proceedings of the 1996 ASME Design Engineering Technical Conferences*, 96-DETC/MECH-1181.

Midha, A., Norton, T.W., and Howell, L.L., 1994, "On the Nomenclature, Classification, and Abstractions of Compliant Mechanisms," *Journal of Mechanical Design*, March 1994, Vol. 116, pp. 270-279.

Millar, A.J., Howell, L.L, and Leonard, J.N., 1996, "Design and Evaluation of Compliant Constant-Force Mechanisms," *Proceedings of the 1996 ASME Design Engineering Technical Conferences*, 96-DETC/MECH-1209.

Murphy, M.D., Midha, A., and Howell, L.L., 1994a, "Type Synthesis of Compliant Mechanisms Employing a Simplified Approach to Segment Type," *Mechanism Synthesis and Analysis*, DE-Vol. 70, 23rd ASME Biennial Mechanisms Conference, pp. 51-60.

Murphy, M.D., Midha, A., and Howell, L.L., 1994b, "Methodology for the Design of Compliant Mechanisms Employing Type Synthesis Techniques with Example," *Mechanism Synthesis and Analysis*, DE-Vol. 70, 23rd ASME Biennial Mechanisms Conference, pp. 51-60.

Murphy, M.D., Midha, A., and Howell, L.L., 1996, "The Topological Synthesis of Compliant Mechanisms," *Mechanism and Machine Theory,* Vol. 31, No. 2, pp. 185-199.

Nielson, A., 1998, "Demonstration of the Pseudo-Rigid-Body Model for Macro- and Micro- Compliant Pantographs", M.S. Thesis, Brigham Young University, Provo, Utah.

Olson, D.G., Erdman, A.G., and Riley, D.R., 1985, "A Systematic Procedure for Type Synthesis of Mechanisms with Literature Review," *Mechanism and Machine Theory*, Vol. 20, No. 4, pp. 285-295.

Opdahl, P.G., 1996, "Modeling and Analysis of Compliant Bi-Stable Mechanisms Using the Pseudo-Rigid-Body Model," M.S. Thesis, Brigham Young University, Provo, Utah.

Opdahl, P.G., Jensen, B.D., and Howell, L.L., 1998, "An Investigation into Compliant Bistable Mechanisms", *Proceedings of the 1998 ASME Design Engineering Technical Conferences*, DETC98/MECH-5914.

Parkinson, M.B., Howell, L.L, and Cox, J., 1997, "A Parametric Approach to the Optimization-Based Design of Compliant Mechanisms," *Proceedings of the 1997 ASME Design Engineering Technical Conferences*, DETC97/DAC-3763.

Paul, B., 1979a, "A Reassessment of Grashof's Criterion," *Journal of Mechanical Design*, Vol. 101, July 1979, pp. 515-518.

Paul, B., 1979b, *Kinematics and Dynamics of Planar Machinery*, Prentice-Hall, Inc., Englewood Cliffs, New Jersey.

Salamon, B.A. and Midha, A., 1992, "An Introduction to Mechanical Advantage in Compliant Mechanisms," *Advances in Design Automation*, (Ed.: D.A. Hoeltzel), DE-Vol. 44-2, 18th ASME Design Automation Conference, pp. 47-51.

Salmon, L.G., Gunyan, D.B., Derderian, J.M, Opdahl, P.G, and Howell, L.L., 1996, "Use of the Pseudo-Rigid-Body Model to Simplify the Description of Compliant Micro-Mechanisms," *1996 IEEE Solid-State Sensor and Actuator Workshop*, Hilton Head Island, SC, pp. 136-139.

Schulze, Erwin F., 1955, "Designing Snap-Action Toggles," *Product Engineering*, November 1955, pp. 168-170.

Sevak, N.M., McLarnan, C.W., 1974, "Optimal Synthesis of Flexible Link Mechanisms with Large Static Deflections," ASME Paper No. 74-DET-83.

Sharpe, W.N., Jr., Yuan, B., Vaidyanathan, R., and Edwards, R.L., 1997, "Measurements of Young's Modulus, Poisson's Ratio, and Tensile Strength of Polysilicon," *IEEE 1997 Micro-Electro-Mechanical Systems*, pp. 424-429.

Shoup, T.E., 1972, "On the Use of the Nodal Elastica for the Analysis of Flexible Link Devices," *Journal of Engineering for Industry*, Trans. ASME, Vol. 94, No. 3, pp. 871-875.

Shoup, T.E. and McLarnan, C.W., 1971a, “A Survey of Flexible Link Mechanisms Having Lower Pairs,” *Journal of Mechanisms,* Vol. 6, No. 3, pp. 97-105.

Shoup, T.E. and McLarnan, C.W., 1971b, “On the Use of the Undulating Elastica for the Analysis of Flexible Link Devices,” *Journal of Engineering for Industry,* Trans ASME, pp. 263-267.

Sigmund, Ole, 1996, “On the Design of Compliant Mechanisms Using Topology Optimization,” *Danish Center for Applied Mathematics and Mechanics*, Technical University of Denmark, Report No. 535.

Simitses, G.J., 1976, *An Introduction to the Elastic Stability of Structures*, Prentice-Hall, Inc., Englewood Cliffs, New Jersey.

Soni, A.H., 1974, *Mechanism Synthesis and Analysis*, Scripta Book Company, Washington, D.C.

Timoshenko, S. and Young, D.H., 1948, *Advanced Dynamics, 1st Ed.*, McGraw-Hill Book Company, Inc., New York.

Timoshenko, S. and Young, D.H., 1951, *Engineering Mechanics 3rd Ed.*, McGraw-Hill Book Company, Inc., New York.

Timoshenko, S., 1961, *Theory of Elastic Stability, 2nd Ed.*, McGraw-Hill Book Company, Inc., New York.

Wagner, B., Quenzer, H.J., Hoershelmann, S., Lisec, T., and Juerss, M., 1996, “Bistable Microvalve with Pneumatically Coupled Membranes,” *Proceedings of IEEE Micro Electro Mechanical Systems 1996*, p. 384-388.

Winter, S.J. and Shoup, T.E., 1972, “The Displacement Analysis of Path Generating Flexible-Link Mechanisms,” *Mechanism and Machine Theory,* Vol. 7, No. 4, pp. 443-451.

Ziegler, H., 1956, “On the Concept of Elastic Stability,” *Advances in Applied Mechanics*, Vol. IV (Ed.: H.L. Dryden and Th. von Karman), Academic Press, Inc., New York, New York.

APPENDIX A *Bistable Snap-Through Buckling Beams in MEMS*

As discussed in section 5.2.3.2, “Solution One - A Snap-Through Buckled Beam,” one possible bistable MEMS design is a simple snap-through buckling beam. This solution to the design problem is attractive because of the simplicity of modeling and analysis of such a beam. By giving the beam some initial curvature, it becomes possible to buckle the beam down into a second stable configuration. The stress at either beam end is greatly reduced if the ends are pinned to the substrate. The result is a functionally binary pinned-pinned segment, as shown in Figure A-1. With the basic configuration of the beam decided, all that remains is to choose dimensions which will allow the beam to toggle between stable positions without exceeding the strength of the material. This appendix discusses the design process used to choose adequate dimensions, and the fabrication and testing of several such beams is considered.

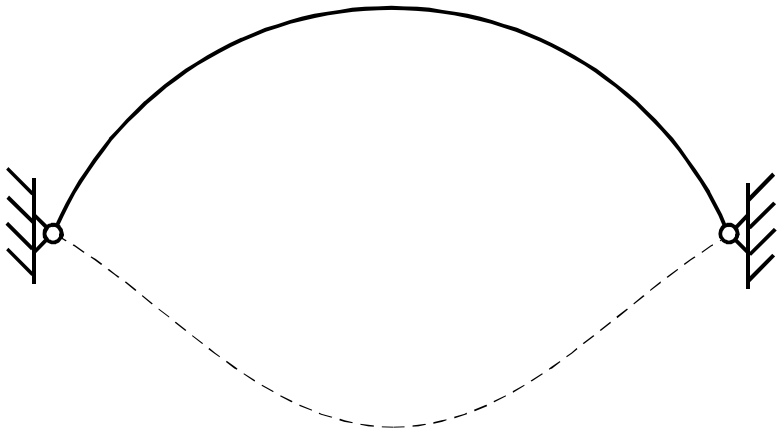

FIGURE A-1: An initially-curve pinned-pinned beam which acts as a snap-through buckling beam.

A.1 The Design of the Snap-Through Buckled Beam

The simplicity of the buckled beam approach lies in the few number of design parameters left once the basic mechanism configuration is decided. A semi-circular beam pinned on both ends may be completely described by three dimensions: *r*, *l*, and *I*, where

- *r* is the radius of curvature of the beam
- *l* is the length of the semi-circular arc, and
- *I* is the cross-sectional moment of inertia of the beam.

For the MUMPS process, *I* is chosen to be 1.5 μm^4, corresponding to a out-of-plane height of 2.0 μm and an in-plane thickness of 3.0 μm (the nominal linewidth). All that remains is to choose an appropriate segment length and radius of curvature. These must be chosen so that the stress in the beam does not exceed the strength of polysilicon. From past experience in the design of compliant MEMS, an adequate strength to Young's modulus ratio is about $1.05X10^{-2}$. It is helpful to specify strength in this way because the Young's modulus of polysilicon is not known with exactness. As the stress in the segment depends

directly on Young's modulus, the strength is given as a ratio so that any errors in the value of Young's modulus are accounted for.

Before the beam can be modeled and dimensions selected, the loads which will be applied to cause toggle must be selected. The beam could be toggled between positions by pushing down on it anywhere along its length until the beam snaps into a second position. However, experience has shown that this method of actuation causes high stress concentrations, resulting in fracture long before the mechanism snapped (Edwards, 1996). Instead, if a moment is applied to one end, the mechanism may be toggled without undue concentrated loading. This moment may be applied using a moment arm attached to one pin joint (see Figure A-2).

A finite element analysis model was constructed to analyze the system and to aid in determining the appropriate values of *r* and *l* such that the beam would have two stable states, but no fracture would occur. The model used *r* and *l* as inputs, and the finite element analysis determined the maximum stress in the segment during toggle and the rotation of the segment's pin joints at the second stable position of the beam. See Appendix C for a copy of the code of the FEA batch file. By analyzing a small number of such beams, some idea of the values required may be seen. Table A-1 shows the maximum stress in the beam for a variety of different lengths and radii. From the table, it can be seen that the stress

TABLE A-1: The ratio of stress in the beam at given levels of *r* and *l* to Young's modulus. All dimensions are in microns.

	r=250	*r*=500	*r*=750
l=250	0.0209	0.0105	0.00705
l=500	0.0208	0.0104	0.00695
l=750	0.0211	0.0104	0.00689

varies a great deal with the radius of curvature but very little with the length. Therefore, based on the analysis, a value for curvature of 500 μm was chosen. Five values for segment length were chosen because both long and short bistable segments may be desirable in different situations. The five lengths chosen were 150, 200, 250, 400, and 500, where all values are in microns. These radius and length values were chosen to give a beam with an acceptable maximum stress and a small size. If the beams become very large, then friction between the beam and the substrate is likely to prevent toggle between the two stable positions.

A very interesting characteristic of these beams was learned through the finite element modeling. As a moment is applied to rotate one pin joint, the pin joint must rotate through some deflection angle, depending on the radius and segment length, until the unstable position is reached. At this point, the segment toggles through toward the second stable position. However, the moment on the pin joint must be released before the second stable position is reached. This is because the deflection angle of the pin joint in the second stable position is actually less than the deflection angle of the pin joint at the unstable position. Thus, care must be exercised in the actuation of these beams so that excessive force is not used to try to push the pin joint past the unstable position. Instead, when the unstable position is reached, the moment on the pin joint should be released, allowing the pin joint to relax into the second stable position.

A.2 Fabrication and Testing

Each of the five designs outlined above was fabricated and tested. While the two longest beams successfully snapped between positions, the three shortest beams proved to

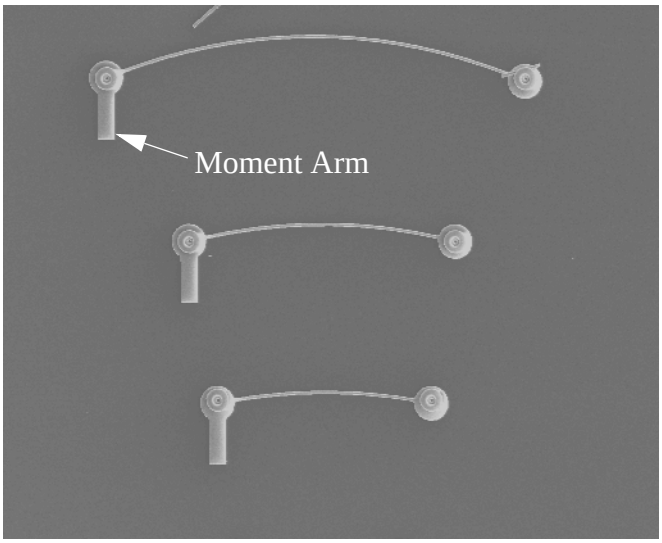

FIGURE A-2: A scanning electron microscope image of the three shortest snap-through beams.

be too stiff to move between positions without fracture. An SEM photograph of the three shortest beams is shown in Figure A-2. The longest beam, with length 500 μm, is shown

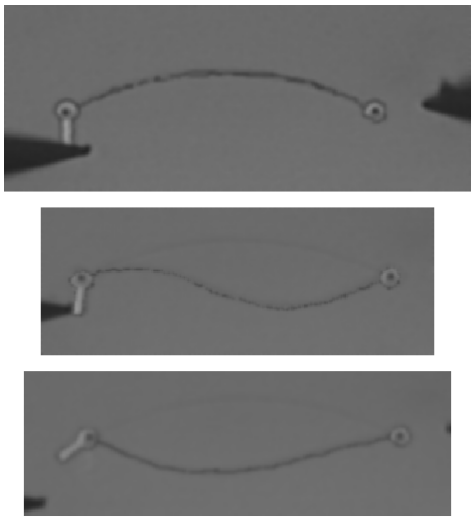

FIGURE A-3: A snap-through buckling micro-beam. These photos have been computer-enhanced to show the beam's shape.

in Figure A-3. This figure shows the beam in its two stable positions as well as while toggling between stable positions.

For use in any application requiring bistable mechanisms, the beam should assume the same position every time it snaps into place. In other words, the stable positions should be very repeatable. The two longest beams were tested to determine the repeatability of their stable positions. This was done by measuring the angle made by the left pin joint at the two stable positions. To reflect the true repeatability of the positions after snapping between positions, each angle was measured only after snapping into position. The number of replicates and the standard deviations of the angles measured are shown in Table A-2. The difference between the means of the angles at each position is also shown for comparison. These standard deviations are fairly low compared to the mean differences (about one twelfth).

One of the problems faced with the bistable snapping micro-beams was their low reliability. The beams rarely toggled before fracture, and they tended to have problems snapping between positions because of friction between the beam and the substrate. In addition, the range of possible bistable states is very limited because the beam can only be up or down. Bistable MEMS based on the four-link mechanism class tend to overcome these problems. Their added complexity of motion makes a variety of stable states possible, and they can be configured in a number of different ways to reduce stress. Chapter 6 discusses the design of mechanisms of this type.

TABLE A-2: The standard deviations of the angle of the left pin joint in each stable position. A small standard deviation indicates the stable position is extremely repeatable.

	Replicates	Difference of Mean Angles	Standard Deviation (Radians)
l=400, first position	5	0.321 rad	0.0228
l=400, second position	5	0.321 rad	0.0261
l=500, first position	4	0.419 rad	0.0325
l=500, second position	4	0.419 rad	0.0330

APPENDIX B *Improved Performance Modifications of Compliant Bistable MEMS*

As mentioned in the Chapter 6, many of the micro-mechanisms which were designed and fabricated either broke before toggling between stable positions or failed to snap when toggling. The probable reason is high frictional forces between the mechanism and the substrate. Therefore, several modifications have been made to some mechanisms to find a way of improving the mechanisms' mean cycles to failure.

Unfortunately, without on-chip actuation, it is very difficult to obtain an accurate measurement of mechanism reliability. This is because it is not feasible to actuate every mechanism to failure by hand using probes. In addition, because the mechanisms are actuated by hand, many of them may break because they have been pushed in the wrong direction due to human error. However, even without on-chip actuation, some idea of which mechanism improvements enhance time to failure may be found by testing a number of such improvements. Therefore, in this appendix, a variety of improvements to the designs of micro-mechanisms are explained, and data is presented which helps to determine which modifications effectively improve reliability.

B.1 Modifications for Mechanism Improvement

The effect of the modifications on a sample of mechanism designs was desired. Three basic mechanism designs were chosen from the list of designs in Table 6-1 on page 110. These were mechanisms 3-I, 5-II, and 11-I. These mechanisms were chosen because experience with earlier testing showed that they were among the most reliable designs. However, because these three mechanisms represent both Classes I and II, the results may be applied to a variety of mechanism designs.

B.1.1 Modifications Tested

Each of the modifications explained here was intended to decrease the friction between the mechanism and the substrate. They fall into four main groups of modifications: methods to increase the distance between the mechanisms and the substrate, modifications of dimples on the mechanisms, stiction-reduction modifications, and mechanisms incorporating new non-fixed pin joints. Each group will be explained separately.

B.1.1.1 Methods of Increasing the Mechanism to Substrate Separation- Two main modifications fall into this category. In the first, the mechanism is constructed from the second layer of polysilicon rather than the first. This is done by increasing the size of the fixed pin joints and attaching the mechanism, fabricated in the second layer, to the outside of the pin joint, fabricated in the first layer. This effectively increases the thickness of the oxide layer under the mechanism by 0.5 μm, resulting in a total separation of 2.5 μm.

To increase the separation distance further, a large sheet of the first layer of polysilicon may be placed under the mechanism. This increases the separation between the mechanism and the substrate by an additional 2.0 μm. The underlying sheet may be pushed

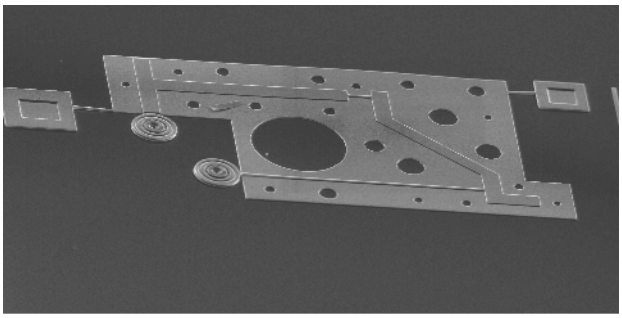

FIGURE B-1: An example mechanism showing the sheet of first layer polysilicon under the mechanism fabricated in the second layer.

out from under the mechanism before it is actuated. This modification results in a total separation distance of about 4.5 μm. An SEM photograph of a mechanism with this modification is shown in Figure B-1 for illustration.

In a similar approach, a layer of polysilicon fixed to the substrate was fabricated under the mechanism in its first stable position. This layer was 0.25 μm thick. When the mechanism switches to its second stable position, it is held above the substrate by this layer.

B.1.1.2 Dimple Modifications- Dimples are depressions made in the first layer of polysilicon, intended to create a small area which extrudes below the rest of the first layer. They may be used to decrease friction by creating a smaller surface area for contact between the mechanism and the substrate. While some dimples were used in the initial mechanism designs presented in Chapter 6, it was not known whether different amounts and sizes of dimples would help to decrease friction.

Therefore, a number of different dimple designs were fabricated. These consisted of dimple designs added to the pin joints and dimple designs added to the mechanism. On the pin joints, square dimples placed radially around the center of the joints were tried, as

well as dimples constructed in the form of circular arcs, hereafter called circular dimples. On the mechanisms, circular dimples placed along the mechanisms were fabricated, as well as dimples in the form of lines down the center of the mechanism links. Square dimples on the mechanisms were also tried.

B.1.1.3 Stiction-Reduction Modifications- Several modifications were done to decrease stiction effects. In the first, triangular tips were added to the ends of mechanism links. These tips have been shown in the past to have some effect on stiction due to the decreased surface area at the end which reduces the capillary forces incurred during the release etch.

Another modification intended to decrease stiction was the use of truss-like structures in place of fully rigid links. These structures were intended to decrease surface area of the mechanism without significantly degrading its strength. They may be applied to mechanisms fabricated in either the first or second layer. A mechanism using the truss modification is shown in Figure B-2 in the second stable position.

The final modification to attempt to decrease stiction was to create a grid under the mechanism fabricated from a thin layer of polysilicon deposited directly on the substrate. This grid causes the mechanism to only contact the surface below it at the points where it touches the grid. Thus, throughout the mechanism's motion, a low surface contact is maintained. Two different grid designs were used: one with lines all going one direction, equally spaced, and another with orthogonal lines which were equally spaced. An SEM photograph showing an orthogonal grid is shown in Figure B-3.

B.1.1.4 Mechanisms with Non-Fixed Pin Joints- Each of the mechanisms described in Chapter 6 had two fixed pin joints due to the difficulty of fabricating moving pin joints.

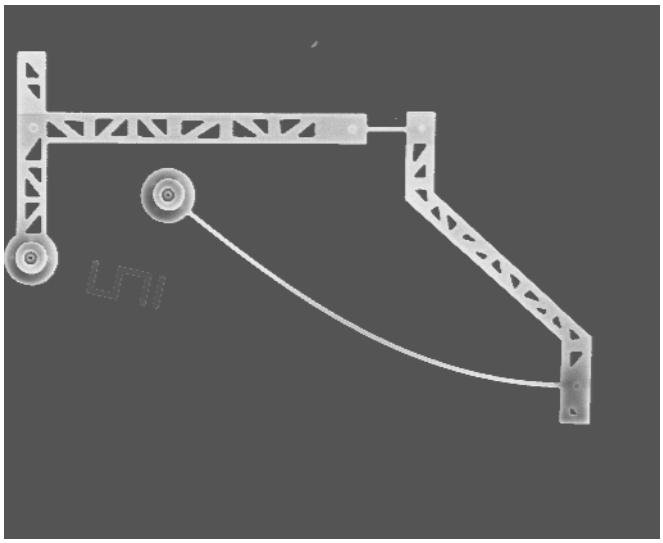

FIGURE B-2: A mechanism using the truss modification shown in the second stable position.

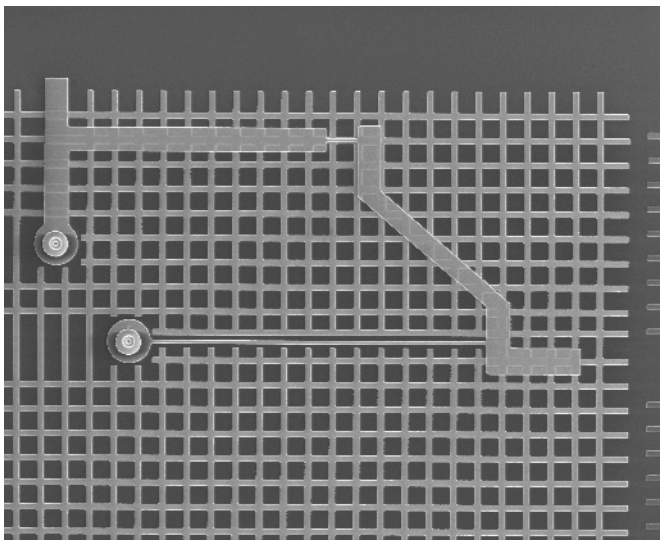

FIGURE B-3: A mechanism design with a fixed grid of polysilicon under the mechanism.

However, successive research identified a possible way of creating moving pin joints which, while not having complete rotation, still approximated rotational motion over some range. A scanning electron microscope picture of such a moving pin joint is shown in

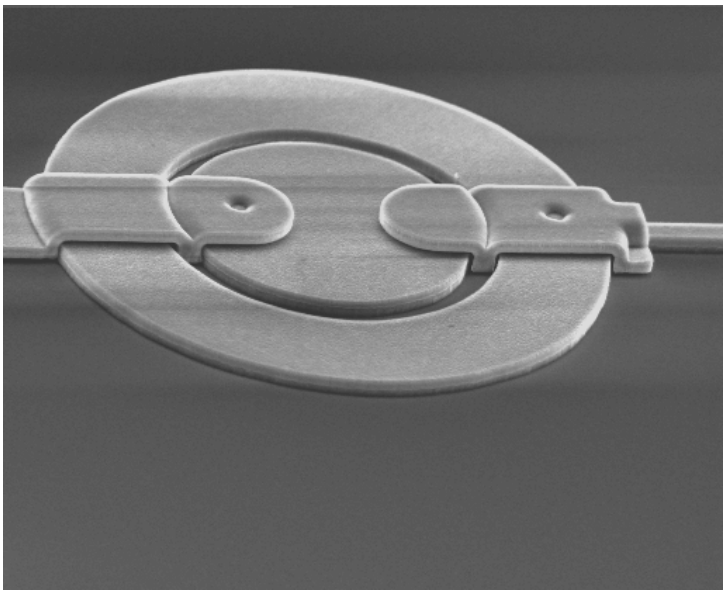

FIGURE B-4: An example of a non-fixed pin joint. The inner disc rotates inside the outer ring.

Figure B-4. These pin joints were implemented by inverting the mechanism, so that one of its moving links became fixed. This means that the mechanism is attached to the substrate through one or both of the compliant segments. This helps to decrease friction because the compliant segments are held above the substrate, while the fixed pin joints could sink down and contact the substrate. Some mechanisms modified in this way contained one fixed and one non-fixed pin joint, and some contained two non-fixed pin joints. Also, two sizes of non-fixed pin joints were used, one with a radius of 30 μm and another with a radius of 40 μm.

B.2 Mechanism Designs and Testing

Twenty-five mechanisms with one or more of the modifications listed above were designed and fabricated, along with three "control" mechanisms identical to the ones

presented in Chapter 6. Each mechanism was given a "modification number" to identify it. These numbers, together with the basic mechanism design number (from Table 6-1 on page 110) and a list of the modifications used, are shown in Table B-1. Microscope pictures of each modification may be found in Appendix E. Each design was fabricated and tested by actuating it up to ten times. The number of cycles before failure and the number of cycles in which the mechanism snapped into position were recorded. Notice that this means that the maximum number of cycles that any one mechanism was tested to was ten. For this reason, no conclusion of total mean cycles to failure can be reached. However, conclusions on the modifications that most improved reliability can be made. Several replicates (or instances) of each mechanism were tested. The resulting data is shown in Table B-2.

The data shows that many of the modifications worked little better or worse than the original mechanism configuration. However, some modifications did seem to have a beneficial effect. For example, modification numbers 4, 16, and 17 all have a grid under the mechanism, and each of these designs performed better than any other design. The other significant modification seems to be designs with dimples, especially dimples in a circular arc on the pin joints. Modification numbers 5, 11, 13, and 14 each had dimples in circular arcs, and they all show a marked improvement in performance over the control design. The other modifications do not seem to have a large effect, though, with the exception of the non-fixed pin joints, which almost never had even one cycle before failure. Thus, improvements in these joints are necessary before they can viably be used in bistable mechanisms.

TABLE B-1: The modification numbers, basic mechanism design numbers, and a list of the modifications used for each test mechanism.

Modification Number	Mechanism Number	Modifications
1	3	No modifications (control)
2	3	Mechanism made from second layer
3	3	Mech. from 2nd layer, with 1st layer sheet
4	3	Orthogonal grid under mechanism
5	3	Circular dimples on pin joints, Line dimples on mech.
6	3	Radial dimples on pin joints
7	5	No modifications (control)
8	5	Mechanism made from second layer
9	5	Mech from 2nd layer, Radial dimples on pin joints
10	5	Mech from 2nd layer, with 1st layer sheet
11	5	Circular dimples on pins, Circular dimples on mech.
12	5	Radial dimples on pins, Circular dimples on mech.
13	5	Circular dimples on pins, Square dimples on mech.
14	5	Circular dimples on pins, Line dimples on mech.
15	5	Anchored polysilicon under mechanism
16	5	Horizontal grid under mechanism
17	5	Orthogonal grid under mechanism
18	5	Two non-fixed pin joints, radius = 30 microns
19	5	Two non-fixed pin joints, radius = 40 microns
20	5	Two non-fixed pin joints, radius = 40 microns, antis-tiction tips
21	5	Two non-fixed pin joints, radius = 30 microns, with truss
22	5	One non-fixed pin joint, radius = 30 microns
23	5	Truss
24	5	Truss with some dimples on mechanism
25	11	No modifications (control)
26	11	Two non-fixed pin joints, radius = 40 microns
27	11	Two non-fixed pin joints, radius = 30 microns
28	11	Two non-fixed pin joints, radius = 30 microns, with truss

TABLE B-2: The results of testing for each of the mechanism modifications shown in Table B-1. The table shows the mean number of cycles, mean number of snapping cycles, and the ratio of snapping to total cycles for each mechanism.

Modification Number	Replicates	Mean No. of Cycles	Mean No. of Snaps	Ratio: Snaps to Cycles
1 (control)	7	0.429	0	0
2	4	0	0	0
3	7	0.0714	0.0714	1
4	4	7.25	5.125	0.707
5	6	0.917	0.333	0.364
6	6	0.167	0.0833	0.5
7 (control)	8	0.688	0.188	0.273
8	7	0	0	0
9	7	0	0	0
10	7	0	0	0
11	7	2.571	1.929	0.75
12	7	0.643	0.143	0.222
13	7	1.857	0.571	0.308
14	6	2.583	1.167	0.452
15	7	1.357	0.357	0.263
16	8	5.25	3.292	0.748
17	7	3.429	3	0.875
18	18	0.111	0.056	0.5
19	6	0	0	0
20	6	0	0	0
21	6	0	0	0
22	64	0.398	0.242	0.608
23	6	0.167	0	0
24	8	2.188	0.688	0.314
25 (control)	6	0.0833	0	0
26	4	0	0	0
27	4	0	0	0
28	5	0	0	0

Further studies on the mean cycles to failure of bistable mechanisms will be possible when on-chip actuation of bistable MEMS has been achieved. However, even without detailed information on the reliability of these systems, the conclusion can be made that the grid under the mechanism is the most effective method studied for improving mechanism performance.

APPENDIX C *Finite Element Analysis Batch File*

This appendix contains the batch file used in the design and analysis of the snap-through bistable micro-beams. The code presented is for the Ansys finite element software.

C.1 Snap-Through Buckling Beam

This batch file takes the radius of curvature, length, width, and thickness of the beam and finds the maximum stress in the beam during motion and the second stable position. The inputs are:

- R - the radius of curvature, in units of centimeters
- h - the in-plane thickness of the beam, in centimeters
- w - the out-of-plane thickness of the beam, in centimeters
- l - the arc length, in centimeters

The data is written to a file called “output.”

```
/BATCH
/COM,ANSYS REVISION  5.2    UP121895         08:09:03    02/25/1997
R=750e-4
h=3e-4
w=2e-4
l=750e-4
```

```
ex=1.9e12
size=5e-4
drotz=.4*l/(3*r)
/PREP7
ET,1,BEAM3
R,1,h*w,w*(h**3)/12,h,1.2, , ,
UIMP,1,EX, , ,ex,
UIMP,1,NUXY, , ,0.3,
UIMP,1,EMIS, , ,1,
k,1,0,0
xpos=r*sin(l/(2*r))
k,2,2*xpos,0
k,3,xpos,-r*cos(l/(2*r))
larc,1,2,3,r
esize,size
type,1
real,1
mat,1
lmesh,1
FINISH
/SOLU
ANTYPE,0
NLGEOM,1
NROPT,AUTO, ,
LUMPM,0
EQSLV,FRONT,1e-08,0,
SSTIF
PSTRES
TOFFST,0,
cnvtol,f,.1,0.001,2, ,
cnvtol,m,.001,0.001,2, ,
neqit,100
DK,1, ,0, ,0,UX,UY
DK,2, ,0, ,0,UX,UY
dk,1,rotz,-drotz
lswrite,1
dk,1,rotz,-2*drotz
lswrite,2
dk,1,rotz,-3*drotz
lswrite,3
dk,1,rotz,-4*drotz
lswrite,4
dk,1,rotz,-5*drotz
lswrite,5
dk,1,rotz,-6*drotz
lswrite,6
dk,1,rotz,-7*drotz
lswrite,7
dk,1,rotz,-7.2*drotz
lswrite,8
dk,1,rotz,-7.4*drotz
lswrite,9
dk,1,rotz,-7.5*drotz
lswrite,10
```

```
dk,1,rotz,-7.6*drotz
lswrite,11
dk,1,rotz,-7.8*drotz
lswrite,12
dk,1,rotz,-8*drotz
lswrite,13
dk,1,rotz,-9*drotz
lswrite,14
dkdel,1,rotz
lswrite,15
save
lssolve,1,15,1
FINISH
/post1
*DIM,smx,ARRAY,15,1,1,
*DIM,smn,ARRAY,15,1,1,
lss=0
lss=lss+1
set,lss
ETABLE,smxi,NMIS,1
ETABLE,smxj,NMIS,3
ETABLE,smni,NMIS,2
ETABLE,smnj,NMIS,4
esort,etab,smxi,0,0
*get,smx(lss,1,1),sort,0,max
esort,etab,smni,0,0
*get,smn(lss,1,1),sort,0,min
eusort
lss=lss+1
set,lss
ETABLE,smxi,NMIS,1
ETABLE,smxj,NMIS,3
ETABLE,smni,NMIS,2
ETABLE,smnj,NMIS,4
esort,etab,smxi,0,0
*get,smx(lss,1,1),sort,0,max
esort,etab,smni,0,0
*get,smn(lss,1,1),sort,0,min
eusort
lss=lss+1
set,lss
ETABLE,smxi,NMIS,1
ETABLE,smxj,NMIS,3
ETABLE,smni,NMIS,2
ETABLE,smnj,NMIS,4
esort,etab,smxi,0,0
*get,smx(lss,1,1),sort,0,max
esort,etab,smni,0,0
*get,smn(lss,1,1),sort,0,min
eusort
lss=lss+1
set,lss
ETABLE,smxi,NMIS,1
ETABLE,smxj,NMIS,3
```

```
ETABLE,smni,NMIS,2
ETABLE,smnj,NMIS,4
esort,etab,smxi,0,0
*get,smx(lss,1,1),sort,0,max
esort,etab,smni,0,0
*get,smn(lss,1,1),sort,0,min
eusort
lss=lss+1
set,lss
ETABLE,smxi,NMIS,1
ETABLE,smxj,NMIS,3
ETABLE,smni,NMIS,2
ETABLE,smnj,NMIS,4
esort,etab,smxi,0,0
*get,smx(lss,1,1),sort,0,max
esort,etab,smni,0,0
*get,smn(lss,1,1),sort,0,min
eusort
lss=lss+1
set,lss
ETABLE,smxi,NMIS,1
ETABLE,smxj,NMIS,3
ETABLE,smni,NMIS,2
ETABLE,smnj,NMIS,4
esort,etab,smxi,0,0
*get,smx(lss,1,1),sort,0,max
esort,etab,smni,0,0
*get,smn(lss,1,1),sort,0,min
eusort
lss=lss+1
set,lss
ETABLE,smxi,NMIS,1
ETABLE,smxj,NMIS,3
ETABLE,smni,NMIS,2
ETABLE,smnj,NMIS,4
esort,etab,smxi,0,0
*get,smx(lss,1,1),sort,0,max
esort,etab,smni,0,0
*get,smn(lss,1,1),sort,0,min
eusort
lss=lss+1
set,lss
ETABLE,smxi,NMIS,1
ETABLE,smxj,NMIS,3
ETABLE,smni,NMIS,2
ETABLE,smnj,NMIS,4
esort,etab,smxi,0,0
*get,smx(lss,1,1),sort,0,max
esort,etab,smni,0,0
*get,smn(lss,1,1),sort,0,min
eusort
lss=lss+1
set,lss
ETABLE,smxi,NMIS,1
```

```
ETABLE,smxj,NMIS,3
ETABLE,smni,NMIS,2
ETABLE,smnj,NMIS,4
esort,etab,smxi,0,0
*get,smx(lss,1,1),sort,0,max
esort,etab,smni,0,0
*get,smn(lss,1,1),sort,0,min
eusort
lss=lss+1
set,lss
ETABLE,smxi,NMIS,1
ETABLE,smxj,NMIS,3
ETABLE,smni,NMIS,2
ETABLE,smnj,NMIS,4
esort,etab,smxi,0,0
*get,smx(lss,1,1),sort,0,max
esort,etab,smni,0,0
*get,smn(lss,1,1),sort,0,min
eusort
lss=lss+1
set,lss
ETABLE,smxi,NMIS,1
ETABLE,smxj,NMIS,3
ETABLE,smni,NMIS,2
ETABLE,smnj,NMIS,4
esort,etab,smxi,0,0
*get,smx(lss,1,1),sort,0,max
esort,etab,smni,0,0
*get,smn(lss,1,1),sort,0,min
eusort
lss=lss+1
set,lss
ETABLE,smxi,NMIS,1
ETABLE,smxj,NMIS,3
ETABLE,smni,NMIS,2
ETABLE,smnj,NMIS,4
esort,etab,smxi,0,0
*get,smx(lss,1,1),sort,0,max
esort,etab,smni,0,0
*get,smn(lss,1,1),sort,0,min
eusort
lss=lss+1
set,lss
ETABLE,smxi,NMIS,1
ETABLE,smxj,NMIS,3
ETABLE,smni,NMIS,2
ETABLE,smnj,NMIS,4
esort,etab,smxi,0,0
*get,smx(lss,1,1),sort,0,max
esort,etab,smni,0,0
*get,smn(lss,1,1),sort,0,min
eusort
lss=lss+1
set,lss
```

```
ETABLE,smxi,NMIS,1
ETABLE,smxj,NMIS,3
ETABLE,smni,NMIS,2
ETABLE,smnj,NMIS,4
esort,etab,smxi,0,0
*get,smx(lss,1,1),sort,0,max
esort,etab,smni,0,0
*get,smn(lss,1,1),sort,0,min
eusort
lss=lss+1
set,lss
ETABLE,smxi,NMIS,1
ETABLE,smxj,NMIS,3
ETABLE,smni,NMIS,2
ETABLE,smnj,NMIS,4
esort,etab,smxi,0,0
*get,smx(lss,1,1),sort,0,max
esort,etab,smni,0,0
*get,smn(lss,1,1),sort,0,min
eusort
fini
/POST26
NSOL,2,1,ROT,Z,rotz
RFORCE,3,1,M,Z,mz
/output,output
*stat,smn,1,ls
*stat,smx,1,ls
prvar,2,3
/output
fini
save
save
```

APPENDIX D *Microscope Images of Fifteen Young Mechanisms*

This appendix contains microscope images for each of the fifteen Young mechanisms designed. Where possible, the mechanism is shown in both stable states, as well as at the unstable state.

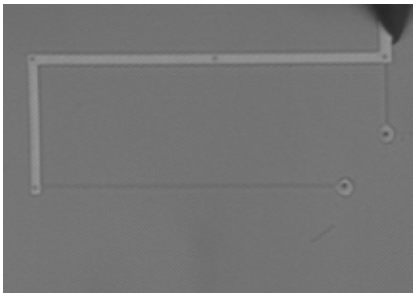

Mechanism 1-I, first stable position

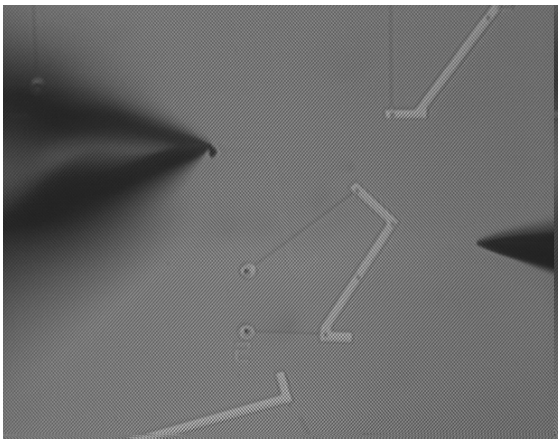

Mechanism 2-I, first stable position

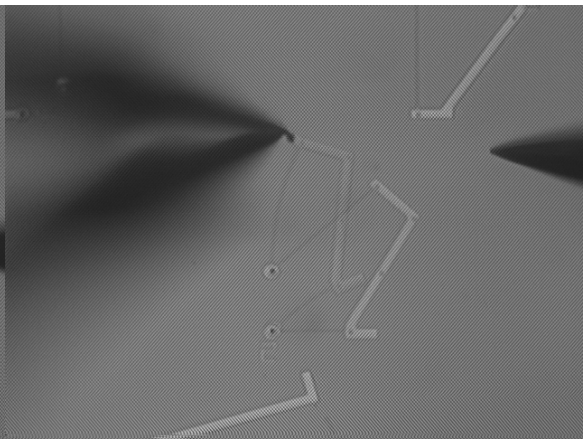

Mechanism 2-I, unstable position

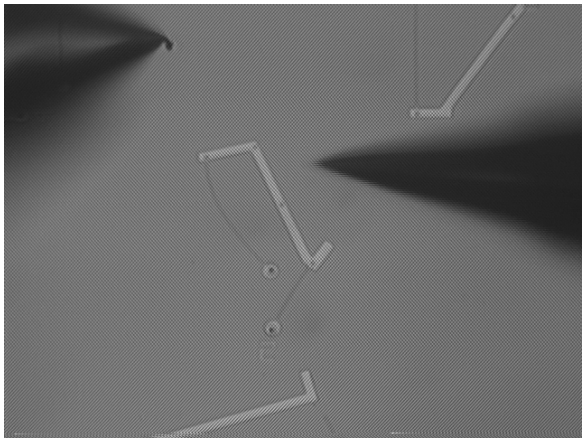

Mechanism 2-I, second stable position

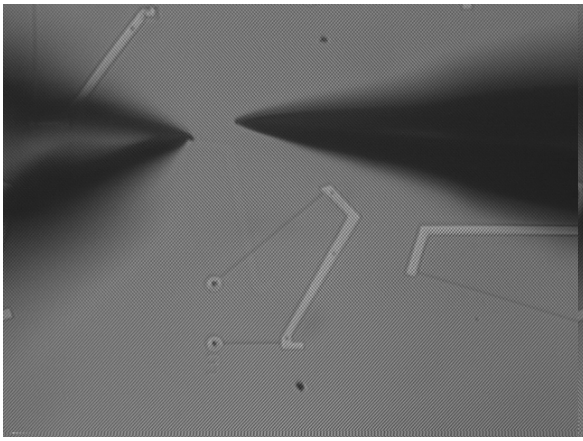

Mechanism 3-I, first stable position

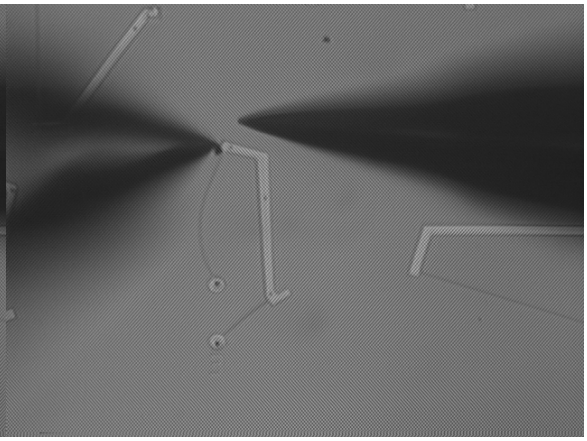

Mechanism 3-I, unstable position

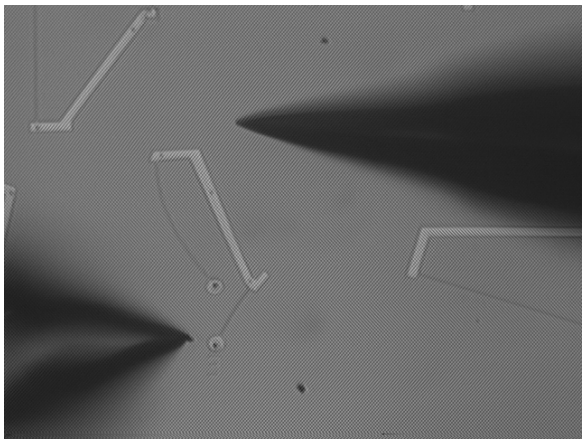

Mechanism 3-I, second stable position

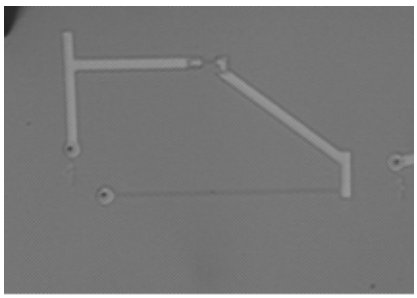

Mechanism 4-II, first stable position

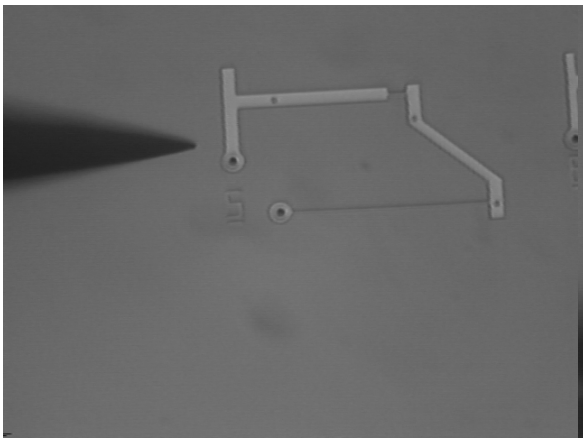

Mechanism 5-II, first stable position

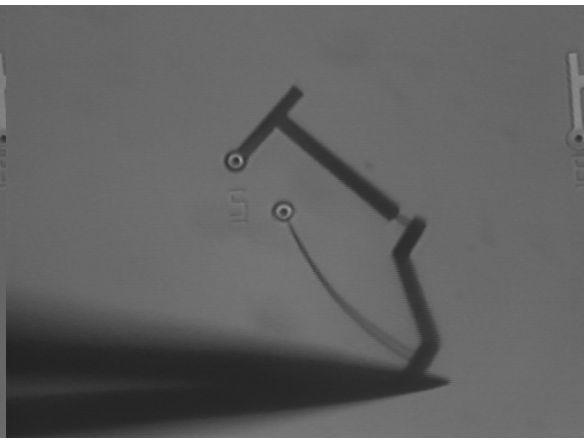

Mechanism 5-II, unstable position

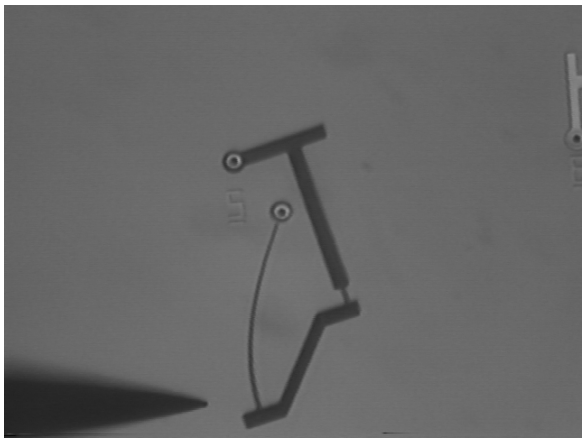

Mechanism 5-II, second stable

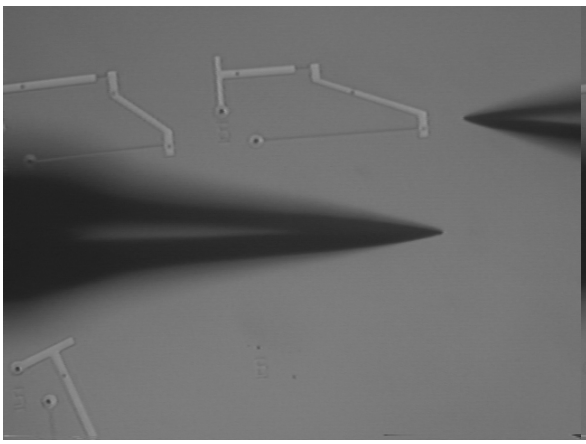

Mechanism 6-II, first stable position

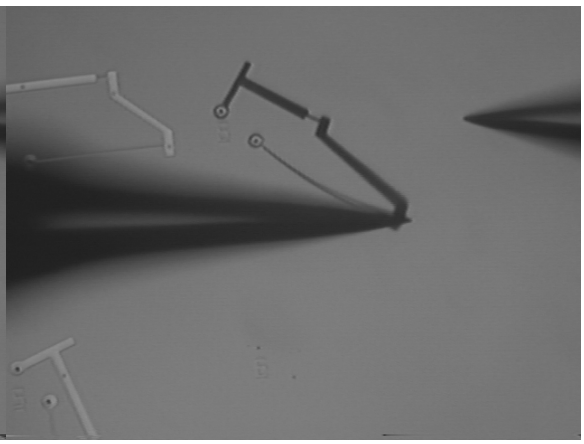

Mechanism 6-II, unstable position

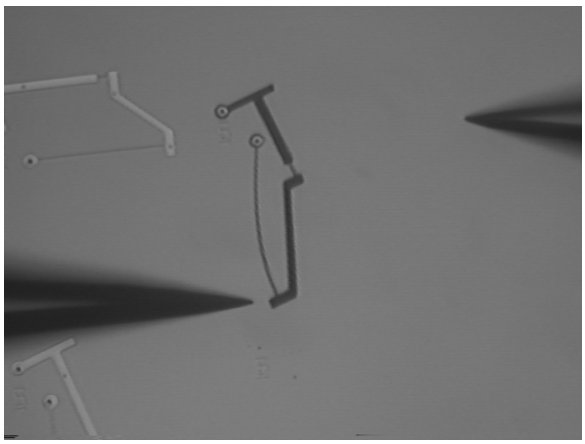

Mechanism 6-II, second stable position

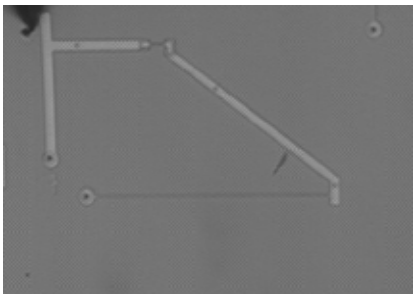

Mechanism 7-II, first stable position

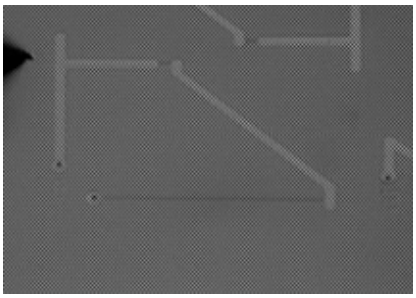

Mechanism 8-II, first stable position

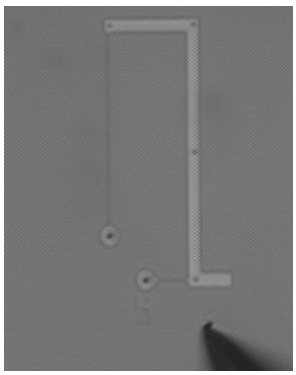

Mechanism 9-I, first stable position

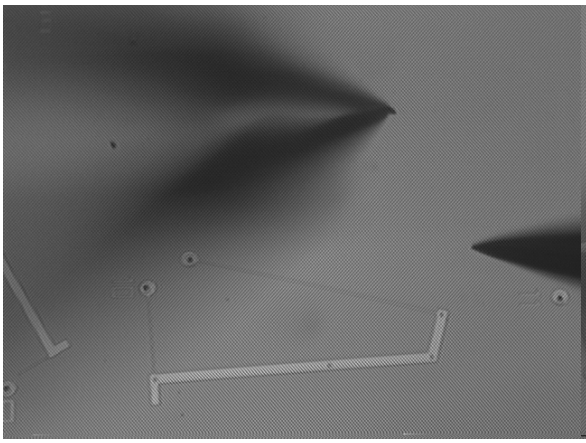

Mechanism 10-I, first stable position

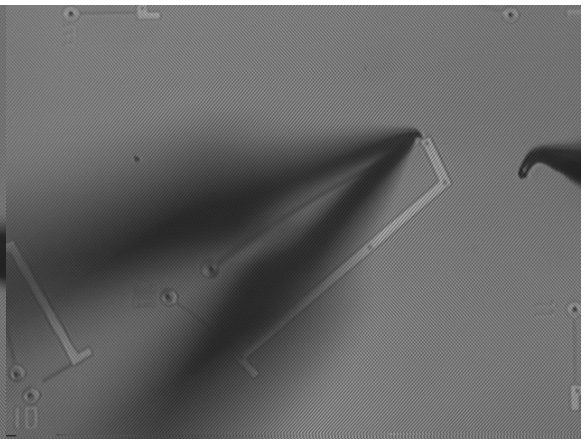

Mechanism 10-I, unstable position

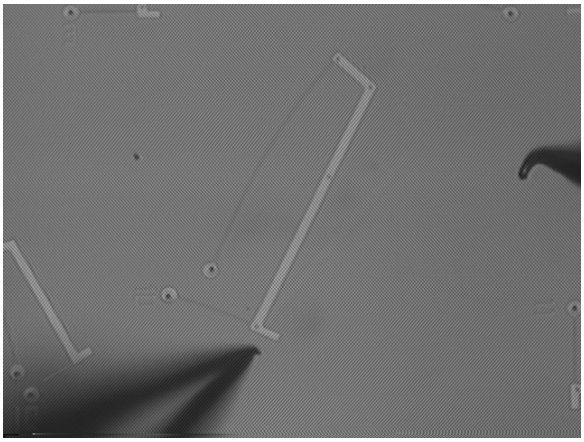

Mechanism 10-I, second stable position

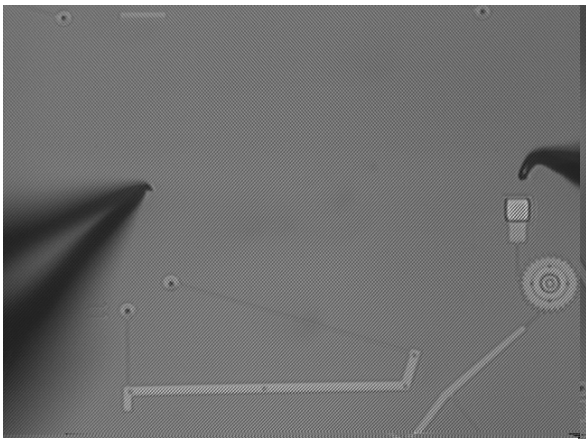

Mechanism 11-I, first stable position

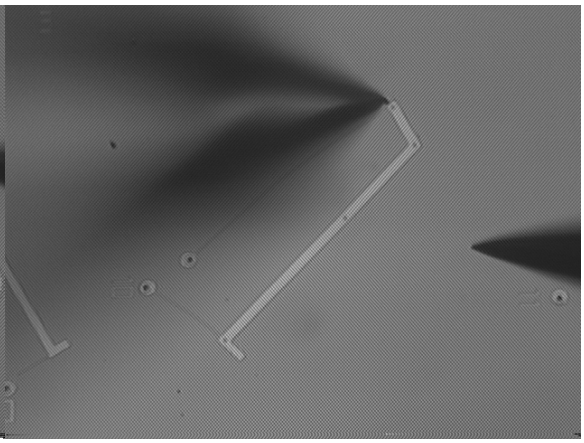

Mechanism 11-I, unstable position

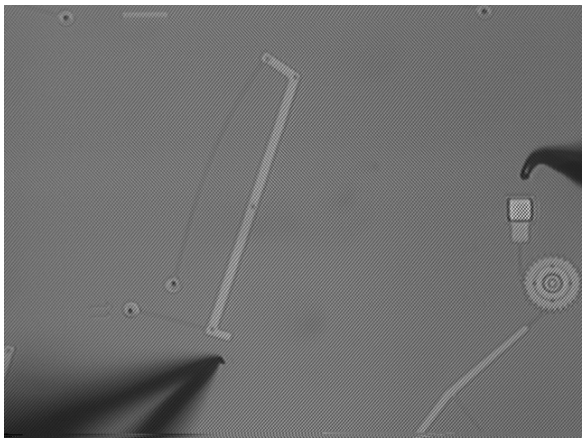

Mechanism 11-I, second stable position

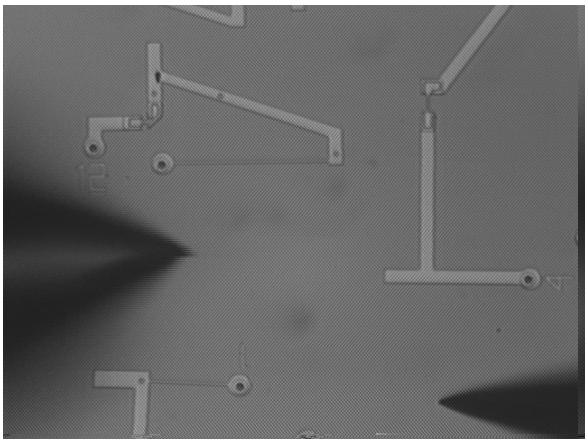

Mechanism 12-II, first stable position

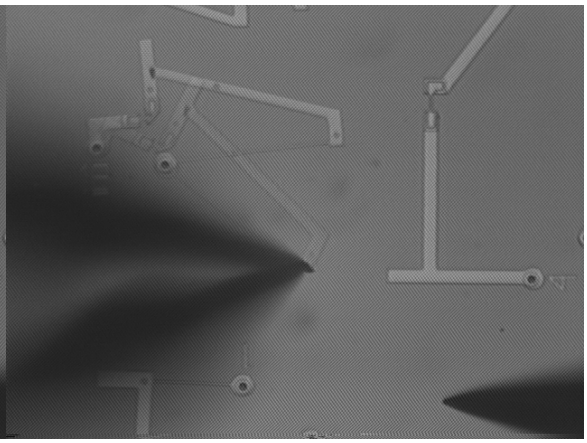

Mechanism 12-II, unstable position

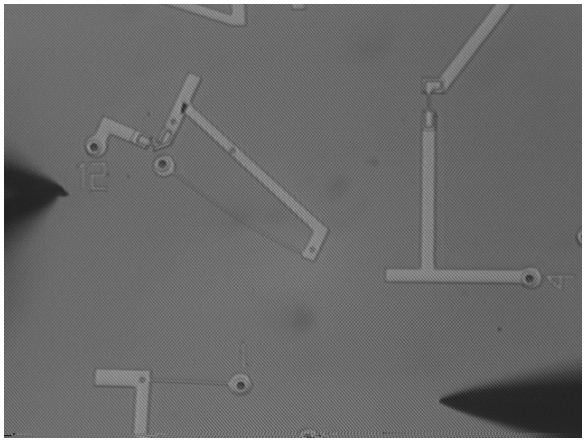

Mechanism 12-II, second stable position

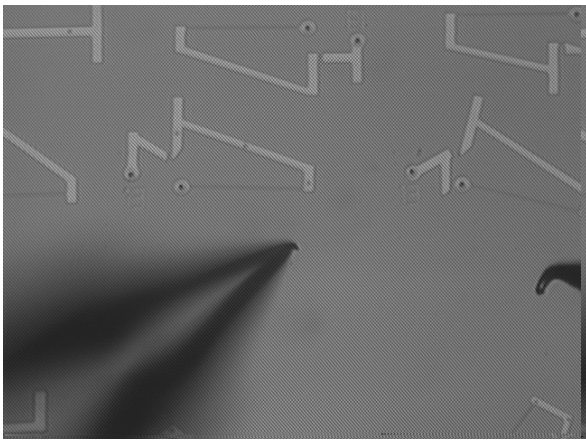

Mechanism 13-II, first stable position

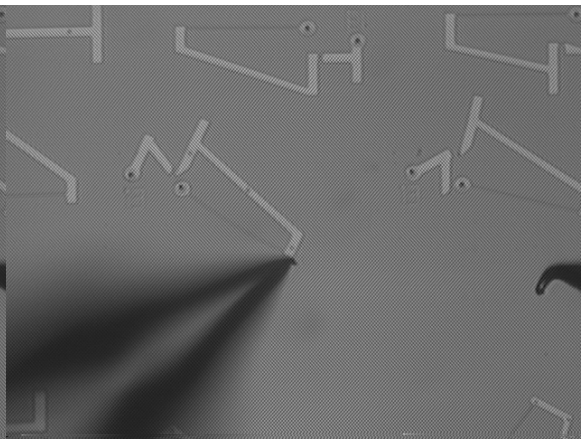

Mechanism 13-II, unstable position

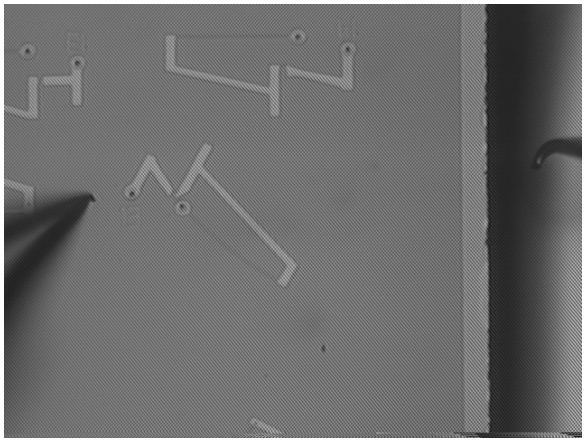

Mechanism 13-II, second stable position

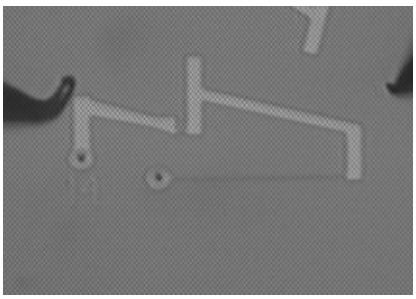

Mechanism 14-II, first stable position

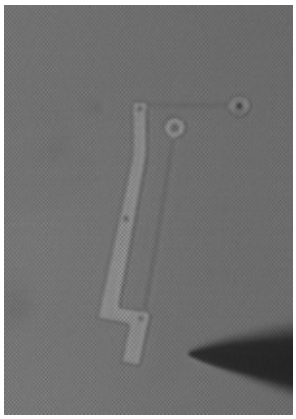

Mechanism 15-I, first stable position

APPENDIX E *Pictures of Mechanism Modifications*

This appendix contains microscope images for each of the twenty-eight modification designs explained in Appendix B. Each modification design is shown in its first stable state.

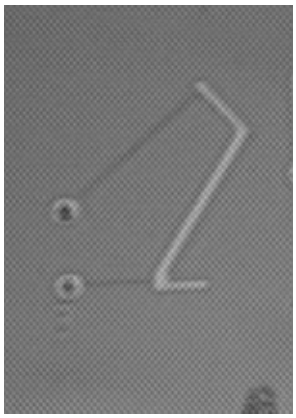

Modification One

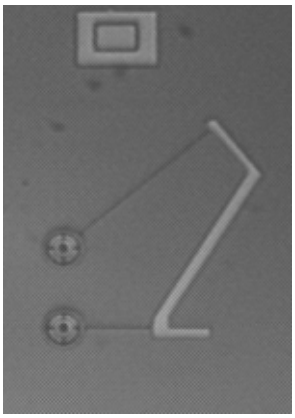

Modification Two

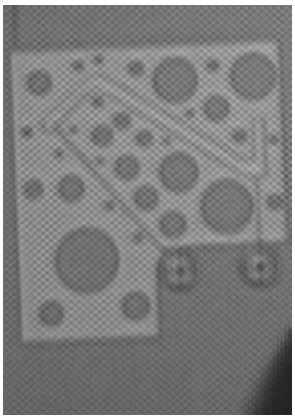

Modification Three

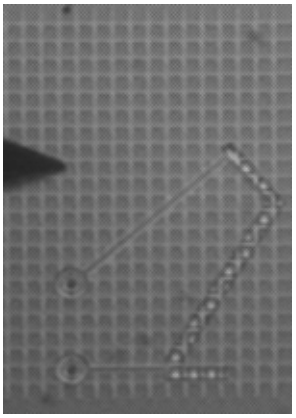

Modification Four

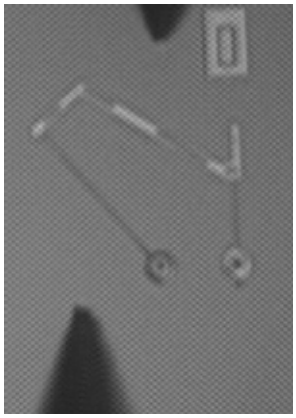

Modification Five

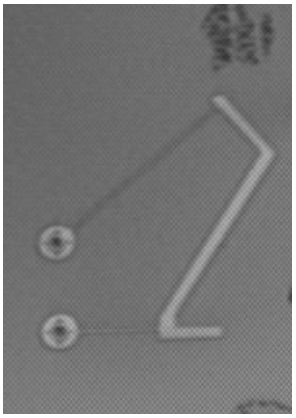

Modification Six

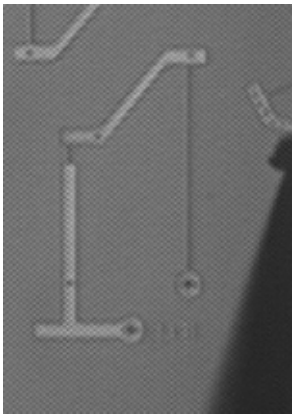

Modification Seven

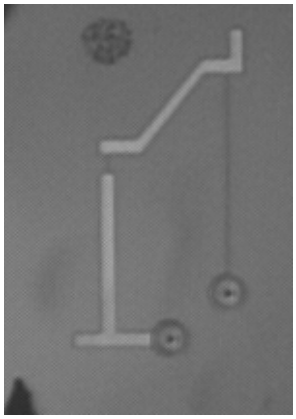

Modification Eight

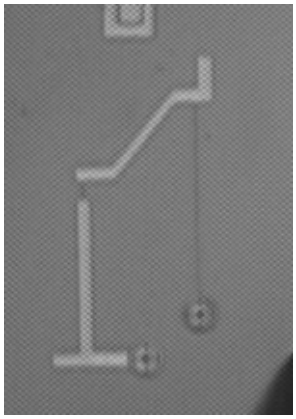

Modification Nine

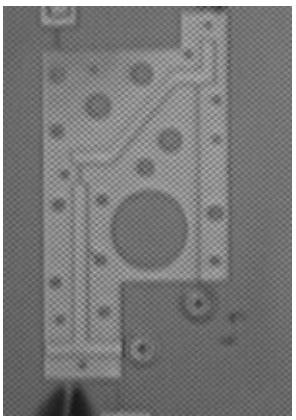

Modification Ten

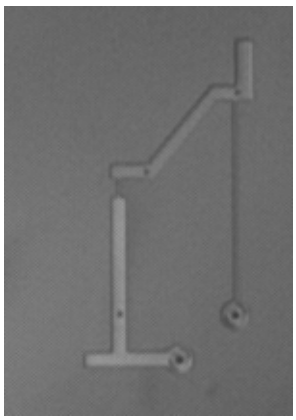

Modification Eleven

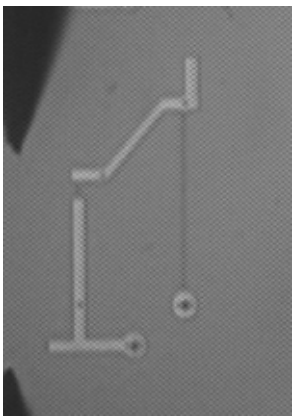

Modification Twelve

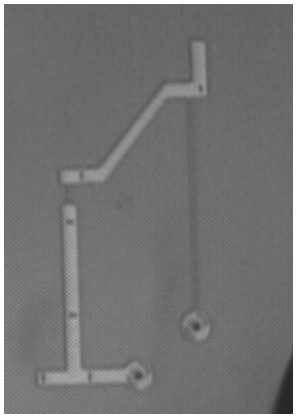

Modification Thirteen

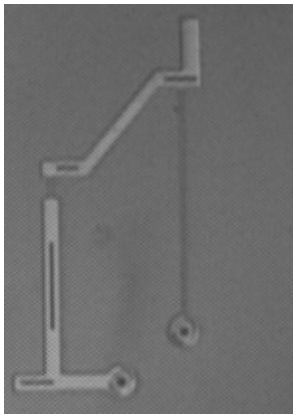

Modification Fourteen

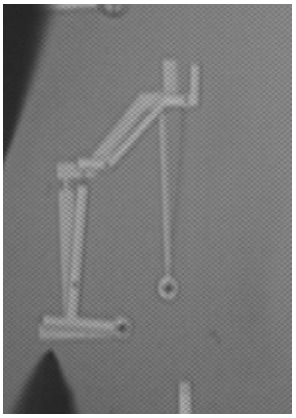

Modification Fifteen

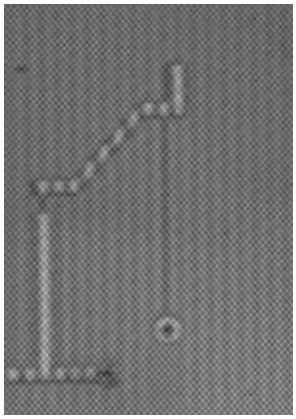

Modification Sixteen

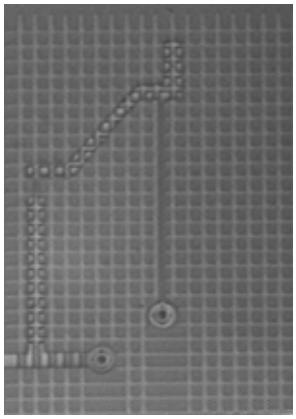

Modification Seventeen

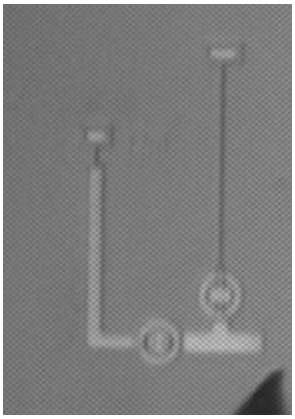

Modification Eighteen

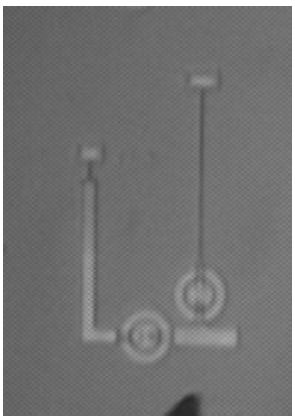

Modification Nineteen

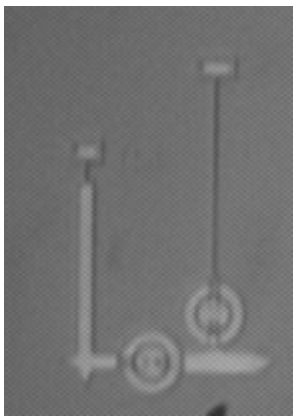

Modification Twenty

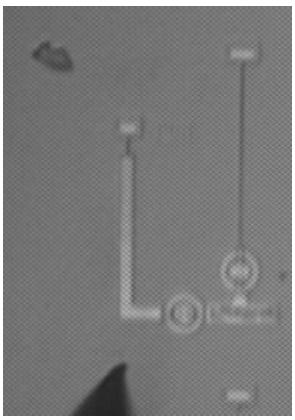

Modification Twenty One

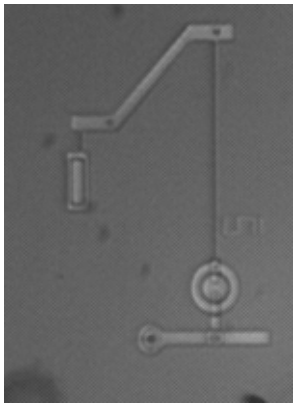

Modification Twenty Two

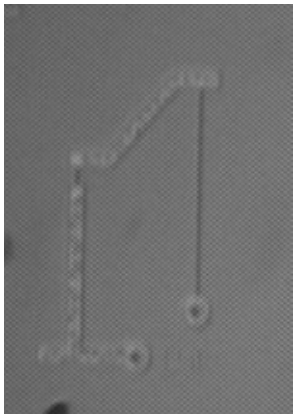

Modification Twenty Three

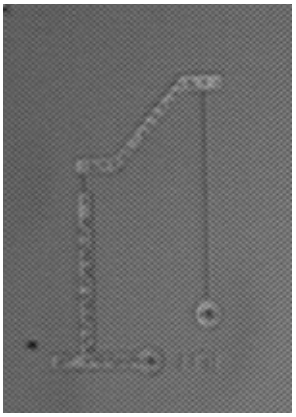

Modification Twenty Four

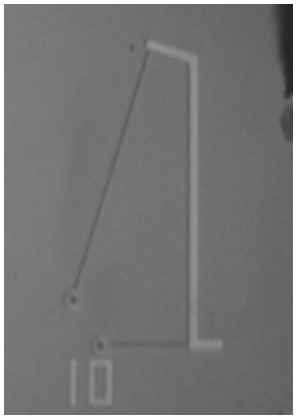

Modification Twenty Five

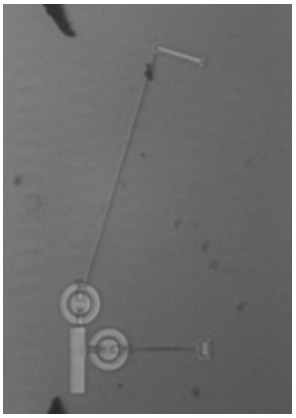

Modification Twenty Six

Modification Twenty Seven

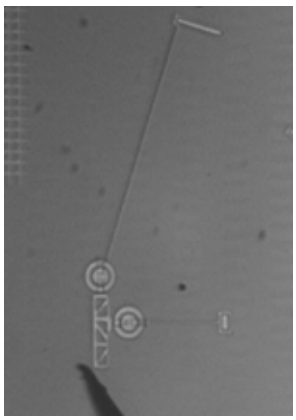

Modification Twenty Eight